CONFIDENTIAL

Copy 6
RM L54L21

NACA RM L54L21

RESEARCH MEMORANDUM

LOW-SPEED WIND-TUNNEL INVESTIGATION OF LEADING-EDGE POROUS SUCTION ON A 4-PERCENT-THICK 60° DELTA WING

By E. Carson Yates, Jr.

Langley Aeronautical Laboratory
Langley Field, Va.

Data Revision 7-20-56
RN-104
8-7-56

CLASSIFIED DOCUMENT

This material contains information affecting the National Defense of the United States within the meaning of the espionage laws, Title 18, U.S.C., Secs. 793 and 794, the transmission or revelation of which in any manner to an unauthorized person is prohibited by law.

NATIONAL ADVISORY COMMITTEE
FOR AERONAUTICS

WASHINGTON
March 1, 1955

CONFIDENTIAL

NASA Technical Library
3 1176 01437 1950

 [redacted]

NATIONAL ADVISORY COMMITTEE FOR AERONAUTICS

RESEARCH MEMORANDUM

LOW-SPEED WIND-TUNNEL INVESTIGATION OF LEADING-EDGE POROUS SUCTION ON A 4-PERCENT-THICK 60° DELTA WING

By E. Carson Yates, Jr.

SUMMARY

A 60° delta-wing—fuselage model employing a 4-percent-thick airfoil section with large leading-edge radius was tested in the Langley 19-foot pressure tunnel to determine the effectiveness of porous-leading-edge suction in delaying and reducing leading-edge separation and the accompanying high drag. Mach numbers for the tests were between 0.06 and 0.20, and Reynolds numbers were between 5.8×10^6 and 17.4×10^6. Lift, drag, and pitching-moment data were compared with leading-edge pressure distributions in order to correlate force changes with the occurrence of separation.

Area suction was shown to provide a means for reducing drag of the delta wing. Maximum drag reduction of 24 percent for the delta-wing—fuselage combination (pump-power equivalent drag not included) at a lift coefficient of 0.65 was attained with a suction flow coefficient of 0.0017. If pump power is efficiently utilized, its inclusion in the total drag should decrease maximum drag reduction to no less than 17 percent. Application of suction caused a slight decrease in lift at moderately high angles of attack but elimimated slight longitudinal instability just before maximum lift. Fences at the outboard end of the suction area and outboard droop-nose chord-extensions were relatively ineffective in delaying the inboard movement of separation over the delta wing outboard of the suction area.

Removing the portion of the wing outboard of the suction area was the only effective means of eliminating the high drag caused by separated flow over that area, but the increased induced drag resulted in about the same total drag coefficient for the clipped wing as for the delta wing. The percentage reduction of drag due to suction on the clipped wing was of a magnitude similar to that for the delta wing. Suction was also effective in reducing the drag of the clipped wing fitted with inboard or full-span split flaps.

Further application of leading-edge suction to delta wings is discussed briefly.

[redacted]

INTRODUCTION

The high drag and low lift-to-drag ratios which accompany moderately high lift on a thin delta wing constitute one of the principal disadvantages of the delta wing at low speed. This characteristic requires that current delta wing airplanes glide with high sinking speeds and use very large amounts of power on landing approaches. Recovery of flying speed following a wave-off, therefore, becomes critical. Previous investigations (for example, ref. 1) have shown that the presence of a separation bubble near the leading edge and wing tips causes a large portion of the drag at high lift. The bubble contributes to early separation of flow over the wing tips, and this separated region, extending inboard with increasing angle of attack, results in large drag. Thus, the drag of the delta wing should be materially decreased if boundary-layer control can be successfully used to delay the inception of leading-edge separation or to reduce the extent of separation or both. For a thin uncambered delta wing the maximum lift-drag ratio normally occurs before separation becomes extensive (ref. 2); thus, this quantity should not change appreciably with the application of leading-edge suction, but lift-drag ratios for lift coefficients above that at which separation normally begins may be considerably increased. The increase in lift-curve slope usually associated with the presence of a leading-edge separation vortex will be delayed and reduced. Hence, lift in the range of moderately high lift coefficient will be adversely affected by reduced separation.

Although porous leading-edge suction is not known to have been previously applied to the delta wing, significant drag reduction as well as increased maximum lift and improved pitching-moment characteristics have been obtained for swept-wing applications (refs. 3 to 11). Some two-dimensional applications of leading-edge suction are discussed in references 12 to 15. Some theoretical work on area suction and on leading-edge suction is given in references 16 and 17.

The present tests were conducted to investigate the extent to which leading-edge separation on a delta wing can be delayed and reduced and to determine the relative magnitude of the effects of reduced separation on the longitudinal characteristics of the delta wing. A 4-percent-thick 60° delta-wing—fuselage model employing an NACA 3-004 airfoil section with a porous leading edge was used in these tests. The tests were conducted in the Langley 19-foot pressure tunnel over a Reynolds number range from 5.80×10^{6} to 17.35×10^{6} and a Mach number range from 0.067 to 0.200.

SYMBOLS

C_L	lift coefficient, $\frac{\text{Lift}}{q_o S}$
C_D	drag coefficient, $\frac{\text{Drag}}{q_o S}$
C_{D_P}	equivalent pump-power drag coefficient, $C_P C_Q$
ΔC_{D_Q}	drag correction caused by loss of suction air momentum, $-2C_Q$
C_m	pitching-moment coefficient, $\frac{\text{Pitching moment about } 0.25\bar{c}}{q_o S \bar{c}}$
C_P	suction-duct pressure coefficient, $\frac{H_d - (p_o + q_o)}{q_o}$
C_Q	suction flow coefficient, $\frac{Q}{V_o S}$
P	pressure coefficient, $\frac{p - p_o}{q_o}$
R	Reynolds number based on mean aerodynamic chord
M_o	free-stream Mach number
M	local Mach number
α	angle of attack, deg
H_d	total pressure inside leading-edge suction compartment, lb/sq ft
Q	volume rate of flow of suction air measured at free-stream density, cu ft/sec
A	aspect ratio
C_l	local lift coefficient

p	local static pressure, lb/sq ft
S	wing area, sq ft
b	wing span, ft or in.
x	chordwise coordinate, ft
$\bar{c}$	mean aerodynamic chord, $\frac{2}{S}\int_0^{b/2} c^2 dy$
c	local wing chord, ft
y	lateral coordinate, ft
q_o	free-stream dynamic pressure, lb/sq ft
p_o	free-stream static pressure, lb/sq ft
T_o	free-stream static temperature, $^{\circ}F$
V_o	free-stream velocity, ft/sec
V_u	inflow velocity just outside of porous skin, ft/sec
$\bar{V}_u$	average inflow velocity just outside of porous skin, ft/sec
ρ_o	free-stream density, slugs/cu ft
Δp	pressure difference across porous skin, in. Hg or lb/sq ft
γ	ratio of specific heat at constant pressure to specific heat at constant volume

MODEL AND APPARATUS

The delta-wing model used in this investigation had leading-edge sweep of 60° and rounded tips. The clipped-wing configuration was formed by cutting off the tips along a streamwise line through the 0.825b/2 station (figs. 1(a) and 1(b)). No attempt was made to round the resulting blunt tips. The streamwise airfoil section was NACA 3-004.

This 4-percent-thick symmetrical section is one of a series of airfoils designed to produce high maximum lift and at the same time retain the principal advantages of thin airfoils at high speeds (ref. 18). These airfoils are principally characterized by large leading-edge radii. For comparison, the (0.400 percent c) leading-edge radius of the NACA 3-004 is the same as the leading-edge radius of a 65-A series airfoil with a thickness of 7.7 percent c (NACA 65A007.7). A 4-percent-thick 65-A series airfoil (NACA 65A004) has a leading-edge radius of 0.102 percent c. Ordinates for the NACA 3-004 are given in table I. The 3-004 airfoil was chosen in the present case because its large nose radius permitted installation of porous suction nearer to the wing tip than would have been possible with a more conventional section. This construction problem would, of course, not exist on a full-size wing, and a small-nose-radius airfoil could be used without difficulty.

The fuselage was a body of revolution which consisted of a cylindrical center section plus nose and tail fairings which were generated by revolving portions of a 274-inch-radius circle about the center line of the fuselage. The general arrangement of the model and principal dimensions are shown in figures 1(a) and 1(b). The wing and nose and tail fairings were of frame and skin aluminum-alloy construction, and the fuselage center section was made of laminated mahogany reinforced with plastic-impregnated fiberglass. A photograph of the model mounted in the tunnel is shown in figure 2. Details of the tip region, including the fences and 0.15c droop-nose chord-extensions used in some of the tests, are shown in figure 1(b). Some tests were made with the clipped wing fitted with 0.20c split flaps deflected 45° perpendicular to the hinge line. The two flap lengths used were full span and fuselage to 0.61b/2 of the clipped wing.

The porous surface of the removable leading edge extended continuously from 0.10c on the upper surface to 0.05c on the lower surface and from the fuselage (0.1828b/2) to the 0.80b/2 station of the full delta wing. It was formed by a three-layer skin which was supported by round-edged leading-edge ribs. The skin consisted of a 1/16-inch perforated-steel supporting plate covered with a spacer layer of 14 × 18 mesh bronze screen and an outer surface of 30 × 250 mesh Dutch weave monel filter cloth. The 30 mesh was in the spanwise direction. From 0.05c to 0.10c on the upper surface a 0.010-inch-thick finely perforated monel sheet was set into the perforated steel plate in order to decrease the permeability over the portion of the leading edge which would experience the largest Δp values. In view of the exploratory nature of this investigation, no attempt was made to minimize suction flow rates by continuous grading of the permeability in the chordwise direction or by dividing the leading edge into small compartments and varying duct pressure across the span.

The permeability characteristics of the two leading-edge skins (designated as porosities 1 and 2) as installed are shown in figure 3. The filter cloth of porosity 1 was rolled from its original thickness of 0.026 inch to 0.018 inch, and the filter cloth of porosity 2 was rolled from 0.026 inch to 0.020 inch. The low permeability of porosity 1 served as a means of keeping suction flow quantity within the limits of system capacity. It was used only on configurations A and B (see table II). From figure 3 it appears that in spite of the finely perforated insert between 0.05c and 0.10c, full open porosity 1 was more permeable than 0 to 0.05c open. The reason for this is not known. These permeability curves, however, were not used in any subsequent calculations; therefore, any discrepancy that may exist will not affect any of the other results.

The leading-edge-suction area was not designed for a specific lift coefficient since the relatively large duct losses which were anticipated made the available suction pressure unknown and since the influence of separated flow at the wing tips on the inflow required to prevent inboard movement of separation cannot be evaluated by Thwaites' criterion (refs. 3 and 19). A variable open area was therefore used and, since maximum thickness for the NACA 3-004 airfoil is at 0.13c, a maximum rearward extent of suction of 0.10c was considered adequate for the present tests.

For tests with the leading edge sealed, the porous area was sprayed with nonporous strippable plastic and a layer of lacquer which was sanded smooth and faired to the wing. For tests with suction the desired porous area was cut out with razor and straight edge, and the plastic was peeled from this surface. The porosity of the skin was maintained by sucking acetone through the porous area before each run.

External pressures on the leading-edge upper surface were measured by means of orifices located (on the full delta wing) at spanwise stations 0.25b/2, 0.35b/2, 0.445b/2, 0.55b/2, 0.70b/2, and 0.796b/2 on the right-wing panel and at stations 0.445b/2 and 0.796b/2 on the left-wing panel. Each orifice station contained eight tubes located at 0c, 0.001c, 0.003c, 0.005c, 0.0125c, 0.025c, 0.05c, 0.10c. Duct static pressures and temperatures were measured by orifices and thermocouples within the leading-edge compartments.

The suction system is outlined in figure 4. Two suction compartments on each wing panel were connected through remotely controlled butterfly valves to a manifold chamber in the fuselage. From this chamber the suction air passed through a 4-inch diameter reinforced-wall rubber hose to a fixed-position 4-inch-diameter vertical pipe which was connected through the floor of the tunnel to the external piping system shown in figure 4. For most of its length this vertical pipe was shielded from tunnel air flow by a streamline fairing. (See fig. 2.) The external system contained a motorized flow control valve, a second length of 4-inch-diameter rubber hose to isolate extraneous forces from the balance

system, a venturi, and a bleed valve. The exhaust end of the suction line was open to atmosphere for some tests and connected to the intake side of the tunnel compressors for others.

TESTS

All tests were made in the Langley 19-foot pressure tunnel with the air in the tunnel compressed to about $2\frac{1}{4}$ atmospheres. Mach numbers for the tests were 0.067, 0.120, and 0.200, and the corresponding Reynolds numbers were 5.80×10^6, 10.41×10^6, and 17.35×10^6. Mach numbers were held within ± 0.002.

For all tests, lift, drag, pitching moment, and suction flow rate were measured up to an angle of attack at which a considerable portion of the flow over the wing was separated. The angle-of-attack range for some tests was extended to include maximum lift. For all tests, measured peak pressures at the outboard orifice stations (0.796b/2 on the full delta wing) were recorded and, for some tests, complete pressure distributions were obtained for the leading-edge upper surface.

For most tests, full available suction was applied to the model, and the differences in C_Q and $\frac{\overline{V_u}}{V_o}$ which occurred were caused by differences in open area. The chordwise and spanwise extents of porous area used are listed in table II. The influence of fences and outboard droop-nose chord-extensions on the full delta wing with suction was determined, as well as the influence of full span and inboard split flaps on the clipped wing with and without suction.

Three procedures for adjusting flow valves were tried because a slight asymmetry of leading-edge radius which existed near the outboard ends of the suction area caused unsymmetrical variations of local pressure. The method yielding greatest drag reduction was based on maintaining approximately the same inflow velocities over left- and right-wing panels. With the outboard-duct butterfly valves full open, the inboard-duct valves about half open (see fig. 4), and maximim suction applied to the model, the angle of attack at which peak pressure occurred at the outboard orifice station was found. At this angle one of the outboard valves was closed until the difference between peak external pressure and outboard duct pressure was the same for the left- and right-wing panels. For this condition the inflow velocities at the outboard stations were approximately the same for both panels. The inboard valves were than adjusted so that inboard-duct pressures were equal and so that the difference between tunnel atmospheric pressure and inboard-duct pressure was about 40 percent of the difference between tunnel pressure and outboard-duct pressure. In a

preliminary theoretical investigation of pressures on the wing, this proportion had been found to yield the highest inboard duct pressure consistent with maintaining inflow over the whole inboard section. In order to produce the same inflow velocities over left and right inboard sections it was only necessary to make the inboard duct pressures equal, since the slight asymmetry of leading-edge radius that existed over the outermost portions of the porous area did not extend inboard. This valve-adjusting process was iterative since all four suction ducts were manifolded within the fuselage. The butterfly-valve settings thus obtained were not changed during a run, but it was necessary to readjust the total flow valve at each angle of attack in order to maintain constant total mass flow and constant suction flow coefficient.

A second procedure was tried on one run. This procedure differed from the one above only in the apportionment of suction to the outboard ducts. Here the outboard valves were adjusted to make the left and right outboard pressure peaks occur at the same angle of attack. Thus, the occurrence of separation over the portion of the wing affected directly by the suction was delayed as long as possible.

A third procedure which was tried on one run was to equalize all duct pressures at the angle of attack of which outboard pressure peaks occurred. Effectiveness of the three methods for adjusting valves is indicated in figure 5.

CORRECTIONS TO DATA

The method of reference 20 was used to evaluate jet-boundary corrections which were applied as follows:

$$\Delta\alpha = 1.388C_L$$

$$\Delta C_D = 0.0192C_L^{\ 2}$$

$$\Delta C_m = 0.0044C_L$$

Angle of attack, drag, and pitching-moment values have been corrected for air-stream misalinement caused by model support and suction pipe fairings. The stream angle due to the model support fairings was determined from tunnel surveys, and the stream angle due to the suction pipe fairing was evaluated from experiments with a similar fairing in an electrolytic tank.

No corrections for support tare and interference have been made. The lift, drag, and pitching-moment data have been corrected for tare caused by external air loads on the vertical suction pipe.

The suction system used required the application of two additional corrections. As shown in figure 4 the suction air was discharged at right angles to the tunnel air stream. The thrust equivalent of the suction air momentum was, therefore, lost. Assuming that the suction air could have been ejected downstream with free-stream velocity and pressure gives the drag correction

$$\Delta C_{D_Q} = -2C_Q$$

as in reference 21. Slight misalinement of the lateral discharge pipe caused the suction air to produce a force in the drag direction. Corrections for this force have been applied to drag and pitching moment.

All tunnel dynamic-pressure measurements were corrected for blockage.

RESULTS AND DISCUSSION

Delta Wing

The results of force measurements on the delta wing with and without leading-edge suction are presented in figures 5 to 9, and leading-edge surface-pressure data are presented in figures 10 to 18.

Drag.- Drag polars (pump-power equivalent drag not included) for the delta-wing—fuselage combination with and without suction are shown in figures 6 and 7. As the Mach number increased, it is seen that drag reduction due to suction began at lower lift coefficients. In all cases, suction benefits persisted to the highest lift coefficients obtained. The greatest percentage of drag decrease was found to occur in the probable-landing-angle range ($\alpha = 14^\circ$ to 17°). At all three Mach numbers maximum drag reduction was approximately 24 percent at a lift coefficient between 0.6 and 0.7. This result is also indicated in figure 9 as a 31-percent increase in lift-drag ratio at $C_L = 0.65$.

The theoretical drag curve for the wing alone with no flow separation is shown in figure 6. The 0.986 factor in the theoretical expression was obtained from reference 22 and unpublished NACA data, and it represents a drag increase due to deviation of the spanwise loading from elliptical. Figure 6 shows the suction test which gave greatest drag reduction (configuration C), and it indicates that the drag for all but the lowest lift coefficients was still considerably greater than the calculated value for the wing alone. Although tuft observations showed separated flow over the wing tips beginning at about $\alpha = 5^\circ$, the tufts indicated no flow separation behind the suction area, and figure 14 does not indicate the presence of a separation bubble near the leading edge below $\alpha = 13^\circ$. It

appears, moreover, from the drag results for the clipped wing discussed below that the variation of fuselage drag with lift is small at low angles of attack. Thus the additional drag (above the theoretical value) for the delta wing was to a great extent caused by separated flow over the tip regions. This outboard separated flow manifested itself as a drag rise beginning at about an angle of attack of 5° but did not become strong enough to influence the lift-curve slope until about 9°.

An attempt was then made to form a more effective barrier against the inward movement of separation by installing wraparound fences just outboard of the porous area (see fig. 1(b)). The results of the fence-on tests as well as tests of other configurations are summarized in figure 5. The addition of wraparound fences to configuration F resulted in a drag increase which tuft observation indicated was caused by separation beginning at the inboard side of the fence at about $\alpha = 7^{\circ}$. The wraparound portion of the fence was removed (see fig. 1(b)) with the hope that the partial fence would have less tendency to initiate separation, but results of both fences on configuration E (fig. 5) indicate approximately the same drag.

Short droop-nose chord-extensions were added to the wing tips for the purpose of delaying separation over that area, and these yielded slight drag improvement up to about $\alpha = 14^{\circ}$ and $C_L = 0.6$ (see fig. 5).

Changes were made in the porous area configuration for the purpose of increasing inflow velocity over the critical outboard section. Results for the various open areas are shown in figures 5, 6, 7, and 12. Comparing configuration G with configuration B in figure 6 shows that approximately the same drag reduction can be obtained with lower C_Q if the inflow velocity is increased by a reduction of open area. Tests of configurations A and B at $C_Q = 0.0008$ (fig. 5) showed that appreciable drag improvement resulted from the decrease in open area and the accompanying increase in inflow velocity. This relationship between C_Q and inflow velocity is, of course, limited since excessive reduction of chordwise extent of suction results in the appearance of the separation bubble behind the porous area. In the present tests tuft observations indicated that reduction of chordwise extent of suction to less than 0.05c at 0.80b/2 caused the bubble to occur behind the porous area. Some results of partial span suction over the outboard portion of the wing are shown by configurations F, G, and H in figure 5. The adverse effect of excessively small chordwise suction extent is apparent particularly at high lift.

Pump power.- The above discussion has not included pump power because interest here is directed solely toward external aerodynamics with no attempt being made to minimize suction flow or power. It should be emphasized, however, that in any application to aircraft, minimizing suction power is extremely important. Even a small amount of excess

power directed to suction can nullify a sizeable portion of the drag reduction due to suction.

An estimate of the order of magnitude of suction power equivalent drag can be quickly obtained (see refs. 7, 21, and 23). Neglecting duct, pump, and exit losses gives for the equivalent drag

$$C_{D_P} = C_P C_Q$$

For the suction test of configuration C shown in figures 6, 8, and 10, $C_Q = 0.0017$, and at $\alpha = 15.2^{\circ}$ $\left(C_L = 0.648\right.$, the approximate condition for maximum drag reduction$\left.\right)$ C_P was -10.2 for the inboard compartment and -20.0 for the outboard compartment. Weighting these on the basis of inboard and outboard exposed porous areas gives an effective C_P of -14.1 and a C_{D_P} of 0.0233. At $\alpha = 0^{\circ}$ and 25.9° the C_{D_P} values are 0.0131 and 0.0260. If C_{D_P} is included in the total drag, the maximum drag reduction due to suction was 7 percent instead of the 24 percent given above. It is believed, however, that by chordwise grading of permeability, spanwise compartmentation, and optimizing the suction area the same external drag benefits could be obtained with less than 40 percent of the C_{D_P} used here. Maximum drag decrease including pump power would then be 17 percent or better.

At $\alpha = 13.1^{\circ}$ for this test (the angle at which P_{max} occurred at the outboard orifice station and also the angle of attack at which the suction duct butterfly valves were set) $C_P = -18.75$ at the outboard end of the porous leading edge. This corresponds to a minimum inflow velocity of $V_u = 3.0$ feet per second at that station.

Lift.- Figure 8 indicates that, as expected, the application of suction caused a lift decrease for angles of attack beyond the point of initial lift-curve-slope increase which extended almost to maximum lift. Maximum lift itself, however, was slightly increased by suction. The suction test shown in figure 8 gave the greatest loss of lift experienced in the tests and also the greatest drag reduction (fig. 6). The lift characteristics shown are typical of the other suction tests, the lift loss being roughly proportional to the drag decrease. Suction did not change the angle of attack at which the characteristic lift-curve-slope increase occurred (about 9°) nor the magnitude of the increase. Since tuft observations in this case did not indicate separation behind the porous area and since figure 14 does not indicate the presence of a separation bubble near the leading edge below $\alpha = 13^{\circ}$, it is concluded that the initial lift-curve-slope increase was caused by a separation bubble on the tips which were unprotected by suction.

The loss of lift in all cases began with a wiggle in the lift curve which occurred when the separated flow region extended inboard to between 0.70 and 0.80b/2 (see figs. 8, 10, and 14(c)). This wiggle is believed to be caused by reduced inflow and suction effectiveness near the outboard end of the suction area. This reduced effectiveness permitted separation to move inboard with relatively little resistance to perhaps 0.75b/2. During this movement there is little difference between the lift curves with or without suction. In the neighborhood of 0.75b/2, the suction barrier to separation became much stronger, and the inward movement of separation was greatly retarded. In this angle-of-attack range as α increased, there was not a corresponding increase in extent of the separation bubble and hence the rate of lift increase was less rapid. This condition existed until separation began to move inboard again; figure 10 indicates that this movement occurred at about 19°. With further increase in angle of attack the lift-curve slope of the wing with suction became greater than that for the no-suction case because (see fig. 10) the inboard movement of the separation bubble was then very rapid on the wing with suction. The location and abruptness of this wiggle in the lift curve would be governed by the location of the outboard end of the suction area and by the spanwise distribution of inflow. It is probable that this wiggle could be smoothed out entirely by appropriate inflow distribution.

Pitching moment.- The pitching-moment curves for the delta wing with and without suction (see fig. 8) deviate at approximately the same lift coefficient as the lift curves. In the lift-coefficient range for which the lift of the wing with suction is less than that for the sealed wing, the pitching moment of the wing with suction is slightly more negative. The rearward center-of-pressure shift indicated by reduced lift and more negative pitching moment is again indicative that the extent of the leading-edge-separation bubble has been appreciably curtailed.

Another effect of suction on the pitching moment occurred near maximum lift. As is characteristic of some thin delta wings with large sweep angles, this wing demonstrated a slight longitudinal instability just before maximum lift, although the stall itself was stable. Application of suction yielded complete stability throughout the entire lift range.

Pressure distributions.- Chordwise pressure distributions at 0.796b/2 for several porous-area configurations are given in figure 12(a). It is seen that for configuration G the reduction of C_Q and the increase of $\frac{\overline{V_u}}{V_o}$ which gave the same polar as configuration B (fig. 6) also gave the same outboard leading-edge pressure peak. Chordwise reduction of suction area inboard (configuration C) increased inflow velocity (at constant C_Q) above that for configuration B and yielded higher outboard peak pressure (fig. 12(a)) as well as greater drag reduction (fig. 6).

Figure 12(b) shows that, with suction allowing high pressure peaks to be held, the chordwise distribution of pressure at the outboard end of the suction area is reasonably represented by combined two-dimensional and simple sweep theory. Since full-chord pressure distributions were not obtained in these tests, $C_{l_{exp}}$ for the calculation of figure 12(b) was found from the spanwise load distribution obtained by the method of reference 24. With suction minimizing flow separation, this procedure is believed to be reasonably accurate. For the wing without suction, theory does not accurately predict the outboard chordwise pressure distribution for which peak pressure occurs since the pressure peak is reached after considerable separation exists behind the leading-edge area.

It has previously been shown that Thwaites' two-dimensional criterion for determining the necessary chordwise extent of suction (ref. 19) is applicable to three-dimensional wings when separation is not present. (See, for example, refs. 3 and 6.) The prime requisite for the use of Thwaites' criterion is the accurate predetermination of chordwise pressure distribution. The agreement in figure 12(b) between the suction test data and the two theoretical curves shown for $2y/b = 0.796$ (one curve for the condition $P_{max_{exp}} = P_{max_{theor}}$ and the other for the condition $C_{l_{exp}} = C_{l_{theor}}$) indicates, therefore, that this criterion might reasonably be used for three-dimensional wings even though separated flow exists adjacent to the porous area.

Peak pressures obtained at $M = 0.067$ were considerably greater than those for $M = 0.120$ (see figs. 10 and 11). This result is attributed to two factors. First, the lower stream velocity permitted a higher C_Q value to be attained. Second, any adverse effect of a rise of local Mach number is less serious at very low stream Mach numbers (see ref. 25). It may be noted that maximum possible pressure coefficient for the condition of infinite local Mach number is $P_{M=\infty} = \frac{-2}{\gamma M_o^2}$. The highest local Mach numbers obtained in the present tests were 0.48 at $M_o = 0.067$ and 0.64 at $M_o = 0.12$.

Clipped Wing

Since no satisfactory means was found to delay separation over the tips where the leading-edge radius became too small to permit the installation of porous suction, the tips of the delta wing were cut off slightly outboard of the porous area. (See figs. 1(a) and 1(b).) Results of tests on the clipped wing are shown in figures 19 to 24.

Drag.- Drag polars for the clipped-wing—fuselage combination with and without suction and flaps are given in figure 19. Pump-power equivalent drag is not included in this figure, but the discussion of pump power given above for the delta wing also applies for the clipped-wing configuration. Removing the tips eliminated the drag caused by separated flow over that area, but the increased induced drag resulting from the lower aspect ratio gave approximately the same total drag coefficient as the delta wing. Without flaps the drag of the clipped wing with suction follows the calculated drag curve much more closely than does the drag of the delta wing with suction. The close agreement between the theoretical and experimental drag curves up to $C_L = 0.4$ indicates that the fuselage drag did not vary much over this low C_L range. No tuft studies were made on the clipped wing, but it is believed that, for the wing without flaps, a separation bubble behind the porous area caused deviation of the drag from the theoretical curve beginning at the same lift coefficient as the beginning of the increase in lift slope. (See figs. 19 and 20.) It should be noted that, for the results presented here, the porous area on the clipped wing extended to only 0.05c at the outboard end. It is believed that, if approximately the same inflow velocity could be maintained while extending the outboard suction area farther rearward, the appearance of the separation bubble behind the porous area could have been further delayed and drag further reduced. This procedure was attempted in the test of configuration J, but sufficient inflow velocity could not be maintained at the tip with the increased open area. In contrast, the delta wing did experience a drag decrease from increased open area at the tip.

The maximum drag reduction and lift-drag increase (fig. 21) for the clipped wing without flaps was approximately the same as that for the delta wing (23-percent drag reduction and 30-percent lift-drag increase with pump-power equivalent drag not included). This condition, however, occurred at a lift coefficient of about 0.75 which is 0.1 higher than that for the delta wing. The effect on drag reduction of adding inboard and then full-span flaps was to increase progressively the lift coefficient at which maximum drag reduction occurred (fig. 19).

Lift.- Figure 20 shows that removing the wing tips and eliminating the accompanying region of strongly separated flow entirely eliminated the wiggle in the lift curve for the wing with suction. For the clipped wing with and without 0.20c split flaps, the initial lift-curve-slope change begins at about $\alpha = 9^{\circ}$, but with suction applied the slope change is very gradual. The slope change for the clipped wing with suction on and flaps off is completed at about an angle of attack of 17°. Pressure data in figures 22 and 23(c) indicate that this is about the attitude at which the leading-edge separation bubble appears at the outboard station. It is believed that the initial lift-curve-slope change for the wing with suction and without flaps was caused by a separation bubble behind the porous area.

Maximum lift coefficient for the clipped wing was approximately the same as that for the delta wing. The addition of flaps with or without suction had little effect on the maximum lift of the clipped wing.

Pitching moment.- Pitching-moment characteristics of the clipped wing without flaps were generally similar to the characteristics of the delta wing, except the slight instability of the delta wing (sealed) near maximum lift was eliminated by removing the wing tips. The addition of flaps introduced an unstable shift of pitching moment at high lift. Below maximum lift, leading-edge suction had little effect on this moment shift, but suction did produce a stable variation of pitching moment at maximum lift with both inboard and full-span flaps.

Comments on the Application of Leading-Edge Suction to Delta Wings

The airfoil used on this wing has a very large leading-edge radius and forward position of maximum thickness. These characteristics resulted in pressure gradients near the leading edge which were much less severe than those for the more conventional high-speed airfoils of similar thickness. This condition would be desirable on a wing without suction and on a wing with porous suction the construction advantages are obvious, but in applying suction it necessitates a large chordwise extent of open area. This problem could be handled satisfactorily by chordwise grading of the permeability. However, if this is not done, an airfoil with a sharper nose and steeper pressure gradients over a smaller fraction of the chord would be desirable. Smaller open area and lower duct pressure would be used. The drag reductions associated with such a model might be greater than those indicated here since sharper nose airfoils usually generate stronger leading-edge separation bubbles.

The addition of at least one more leading-edge suction compartment is strongly indicated by the present tests. If lower duct pressures could have been held over the outboard 10 percent of the suction area, outboard pressure peaks could have been held to higher angles of attack, and greater drag reduction would have been realized. Maintaining very low duct pressures near the outboard end of the suction area is particularly important for the delta wing. Theoretically delta-wing leading-edge pressure peaks tend to increase without limit as the tip is approached; thus, practically, if separation near the tips is to be appreciably delayed, extremely high pressure peaks must be dealt with.

Finally, the application of leading-edge suction to a clipped wing seems to offer more benefits than application to a delta wing. Thickness reduction toward the tip of the delta wing limits the possible spanwise extent of a porous suction system. It has been shown that the tip areas

beyond the reach of leading-edge suction are responsible for a large part of the drag at moderate lift.

CONCLUSIONS

Tests in the Langley 19-foot pressure tunnel of a 60° delta-wing—fuselage model equipped with porous leading-edge suction and of the model with the wing tips removed indicate the following conclusions:

1. Application of porous leading-edge suction to a delta wing provides a means for reducing the extent of leading-edge separation, increasing leading-edge pressure peaks, and reducing drag in the range of moderately high lift coefficient.

2. The maximum drag reduction of 24 percent for the delta-wing—fuselage combination (pump-power equivalent drag not included) at a lift coefficient of 0.65 could have been appreciably increased by the provision of an additional suction compartment at the outboard end of the porous area so that lower duct pressures could have been maintained there.

3. Inclusion in the total drag of the pump-power equivalent drag required by a reasonably efficient suction system would yield a maximum drag reduction of an estimated 17 percent or better for the present delta-wing tests. This value was not actually attained in this investigation because no attempt was made to reduce pump power to low values.

4. Application of suction caused a slight decrease in lift at moderately high angles of attack but eliminated slight longitudinal instability of the delta wing just before maximum lift.

5. Fences at the outboard end of the suction area and outboard droop-nose chord-extensions were relatively ineffective in delaying the inboard movement of separation over the delta wing outboard of the suction area.

6. Removing the portion of the wing outboard of the suction area was the only effective means of eliminating the high drag caused by separated flow over that area. However, the increased induced drag resulting from the lower aspect ratio gave approximately the same total drag coefficients as the delta wing. Percentage of drag reduction due to suction on the clipped wing was of magnitude similar to that for the delta wing.

7. Leading-edge area suction reduced the drag of the clipped wing fitted with inboard or full-span split flaps.

Langley Aeronautical Laboratory,
National Advisory Committee for Aeronautics,
Langley Field, Va., December 16, 1954.

[redacted]

REFERENCES

15379 1. Pocock, P. J., and Westell, J. R.: The Induced Drag Factor of Highly Swept Delta Wings at Subsonic Speeds. Lab. Memo. AE-6b, Nat. Aero. Establishment (Ottawa) Apr. 22, 1952.

2. Palmer, William E.: Effect of Reduction in Thickness from 6 to 2 Percent and Removal of the Pointed Tips on the Subsonic Static Longitudinal Stability Characteristics of a 60° Triangular Wing in Combination With a Fuselage. NACA RM L53F24, 1953.

3. Cook, Woodrow L., Griffin, Roy N., Jr., and McCormack, Gerald M.: The Use of Area Suction for the Purpose of Delaying Separation of Air Flow at the Leading Edge of a 63° Sweptback Wing. NACA RM A50H09, 1950.

4. Holzhauser, Curt A., and Martin, Robert K.: The Use of a Leading-Edge Area-Suction Flap To Delay Separation of Air Flow From the Leading Edge of a 35° Sweptback Wing. NACA RM A53J26, 1953.

5. Pasamanick, Jerome, and Scallion, William I.: The Effects of Suction Through Porous Leading-Edge Surfaces on the Aerodynamic Characteristics of a 47.5° Sweptback Wing-Fuselage Combination at a Reynolds Number of 4.4×10^6. NACA RM L51K15, 1952.

6. Cook, Woodrow L., and Kelly, Mark W.: The Use of Area Suction for the Purpose of Delaying Separation of Air Flow at the Leading Edge of a 63° Swept-Back Wing - Effects of Controlling the Chordwise Distribution of Suction-Air Velocities. NACA RM A51J24, 1952.

6733 RES 7. Poppleton, E. D.: Wind Tunnel Tests on a Swept-Back Wing Having Distributed Suction on the Leading Edge. Tech. Note. No. Aero. 2081, British R.A.E., Nov., 1950.

U 38712 8. Poppleton, E. D.: Boundary Layer Control by Suction on the Leading Edge of a Swept-Back Wing. Rep. No. Aero. 2440, British R.A.E., 1951.

9. Spillman, J., and Dean, J.: Wind Tunnel Tests of Devices To Prevent Tip Stalling on a Swept Wing. Part I. Leading Edge Porous Suction With, and Without, Fences. W. T. Rep. No. 1847, Vickers-Armstrong, Ltd. (Surrey), Apr. 1, 1950.

10. Cook, Woodrow L., Holzhauser, Curt A., and Kelly, Mark W.: The Use of Area Suction for the Purpose of Improving Trailing-Edge Flap Effectiveness on a 35° Sweptback Wing. NACA RM A53E06, 1953.

11. Holzhauser, Curt A., and Martin, Robert K.: The Use of Leading-Edge Area Suction to Increase the Maximum Lift Coefficient of a 35° Swept-Back Wing. NACA RM A52G17, 1952.

12. Nuber, Robert J., and Needham, James R., Jr.: Exploratory Wind-Tunnel Investigation of the Effectiveness of Area Suction in Eliminating Leading-Edge Separation Over an NACA 64_1A212 Airfoil. NACA TN 1741, 1948.

13. Anderson, K. G.: Investigation of Boundary-Layer Control at High Subsonic Speeds. USAF Tech. Rep. No. 6344, Pt. I, Wright Air Dev. Center, U. S. Air Force, Jan. 1951.

14. Dannenberg, Robert E., and Weiberg, James A.: Section Characteristics of a 10.5-Percent-Thick Airfoil With Area Suction as Affected by Chordwise Distribution of Permeability. NACA TN 2847, 1952.

15. Von Doenhoff, Albert E., and Loftin, Laurence K., Jr.: Present Status of Research on Boundary-Layer Control. NACA RM L8J29, 1949.

16. Braslow, Albert L., Burrows, Dale L., Tetervin, Neal, and Visconti, Fioravanti: Experimental and Theoretical Studies of Area Suction for the Control of the Laminar Boundary Layer on an NACA 64A010 Airfoil. NACA Rep. 1025, 1951. (Supersedes NACA TN 1905 by Burrows, Braslow, and Tetervin and NACA TN 2112 by Braslow and Visconti.)

17. Lighthill, M. J.: A Theoretical Discussion of Wings With Leading-Edge Suction. R. & M. No. 2162, British A.R.C., May 1945.

18. Loftin, Laurence K., Jr., and Von Doenhoff, Albert E.: Exploratory Investigation at High and Low Subsonic Mach Numbers of Two Experimental 6-Percent-Thick Airfoil Sections Designed To Have High Maximum Lift Coefficients. NACA RM L51F06, 1951.

19. Thwaites, B.: A Theoretical Discussion of High-Lift Aerofoils With Leading-Edge Porous Suction. R. & M. No. 2242, British A.R.C., 1946.

20. Sivells, James C., and Salmi, Rachel M.: Jet-Boundary Corrections for Complete and Semispan Swept Wings in Closed Circular Wind Tunnels. NACA TN 2454, 1951.

21. Graham, Robert R., and Jacques, William A.: Wind-Tunnel Investigation of Stall Control by Suction Through a Porous Leading Edge on a 37° Sweptback Wing of Aspect Ratio 6 at Reynolds Numbers From 2.50×10^6 to 8.10×10^6. NACA RM L52L05, 1953.

[redacted]

22. Furlong, G. Chester, and McHugh, James G.: A Summary and Analysis of the Low-Speed Longitudinal Characteristics of Swept Wings at High Reynolds Number. NACA RM L52D16, 1952.

23. Pankhurst, R. C., Raymer, W. G., and Devereux, A. N.: Wind-Tunnel Tests of the Stalling Properties of an 8 Per Cent Thick Symmetrical Section With Nose Suction Through a Porous Surface. R. & M. No. 2666, British A.R.C., June 1948.

24. DeYoung, John, and Harper, Charles W.: Theoretical Symmetric Span Loading at Subsonic Speeds for Wings Having Arbitrary Plan Form. NACA Rep. 921, 1948.

25. Edwards, George G., and Boltz, Frederick W.: An Analysis of the Forces and Pressure Distribution on a Wing With the Leading Edge Swept Back 37.25°. NACA RM A9K01, 1950.

TABLE I.- NACA 3-004 AIRFOIL SECTION ORDINATES

[Stations and ordinates are in percent of wing chord]

Station percent chord	Ordinates percent chord
0	0
.533	.642
2.132	1.208
4.796	1.639
8.517	1.904
13.253	2.000
15.0	1.998
20.0	1.984
25.0	1.953
30.0	1.907
35.0	1.845
40.0	1.769
45.0	1.680
50.0	1.578
55.0	1.465
60.0	1.340
65.0	1.206
70.0	1.061
75.0	.908
80.0	.747
85.0	.579
90.0	.405
95.0	.225
100.0	.040
L.E. radius, 0.400 percent chord	

TABLE II.- CONFIGURATIONS OF POROUS AREA

[When chordwise extent of porous area was not constant along the span, a straight-line taper was used between the spanwise end points]

(a) Delta Wing

Configuration	Chordwise extent	Spanwise extent	Total open area, sq ft	Porosity (see fig. 3)
Sealed	0	0	0	-
A	0 to 0.05c	0.1828 to 0.80b/2	1.761	1
A'	0 to 0.05c	0.1828 to 0.80b/2	1.761	2
B	0 to 0.10c	0.1828 to 0.80b/2	3.234	1
C	0 to 0.05c at 0.1828 0 to 0.10c at 0.80	0.1828 to 0.80b/2	2.042	2
D	-0.005 to 0.05c	0.1828 to 0.80b/2	2.142	2
E	0 to 0.025c at 0.30 0 to 0.05c at 0.80	0.30 to 0.80b/2	.864	2
E with full fence	0 to 0.025c at 0.30 0 to 0.05c at 0.80	0.30 to 0.80b/2	.864	2
E with partial fence	0 to 0.025c at 0.30 0 to 0.05c at 0.80	0.30 to 0.80b/2	.864	2
E with chord-extensions	0 to 0.025c at 0.30 0 to 0.05c at 0.80	0.30 to 0.80b/2	.864	2
E with partial fence and chord-extensions	0 to 0.025c at 0.30 0 to 0.05c at 0.80	0.30 to 0.80b/2	.864	2
F	0 to 0.025c at 0.40 0 to 0.05c at 0.80	0.40 to 0.80b/2	.626	2
F with full fence	0 to 0.025c at 0.40 0 to 0.05c at 0.80	0.40 to 0.80b/2	.626	2
G	0 to 0.025c	0.40 to 0.80b/2	.535	2
H	0 to 0.015c at 0.40 0 to 0.025c at 0.80	0.40 to 0.80b/2	.415	2
I	0 to 0.025c	0.48 to 0.80b/2	.400	2

TABLE II.- CONFIGURATIONS OF POROUS AREA - Concluded

(b) Clipped wing

Configuration	Chordwise extent	Spanwise extent	Total open area, sq ft	Porosity (see fig. 3)
Sealed	0	0	0	-
Sealed and with full flap	0	0	0	2
Sealed and with inboard flap	0	0	0	2
A	0 to 0.05c	0.1828 to 0.80b/2	1.761	2
E	0 to 0.025c at 0.30 0 to 0.05c at 0.80	0.30 to 0.80b/2	.864	2
E with full flap	0 to 0.025c at 0.30 0 to 0.05c at 0.80	0.30 to 0.80b/2	.864	2
E with inboard flap	0 to 0.025c at 0.30 0 to 0.05c at 0.80	0.30 to 0.80b/2	.864	2
J	0 to 0.05c at 0.30 0 to 0.075c at 0.80	0.30 to 0.80b/2	1.372	2

	Delta Wing	Clipped Wing
Leading-edge sweep	60°	60°
Aspect ratio	2.06	1.62
Taper ratio	0	0.175
Twist	0	0
Dihedral	0	0
Incidence	0	0
Airfoil	NACA 3-004	
Wing area	43.30 sq ft	41.98 sq ft
Mean aerodynamic chord	69.28 in.	71.13 in.
Tip radius	4.70 in.	--
Outboard end of porous area	0.80b/2	0.97b/2
Outboard end of full flap	--	1.00b/2
Outboard end of inboard flap	--	0.61b/2
Flap chord	--	0.20c
Fuselage fineness ratio	9.86	9.86
Ratio of maximum fuselage diameter to wing span	0.1935	0.2211

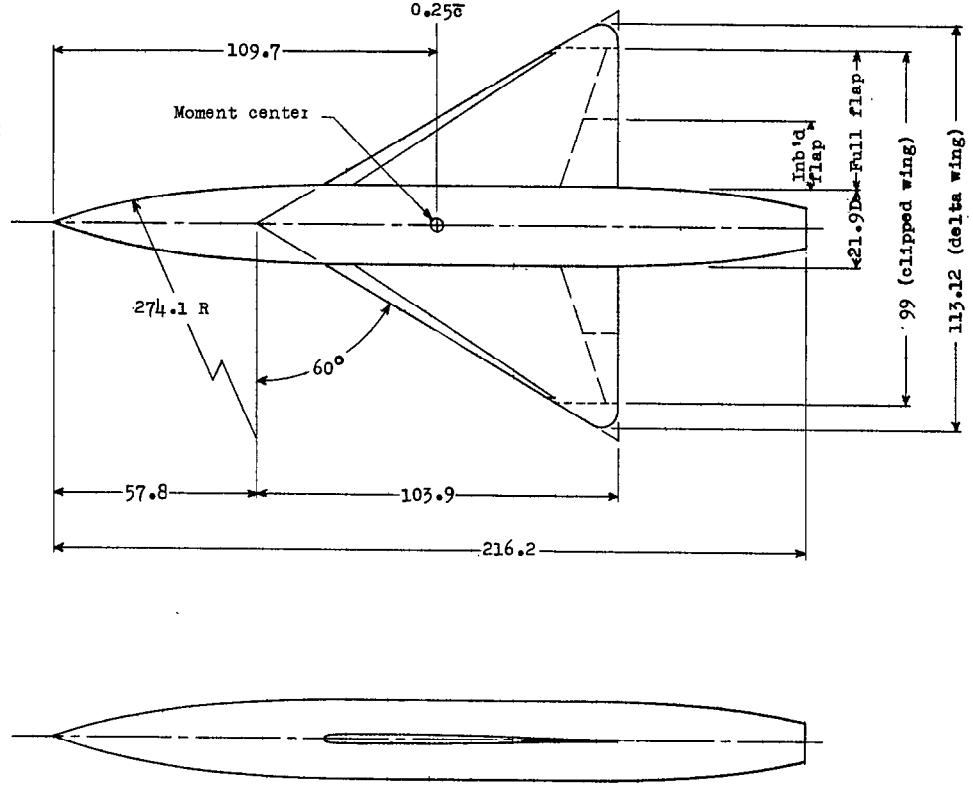

(a) Arrangement and dimensions of model.

Figure 1.- Description of model. (Dimensions are in inches unless otherwise noted.)

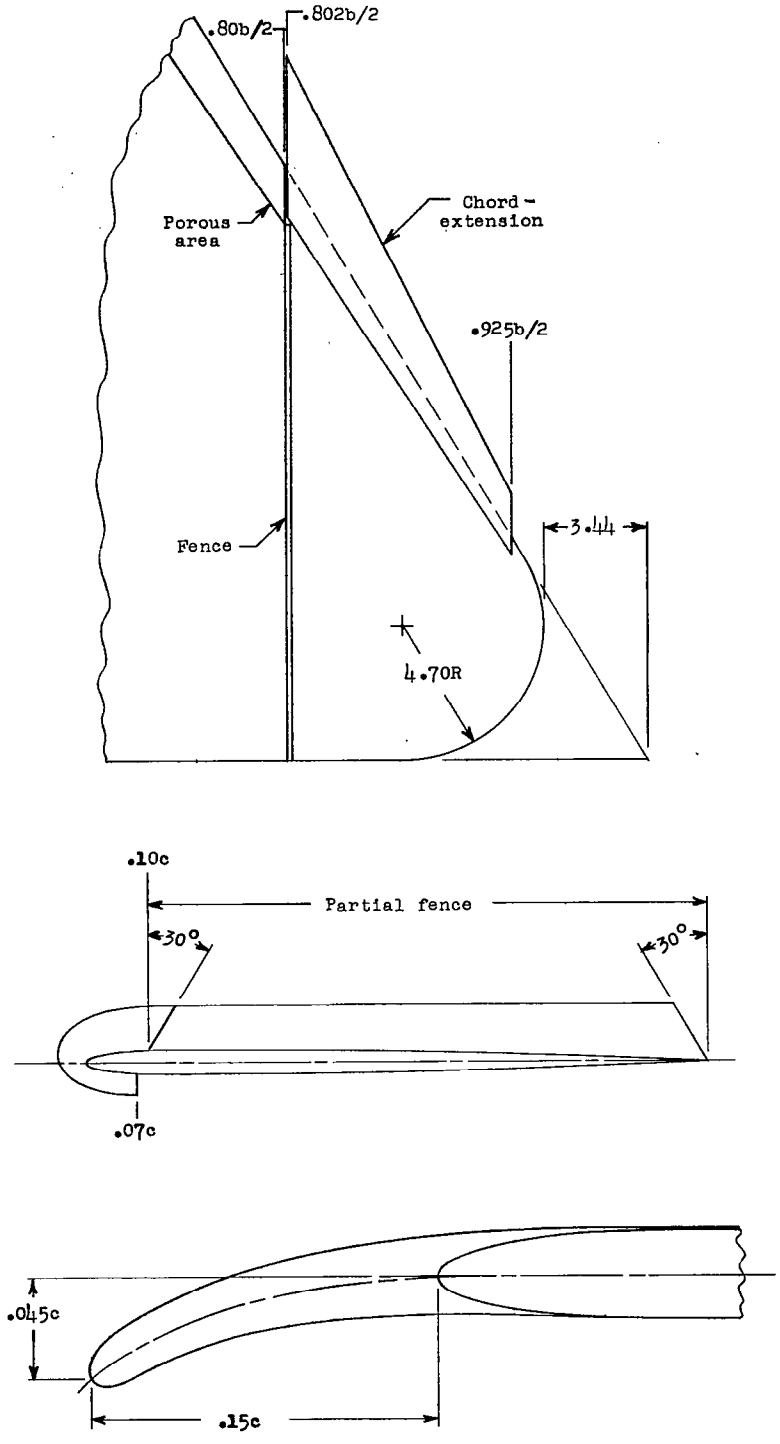

(b) Details of tip region, fences, and chord-extensions.

Figure 1.- Concluded.

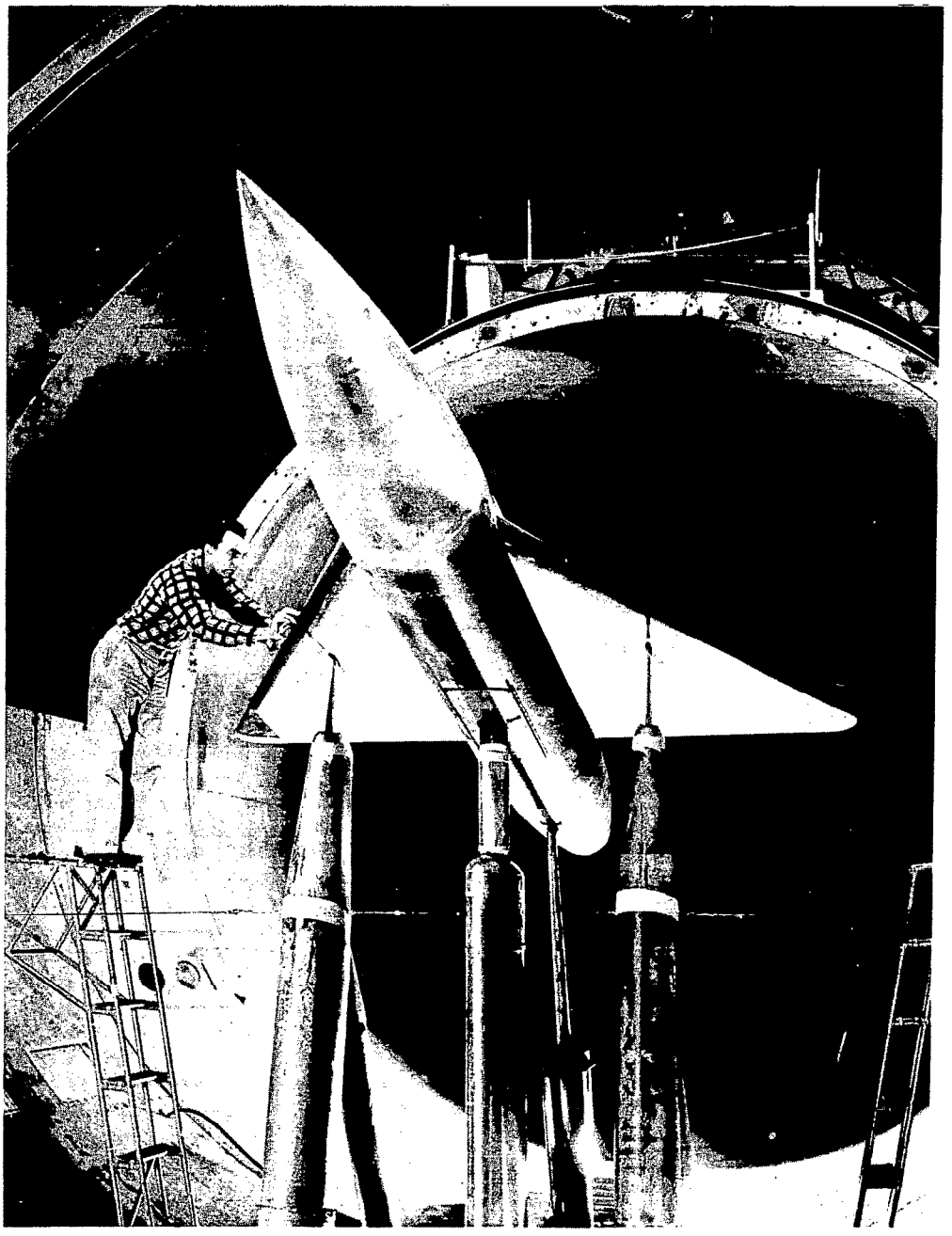

L-84699

Figure 2.- Delta-wing model in the Langley 19-foot pressure tunnel.

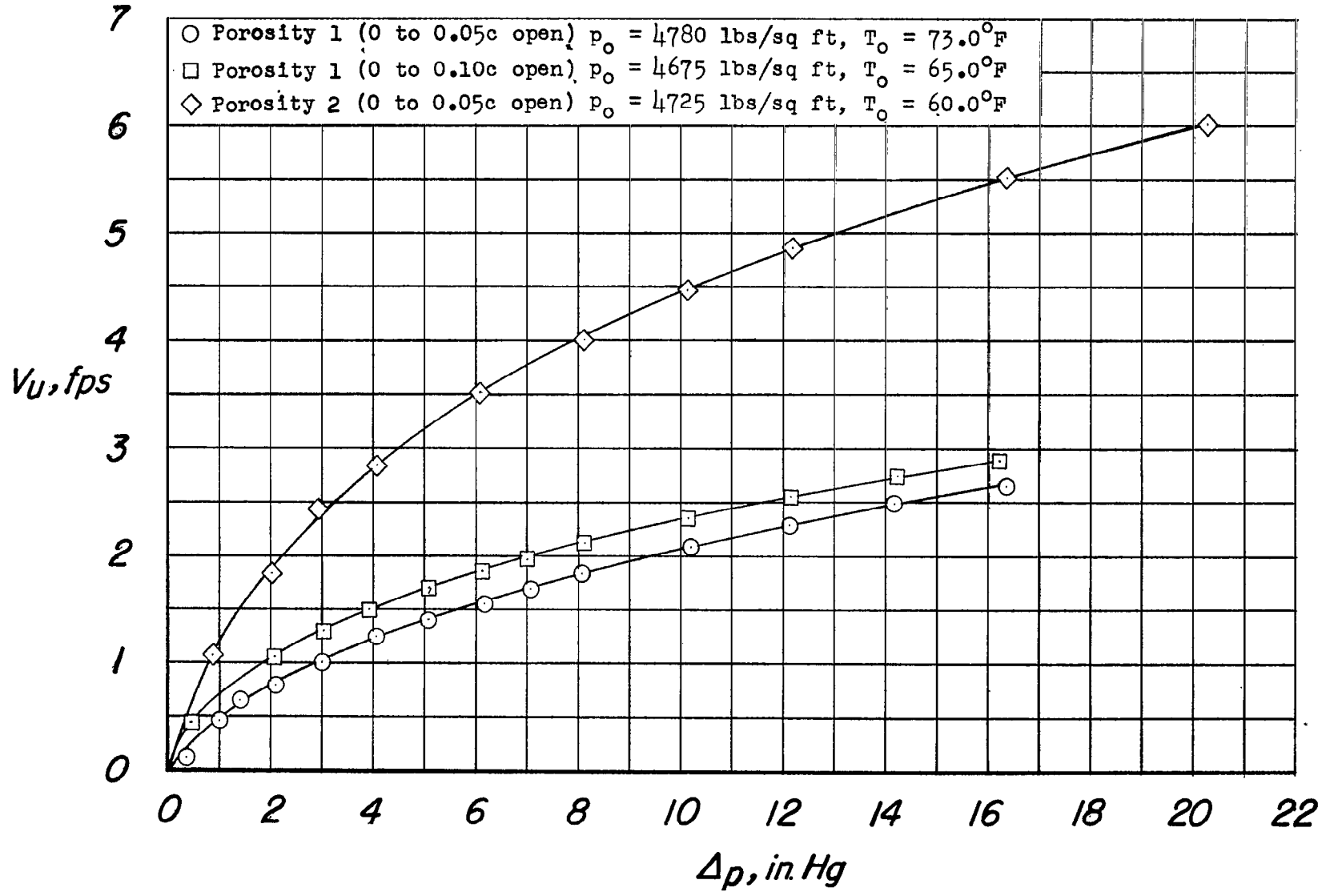

Figure 3.- Permeability characteristics of leading-edge skins. Pressure upstream of porous material approximately $2\frac{1}{4}$ atmospheres.

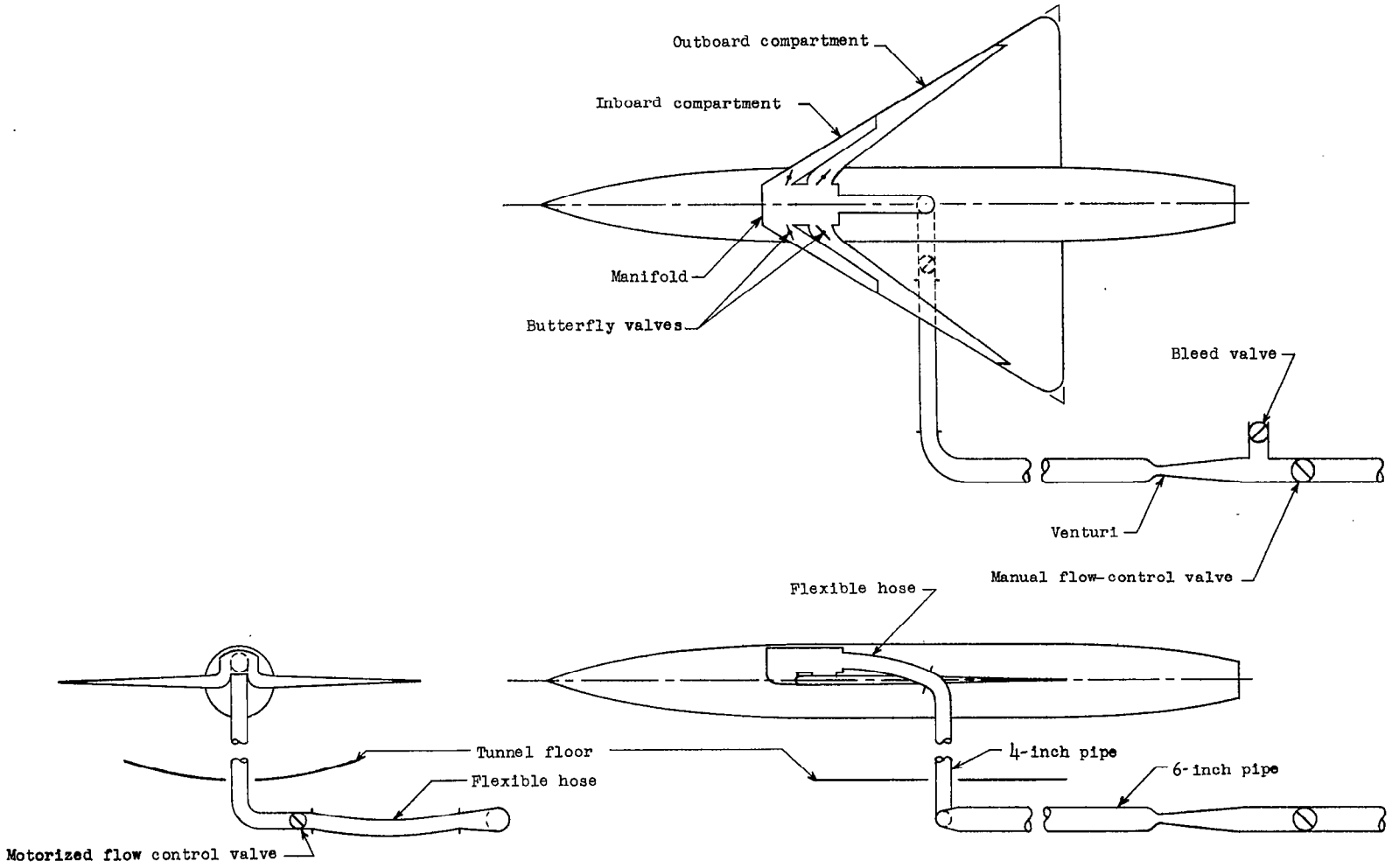

Figure 4.- Outline of suction system.

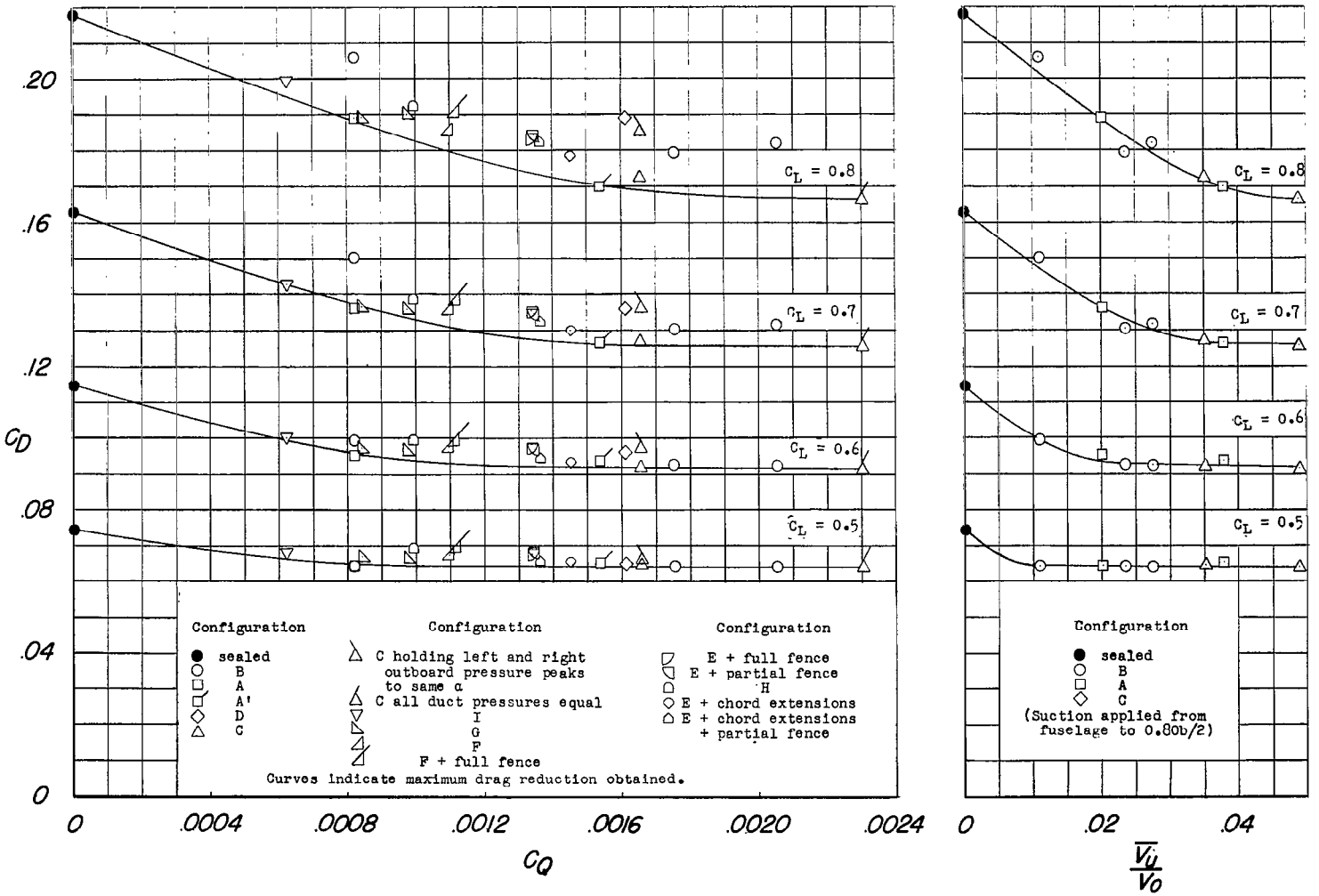

Figure 5.- Summary of delta-wing drag characteristics for various porous area configurations. M = 0.12; R = 10.4×10^6. Pump-power equivalent drag not included.

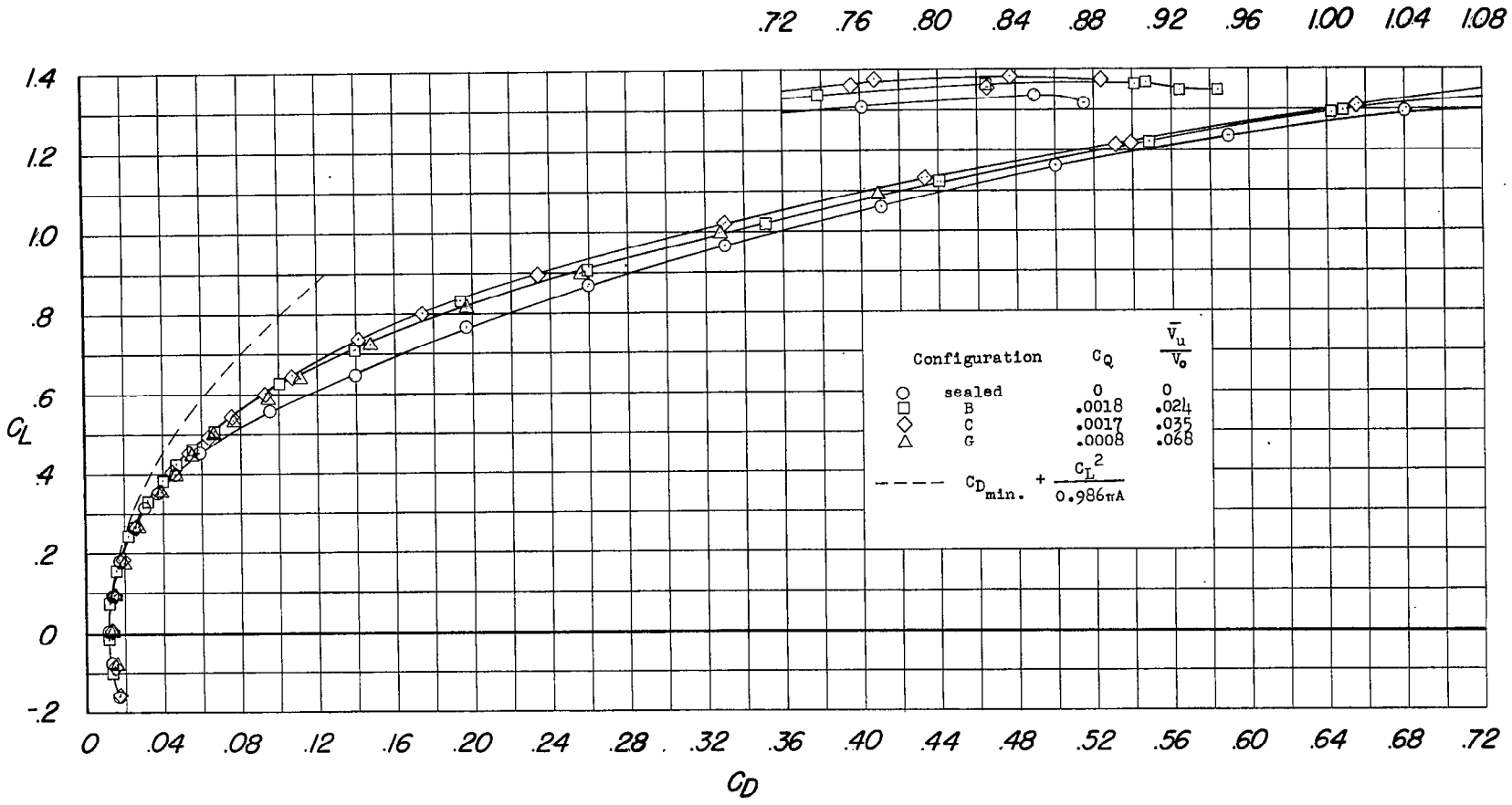

Figure 6.- Effect of suction on the drag of the delta wing at $M = 0.12$; $R = 10.4 \times 10^6$. (Insert shows maximum lift.) Pump-power equivalent drag not included.

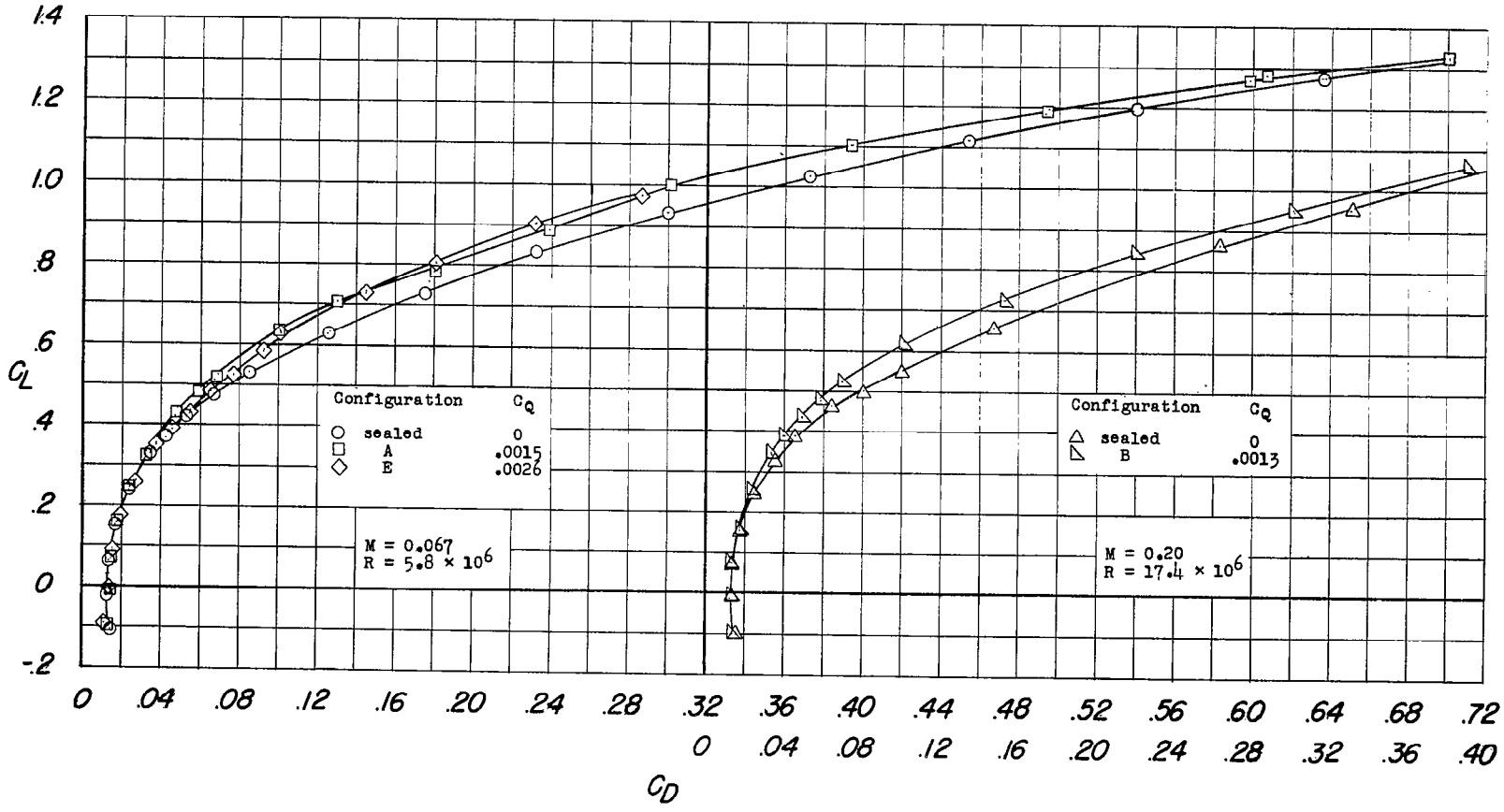

Figure 7.- Effect of suction on the drag of the delta wing at M = 0.067 and M = 0.20. Pump-power equivalent drag not included.

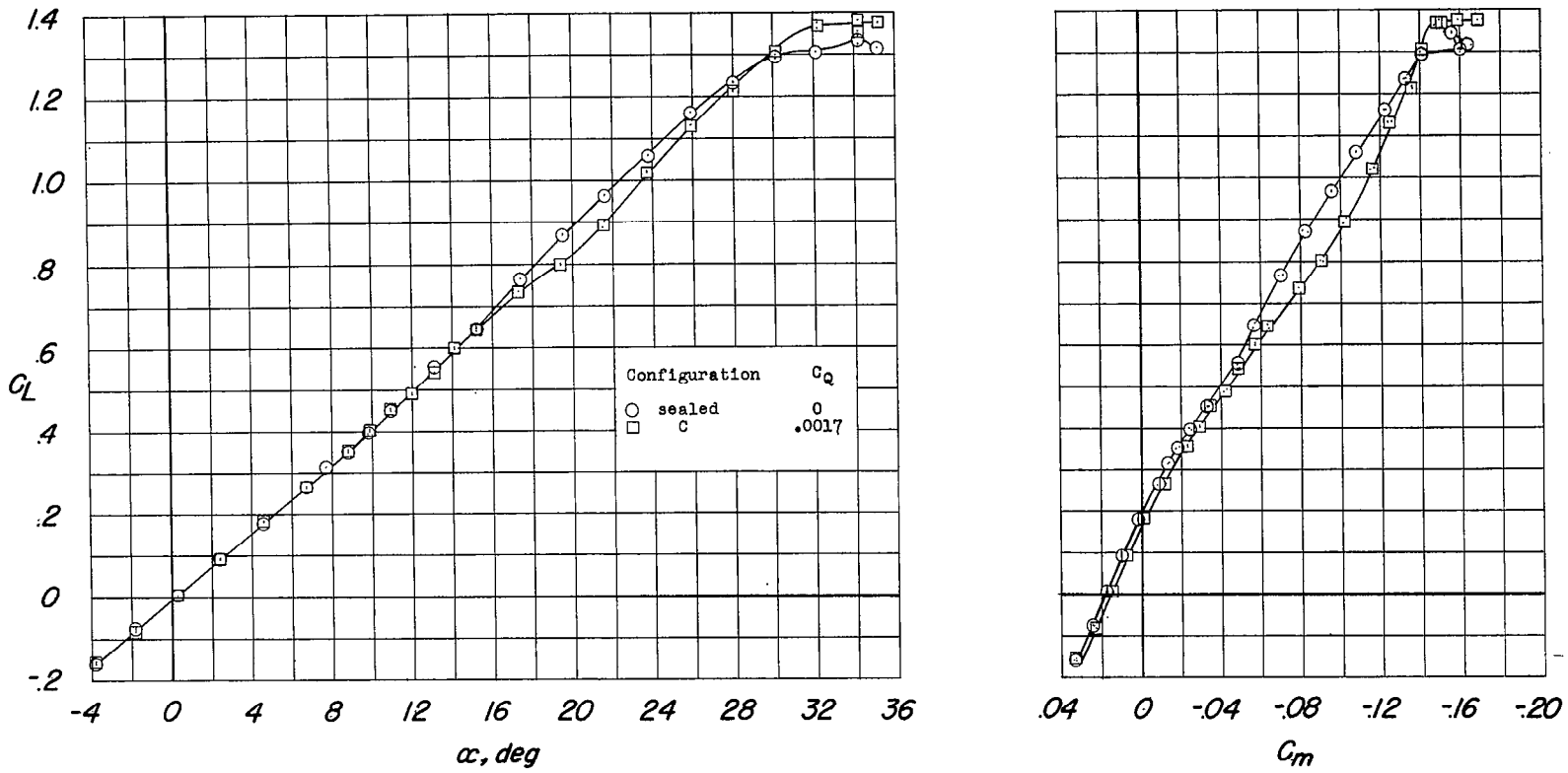

Figure 8.- Effect of suction on the lift and pitching-moment characteristics of the delta wing. M = 0.12; R = 10.4×10^6.

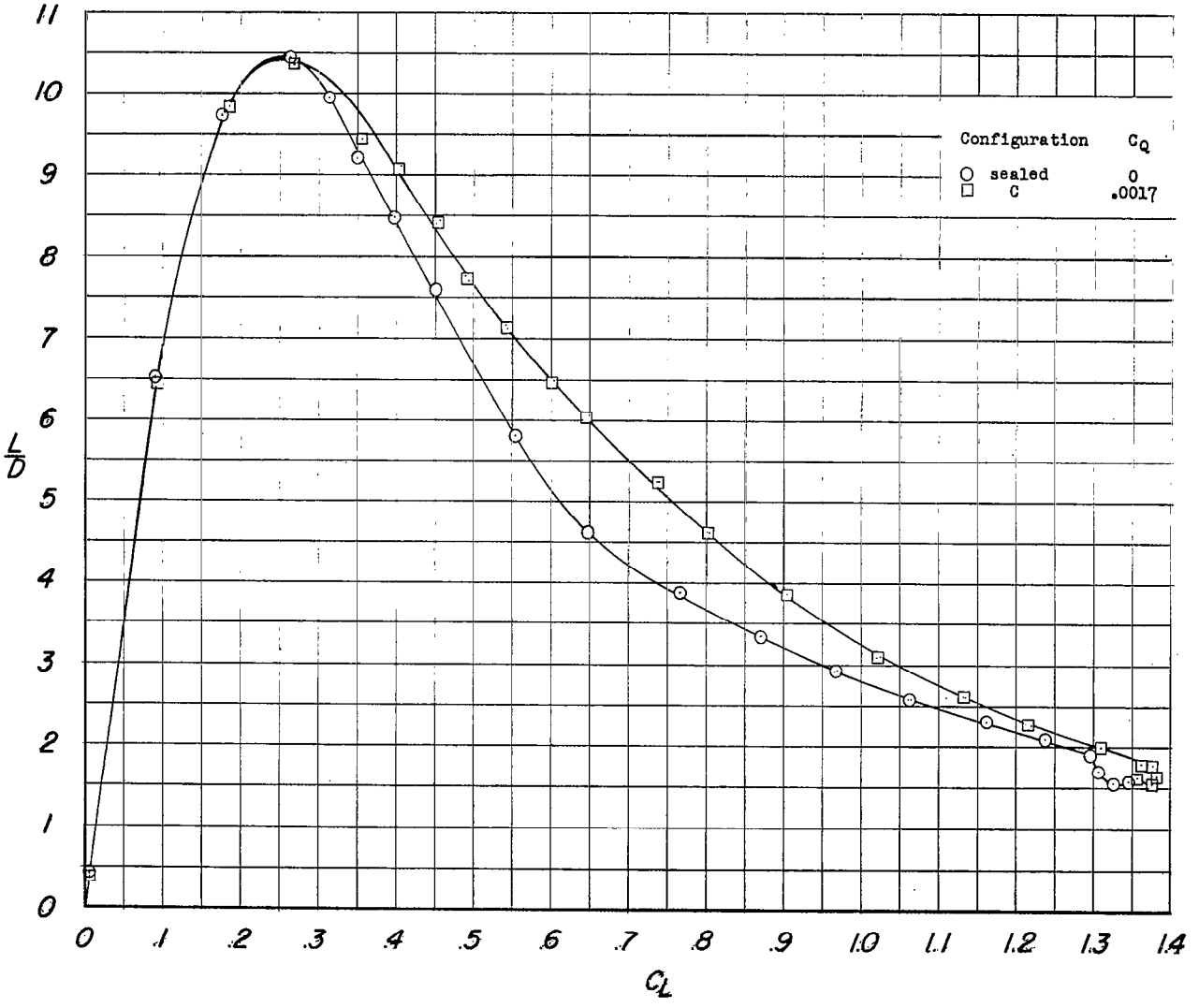

Figure 9.- Effect of suction on lift-drag ratio of delta wing. M = 0.12; R = 10.4×10^6. Pump-power equivalent drag not included.

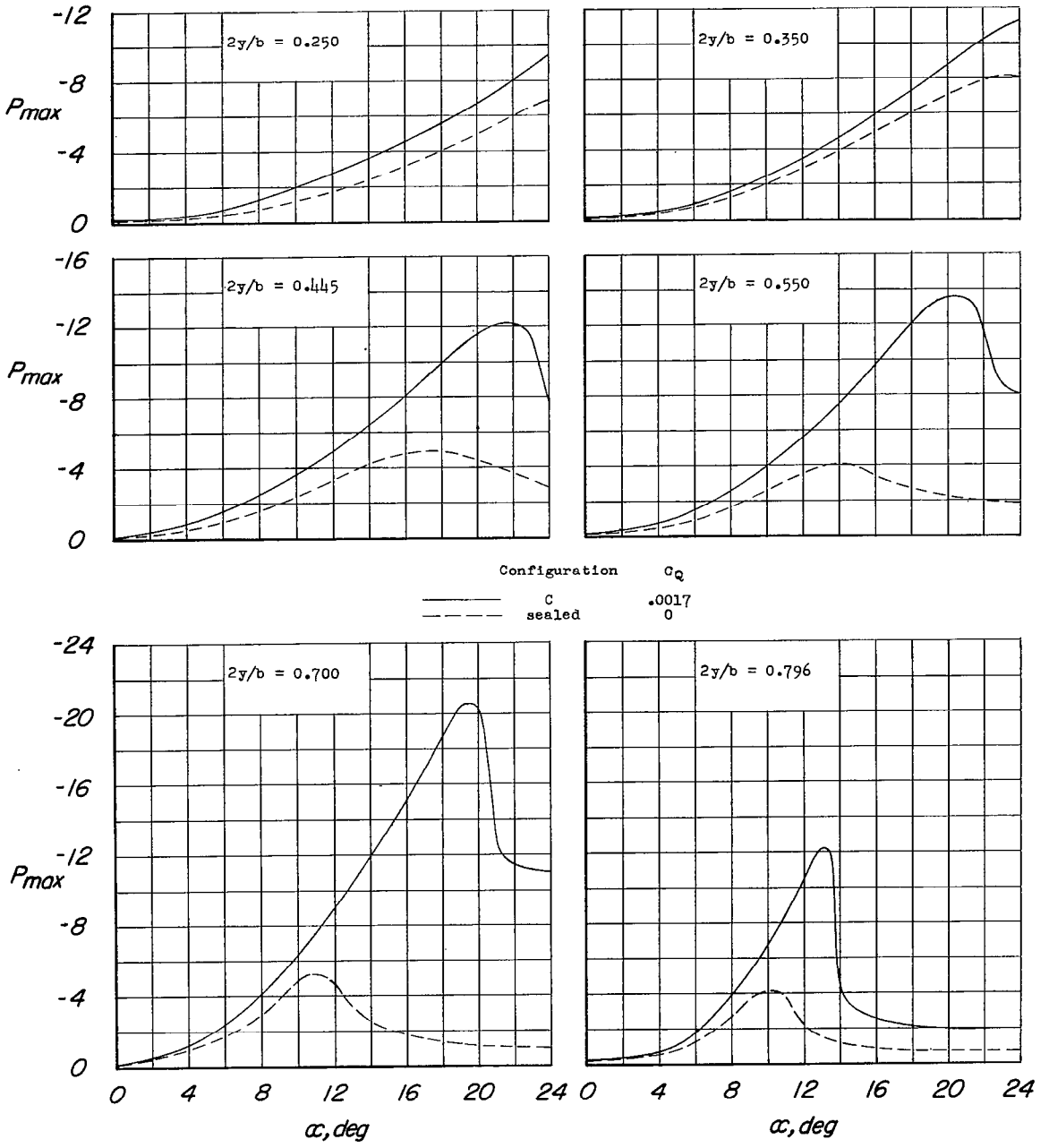

Figure 10.- Effect of suction on peak measured pressure at several spanwise stations on the delta wing. $x/c = 0.001$; $M = 0.12$; $R = 10.4 \times 10^6$.

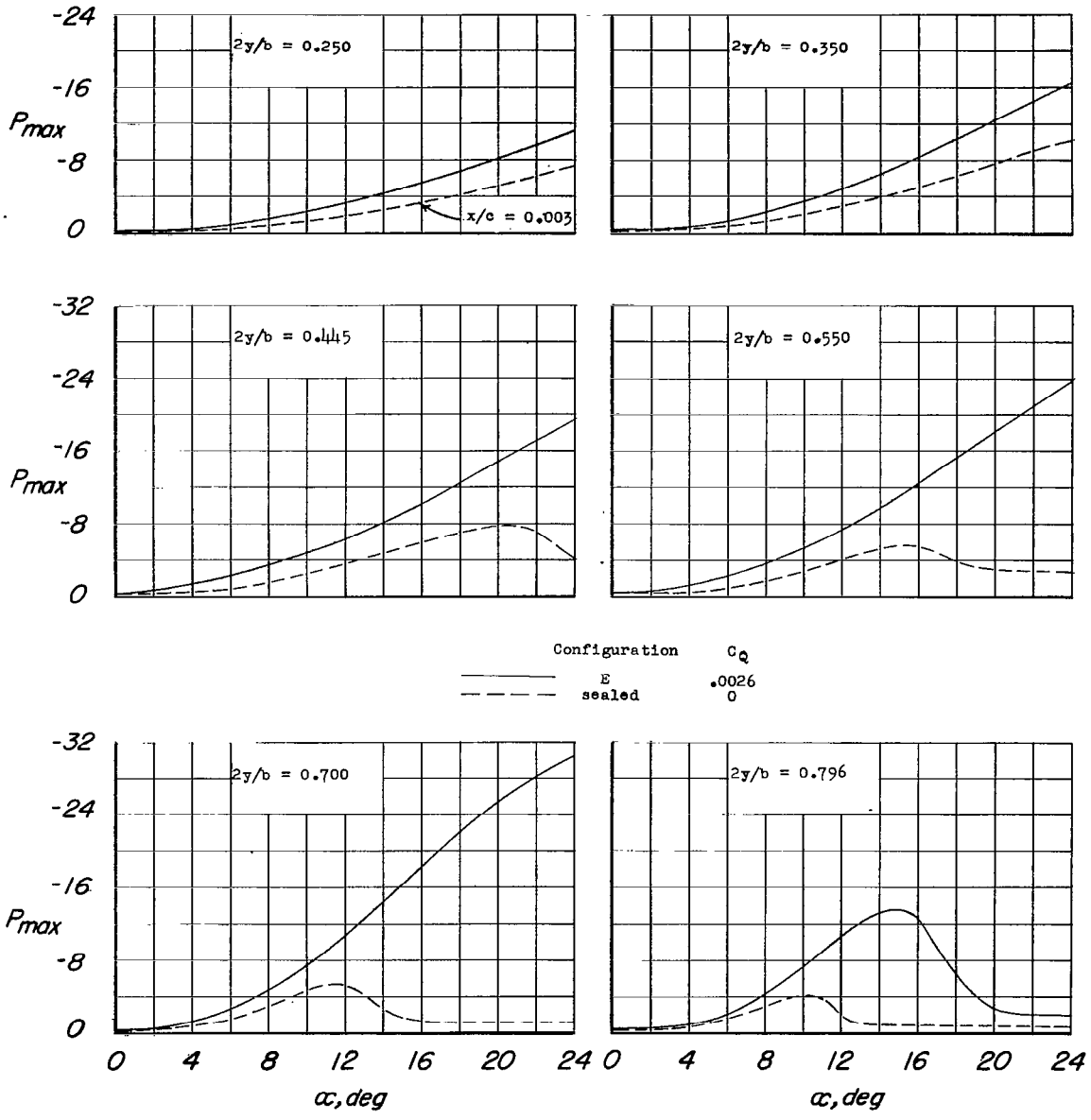

Figure 11.- Effect of suction on peak measured pressure at several spanwise stations on the delta wing. $x/c = 0.001$; $M = 0.067$; $R = 5.8 \times 10^6$.

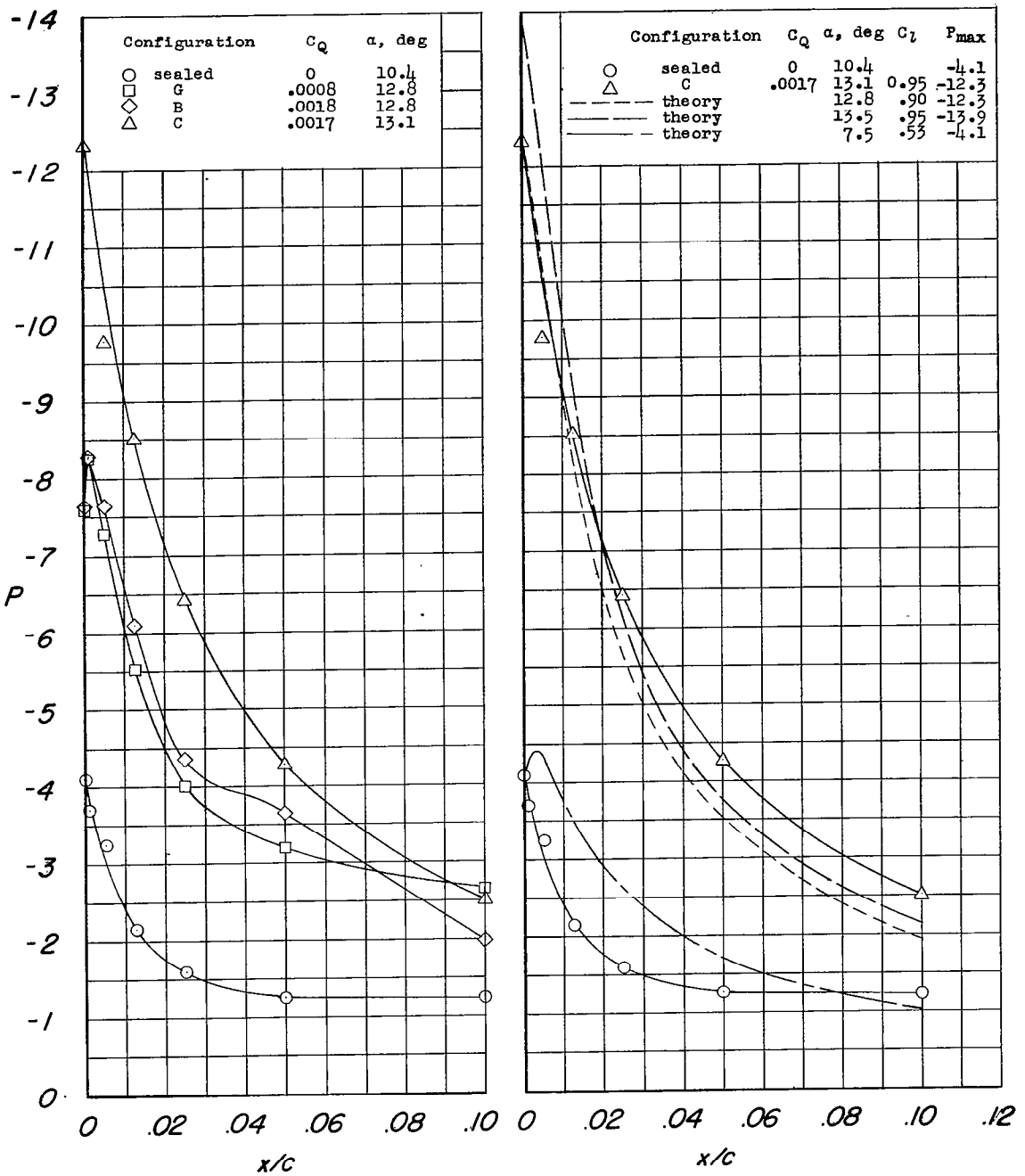

(a) Comparison of leading-edge configurations.

(b) Comparison of experiment with combined two-dimensional and simple sweep theory.

Figure 12.- Delta-wing pressure distribution at $2y/b = 0.796$ at angle of attack for which maximum pressure peak occurs. $M = 0.12$; $R = 10.4 \times 10^6$.

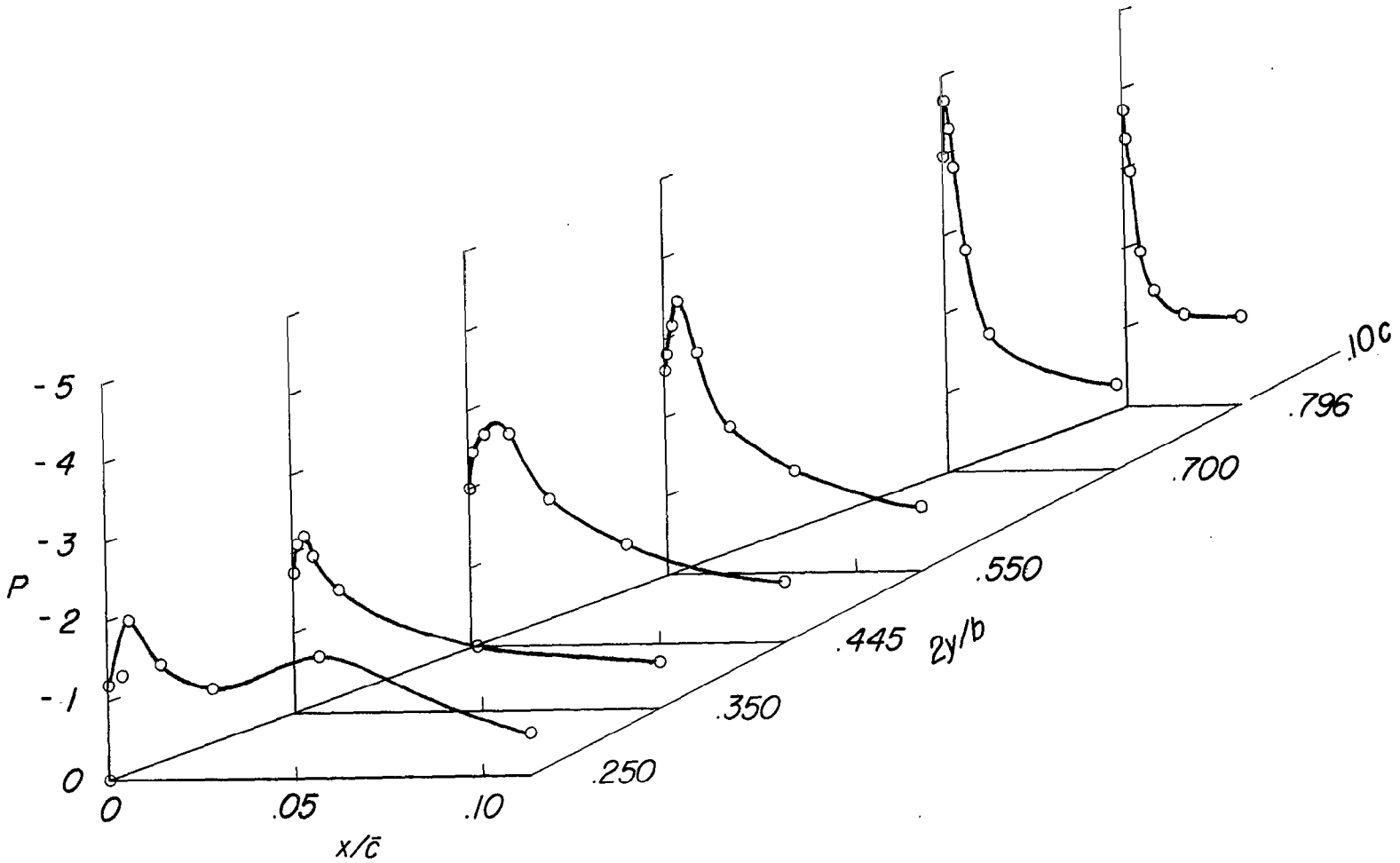

(a) $\alpha = 10.4^{\circ}$.

Figure 13.- Pressure distribution on the leading-edge upper surface of the delta wing. Leading edge sealed; M = 0.12; R = 10.4 × 10^6.

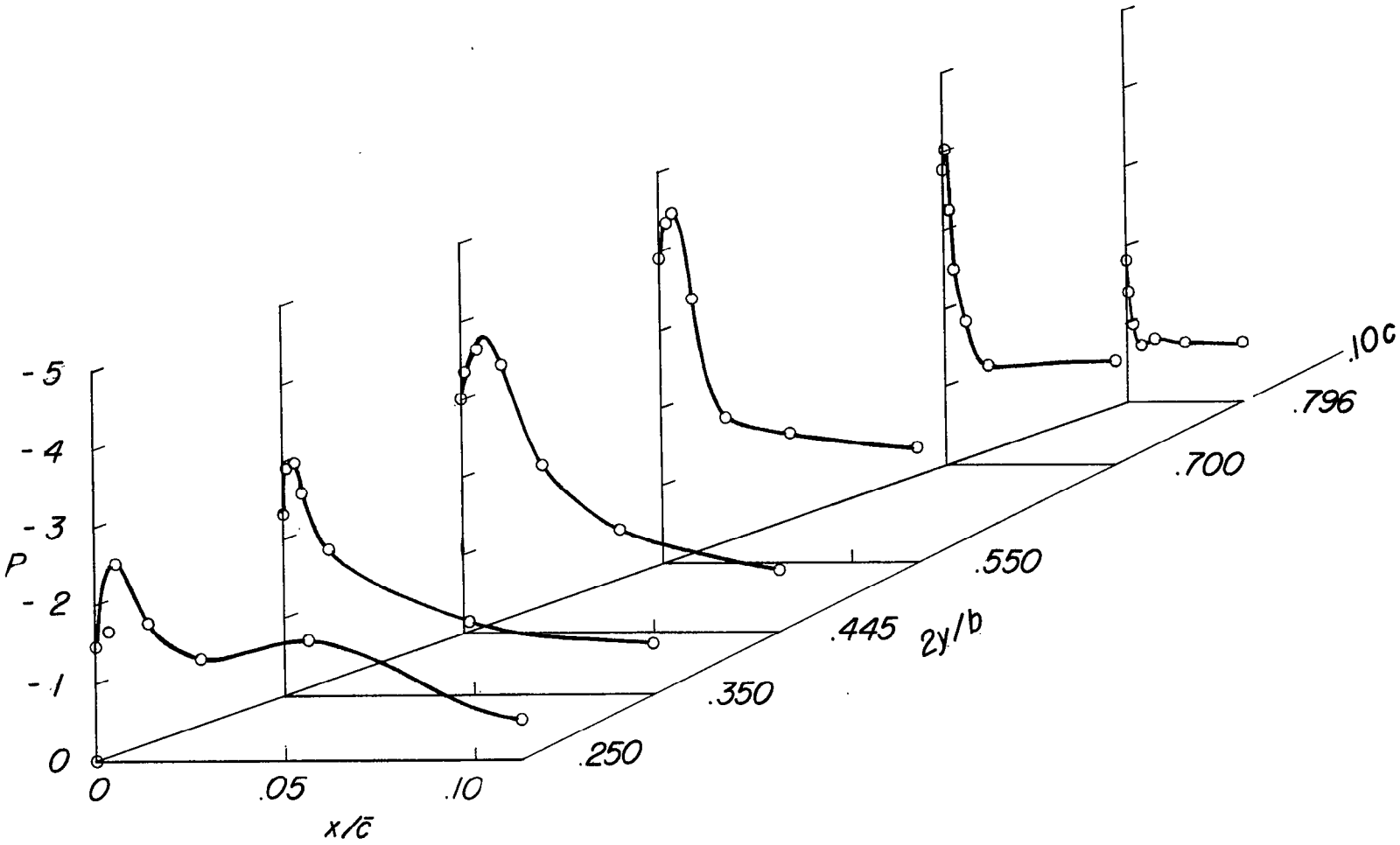

(b) $\alpha = 12.5^{\circ}$.

Figure 13.- Continued.

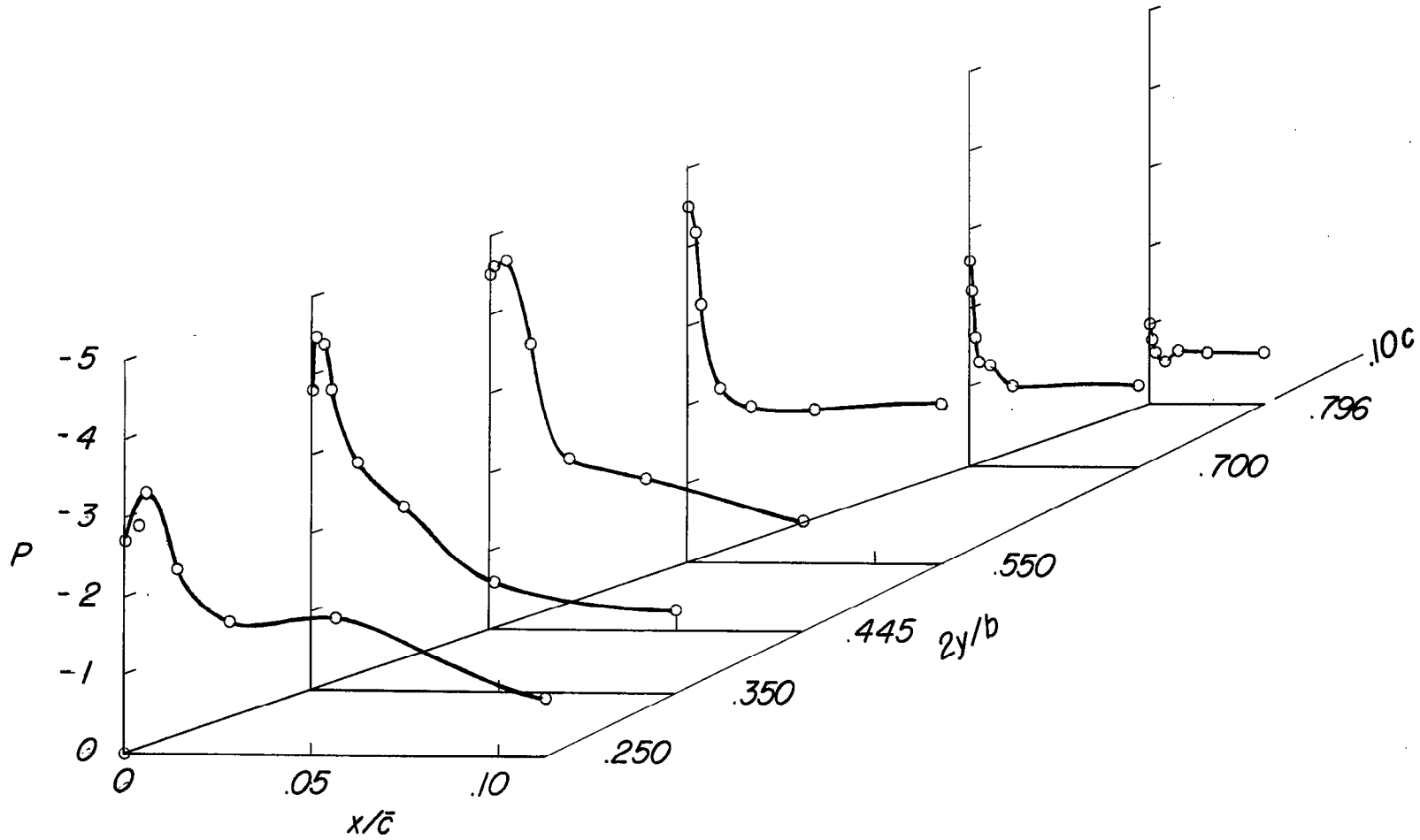

(c) $\alpha = 14.7^{\circ}$.

Figure 13.- Continued.

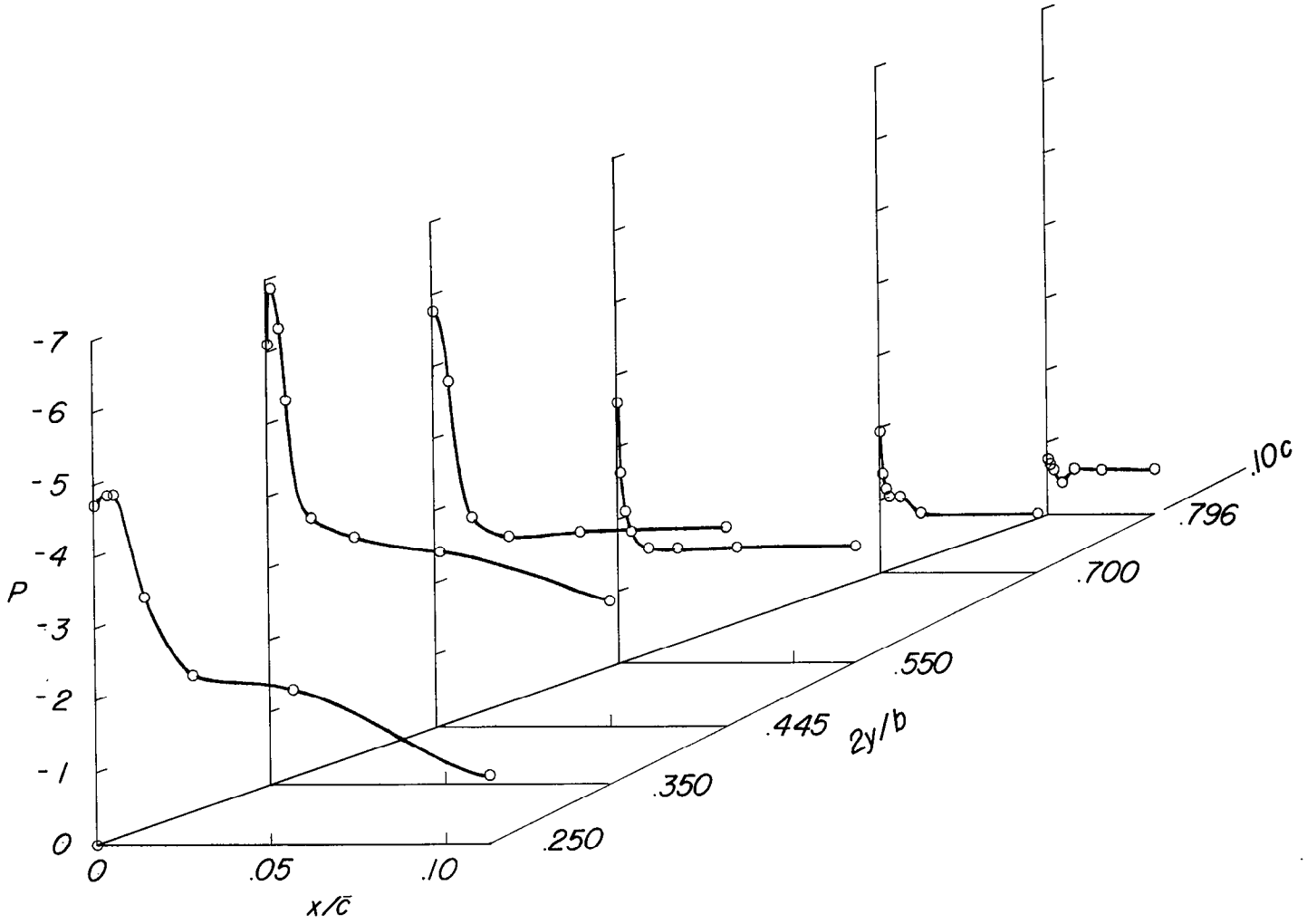

(d) $\alpha = 19.0^{\circ}$.

Figure 13.- Continued.

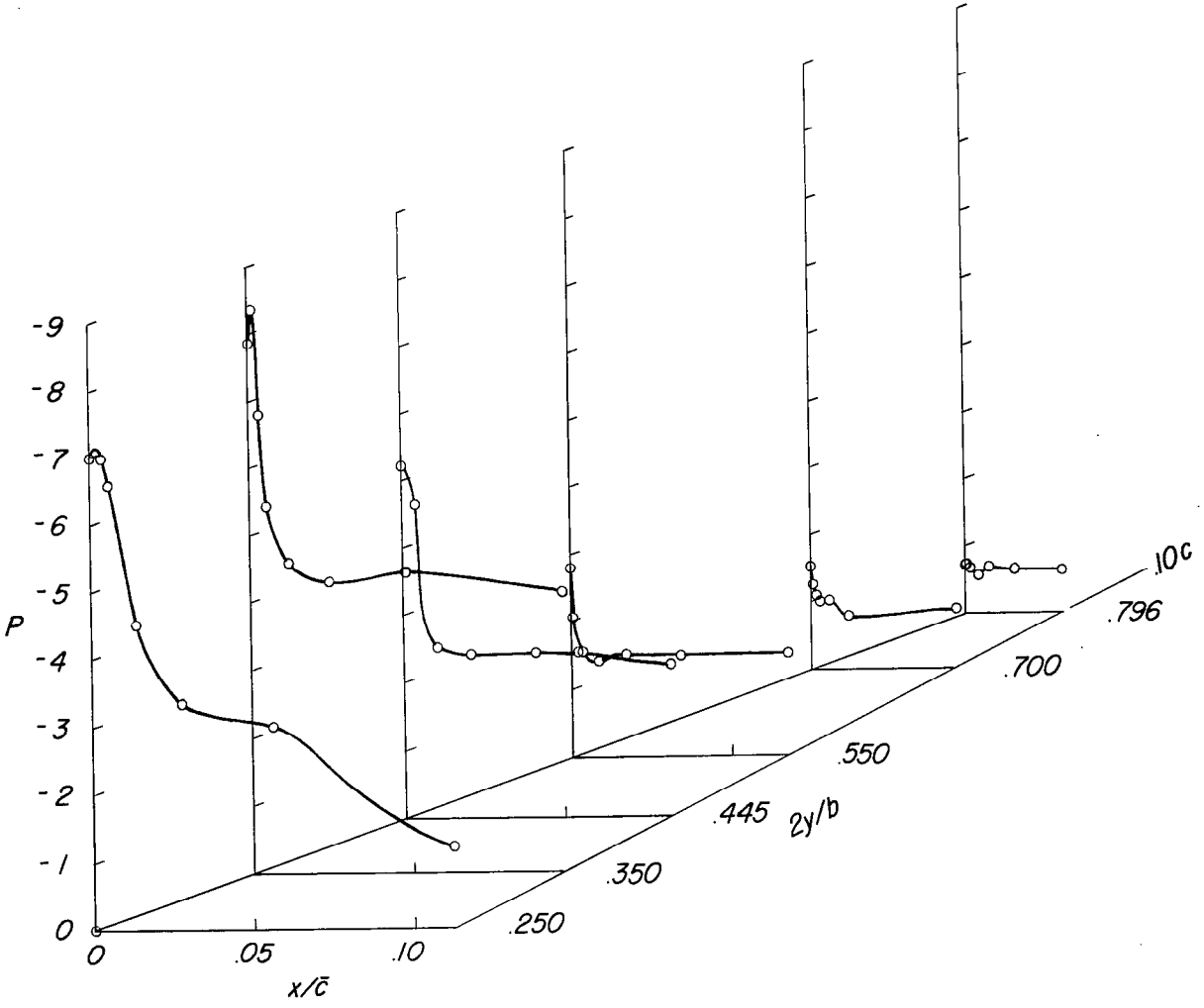

(e) $\alpha = 23.2^{\circ}$.

Figure 13.- Concluded.

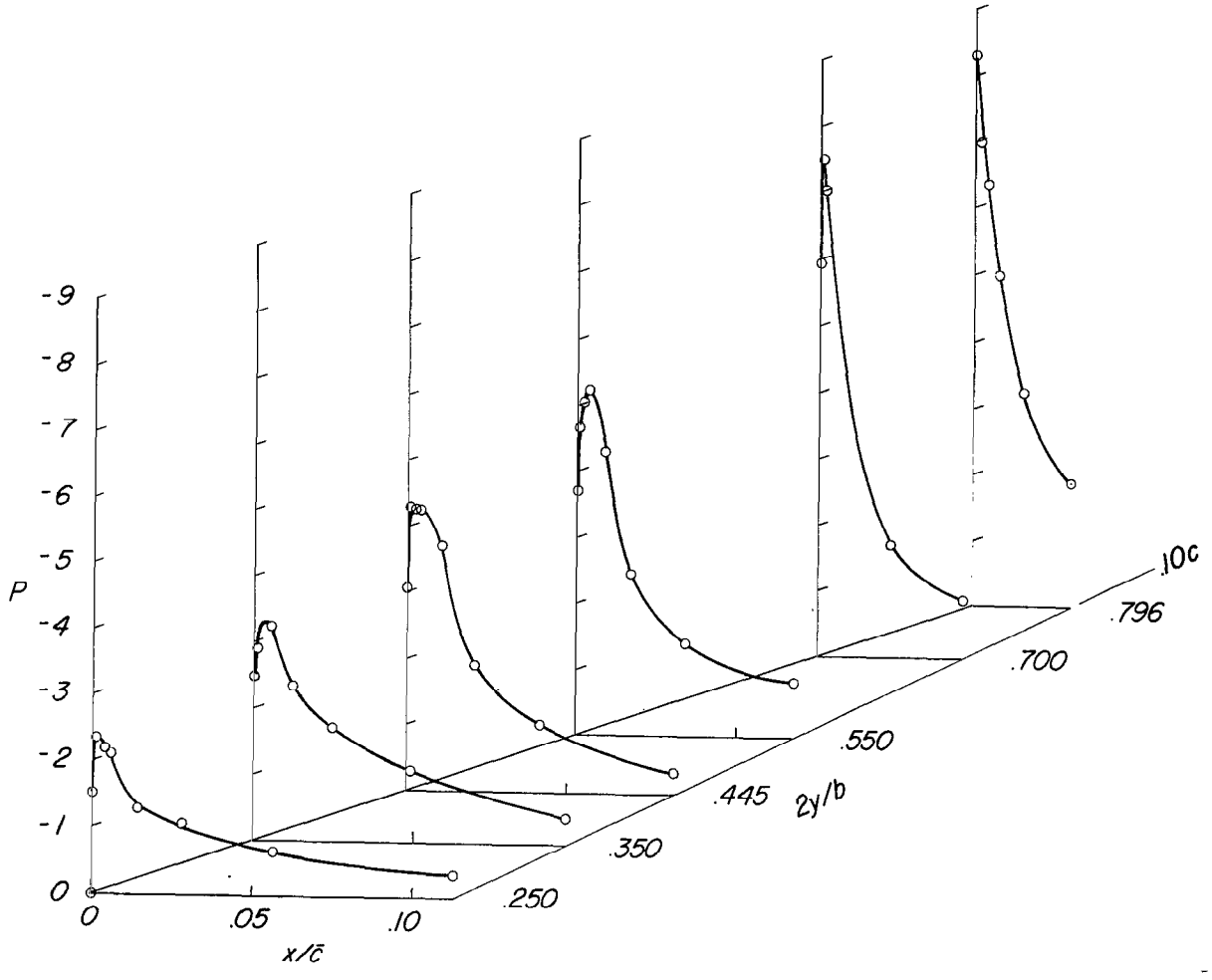

(a) $\alpha = 10.9^{\circ}$.

Figure 14.- Pressure distribution on the leading-edge upper surface of the delta wing. Configuration C; $C_Q = 0.0017$; $M = 0.12$; $R = 10.4 \times 10^6$.

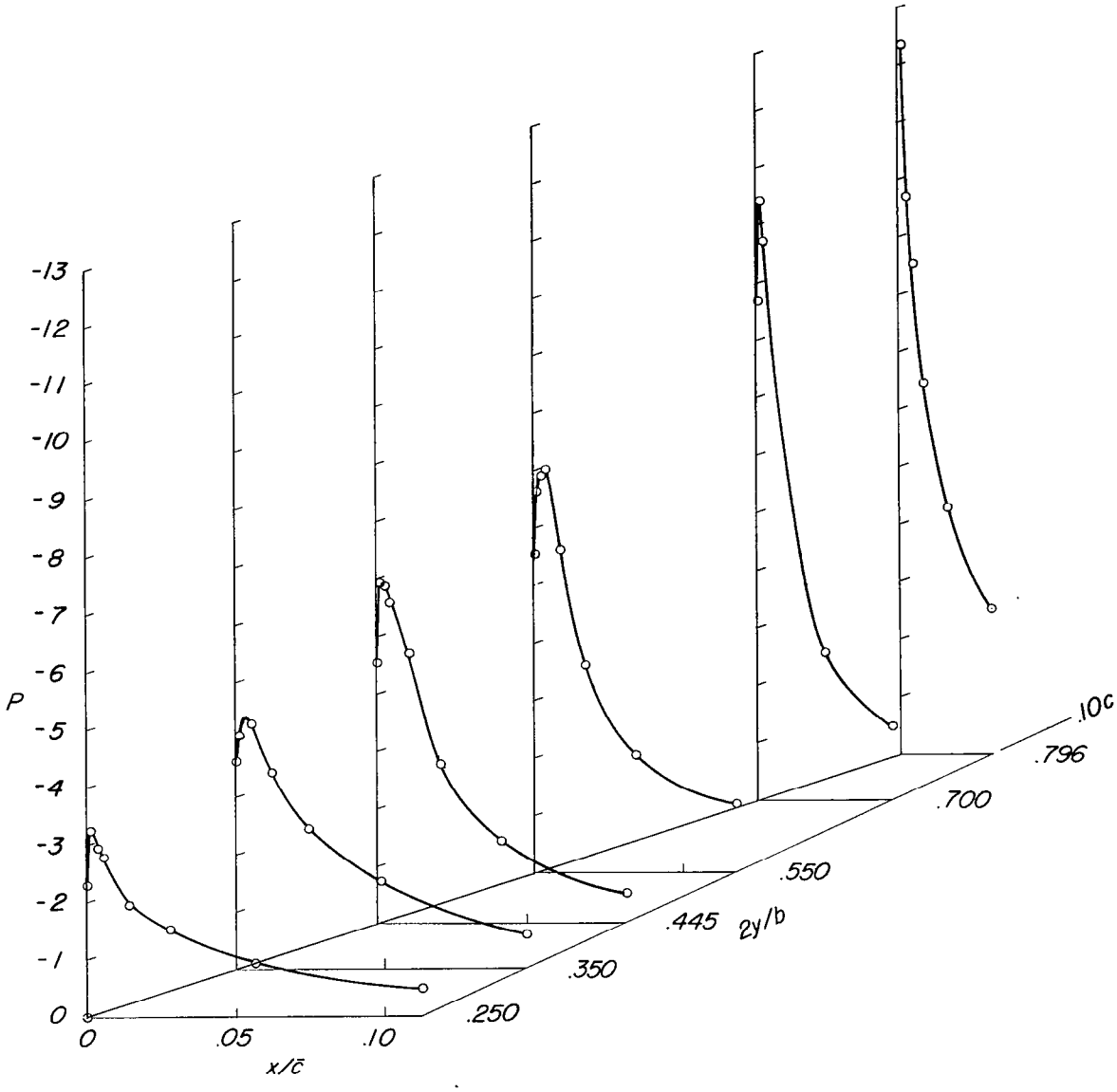

(b) $\alpha = 13.0^{\circ}$.

Figure 14.- Continued.

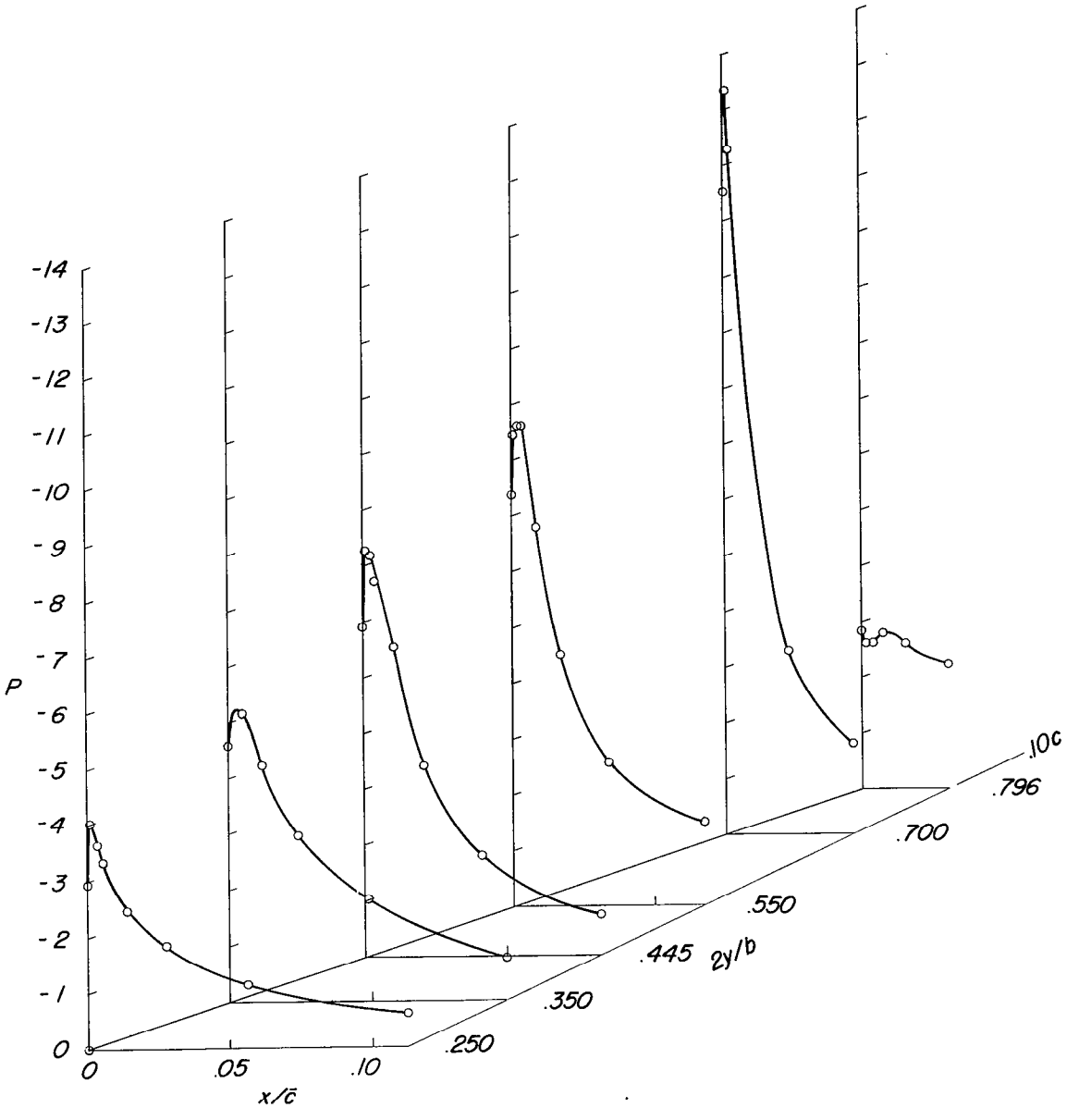

(c) $\alpha = 15.2^{\circ}$.

Figure 14.- Continued.

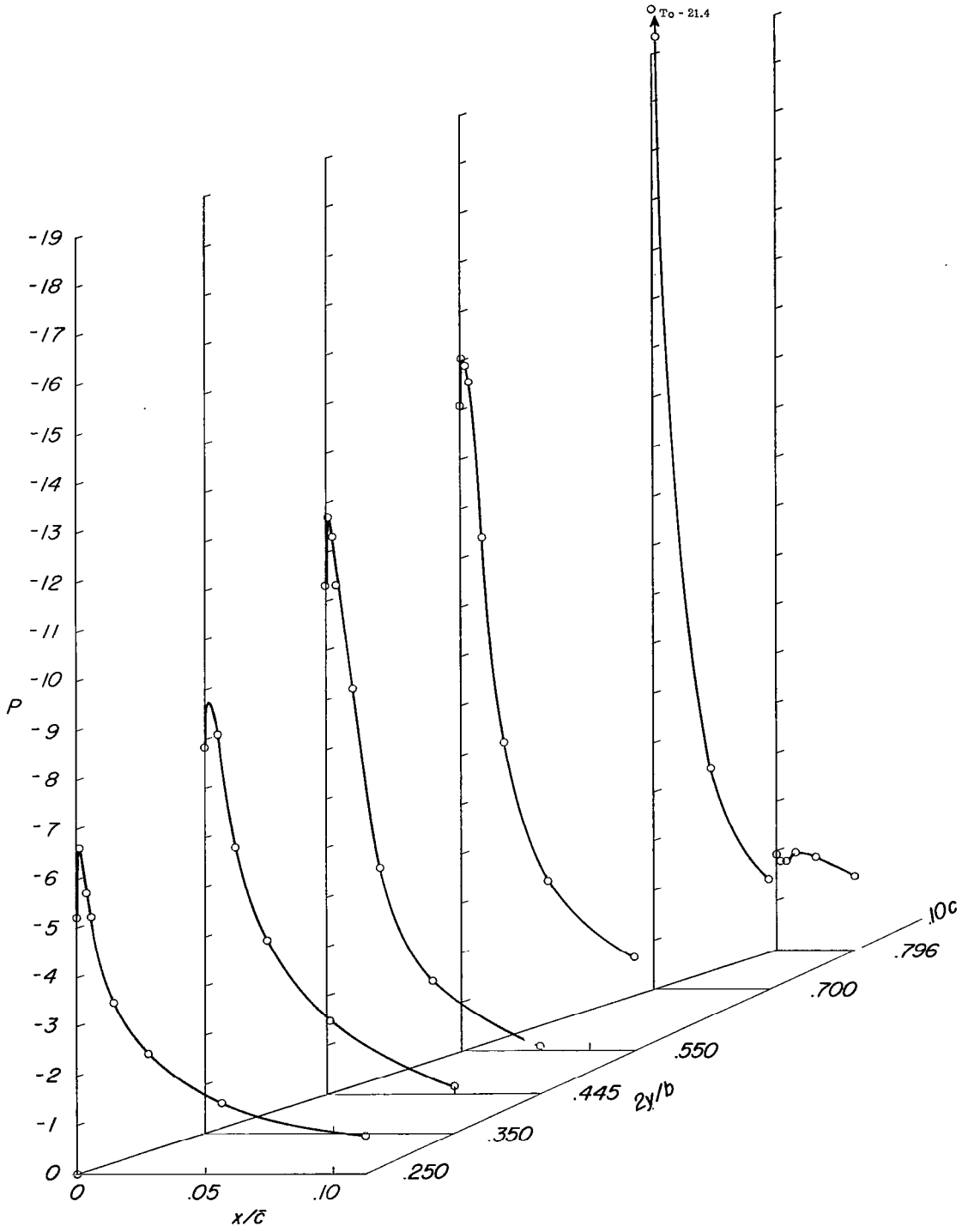

(d) $\alpha = 19.4^{\circ}$.

Figure 14.- Continued.

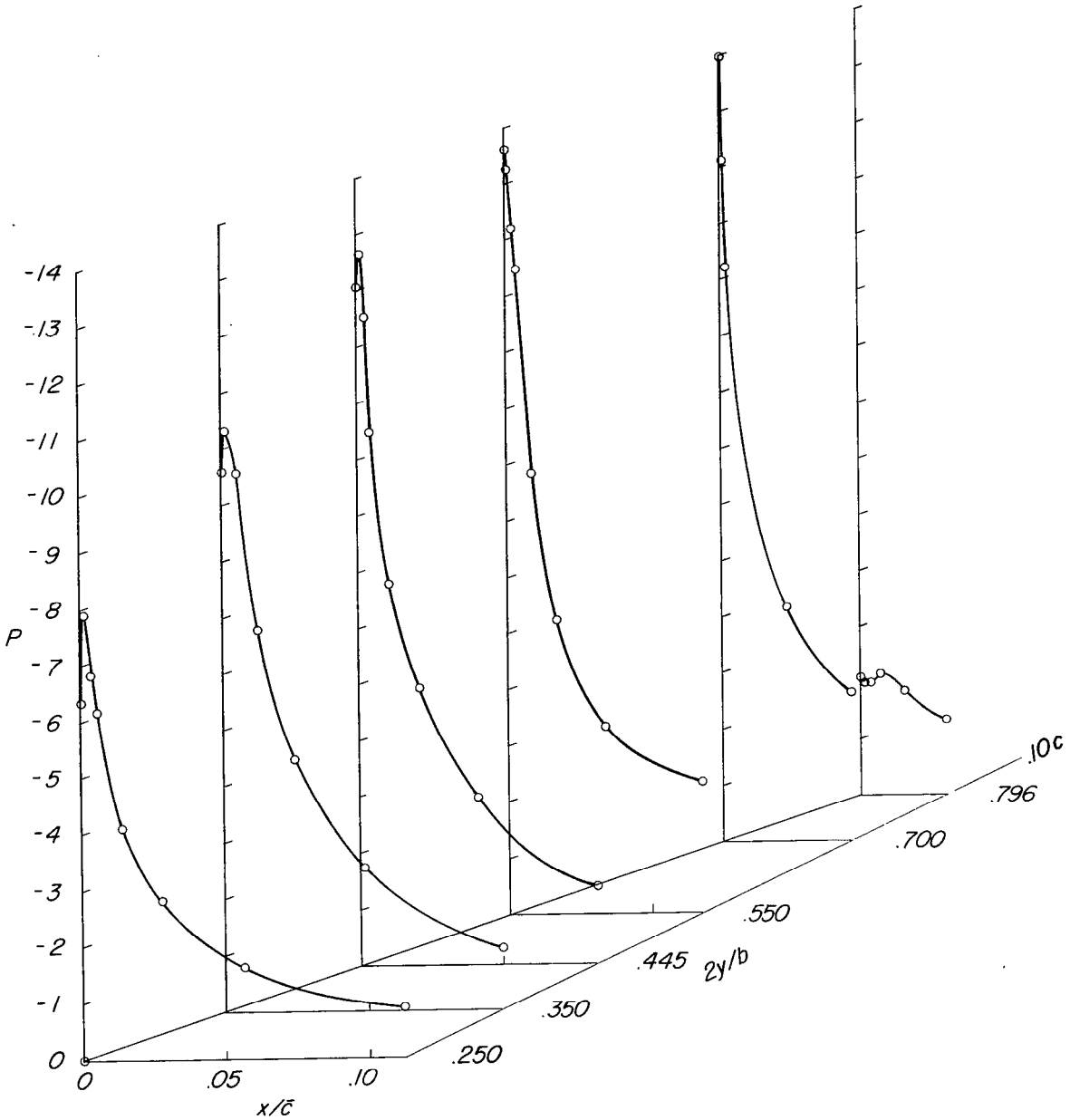

(e) $\alpha = 21.6^{\circ}$.

Figure 14.- Concluded.

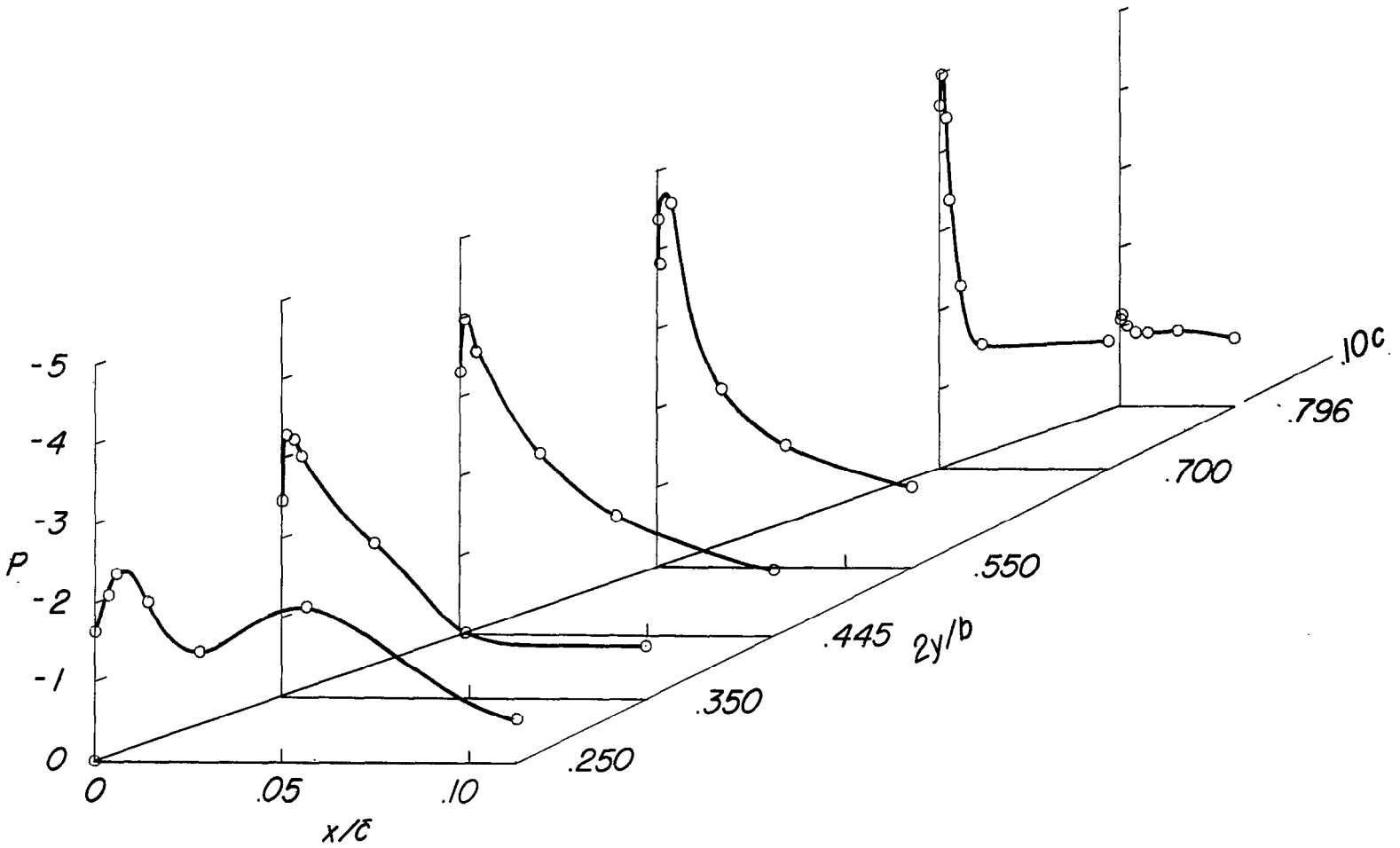

(a) $\alpha = 12.5^{\circ}$.

Figure 15.- Pressure distribution on the leading-edge upper surface of the delta wing. Leading edge sealed; $M = 0.067$; $R = 5.8 \times 10^{6}$.

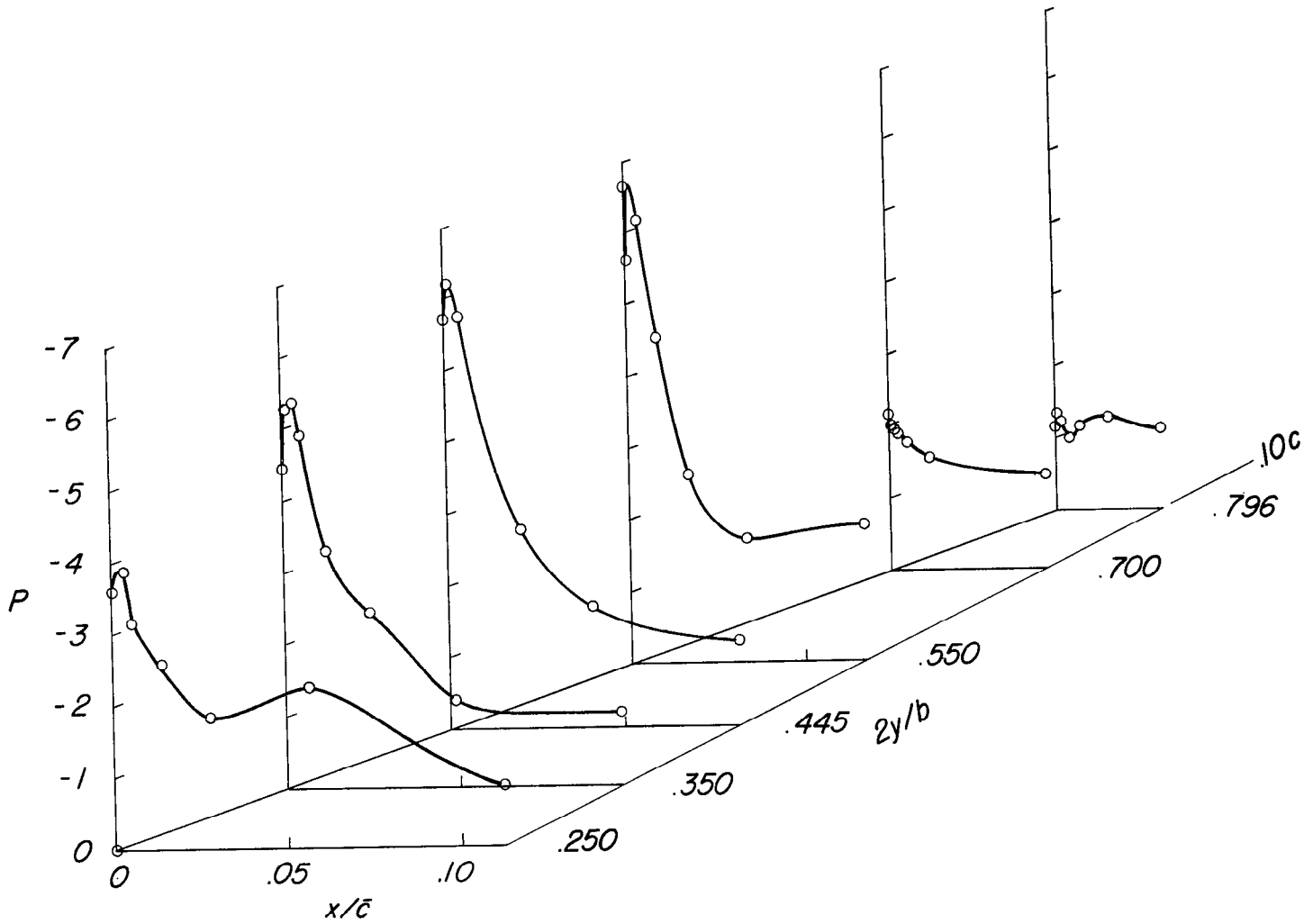

(b) $\alpha = 14.7^{\circ}$.

Figure 15.- Continued.

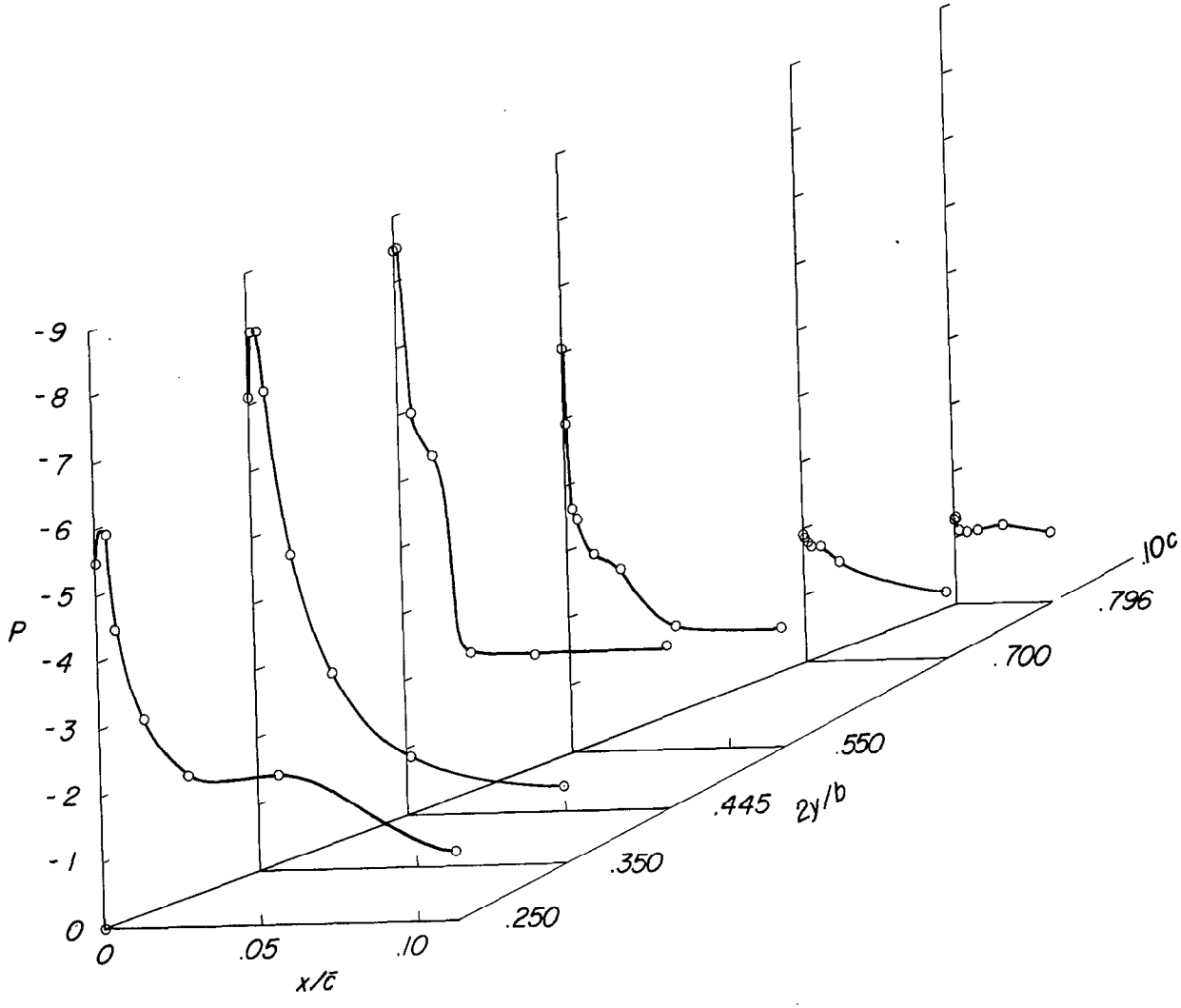

(c) $\alpha = 19.0^{\circ}$.

Figure 15.- Continued.

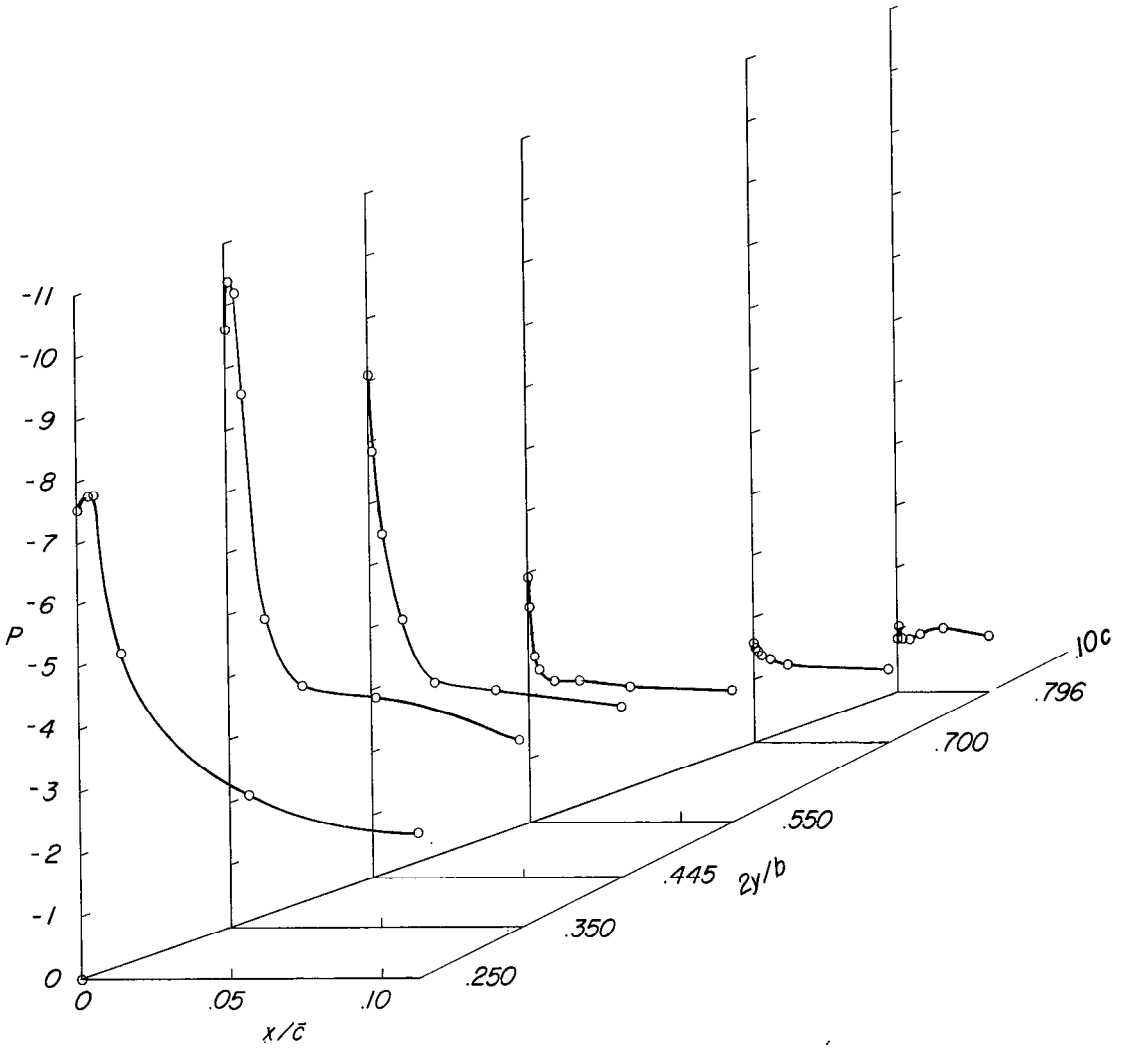

(d) $\alpha = 23.2^{\circ}$.

Figure 15.- Concluded.

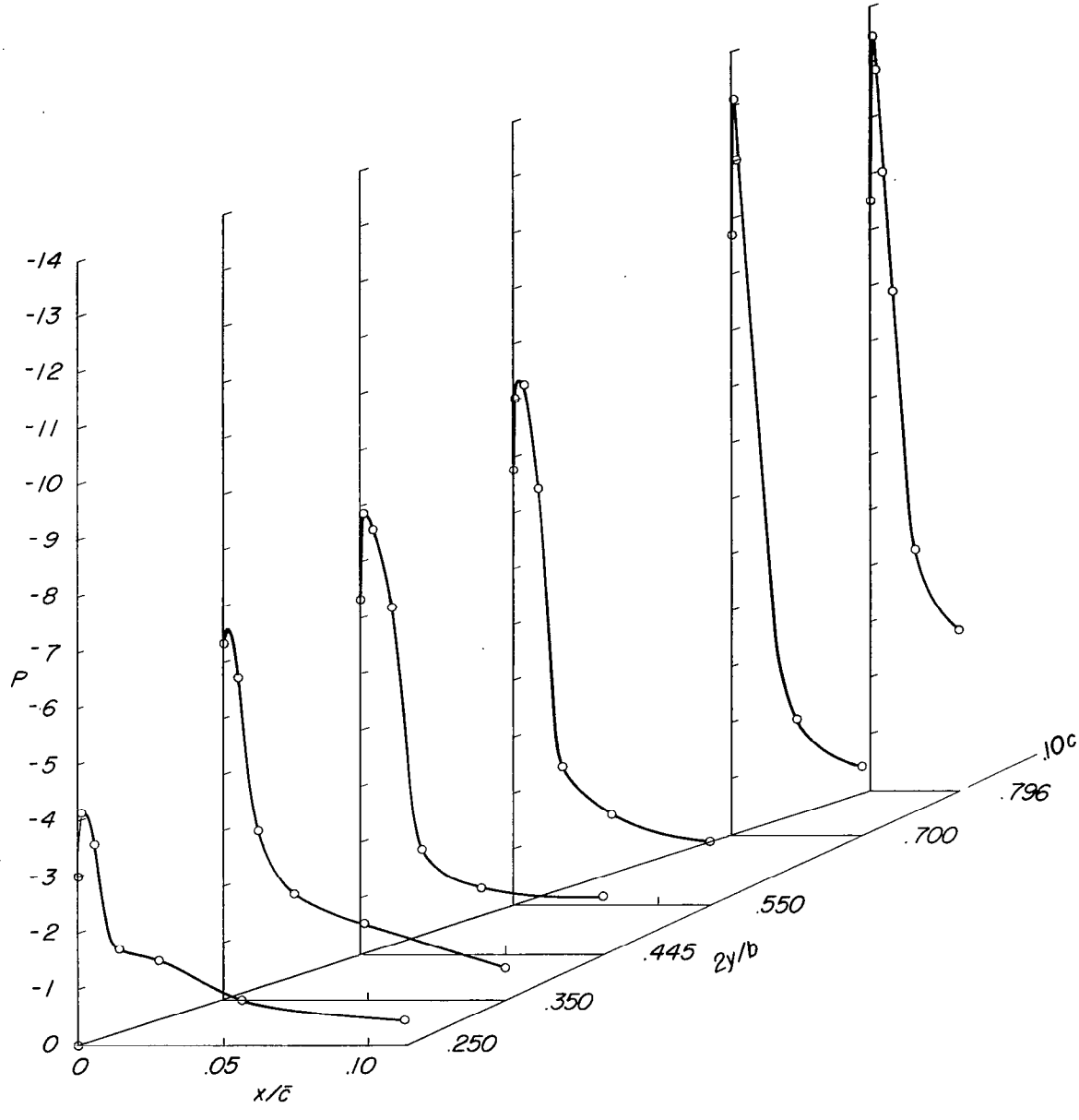

(a) $\alpha = 13.0^{\circ}$.

Figure 16.- Pressure distribution on the leading-edge upper surface of the delta wing. Configuration E; $C_Q = 0.0026$; $M = 0.067$; $R = 5.8 \times 10^6$.

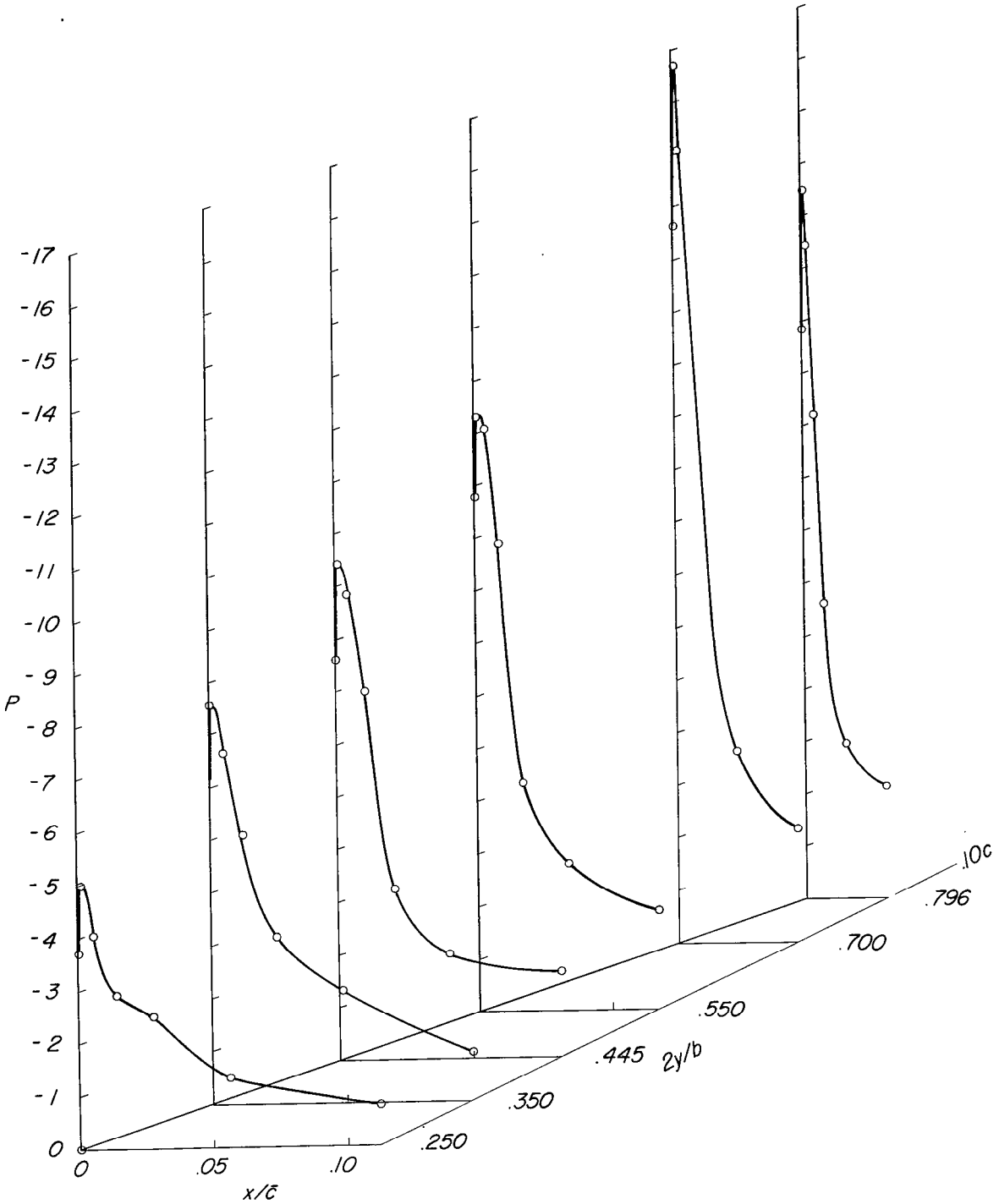

(b) $\alpha = 15.2^{\circ}$.

Figure 16.- Continued.

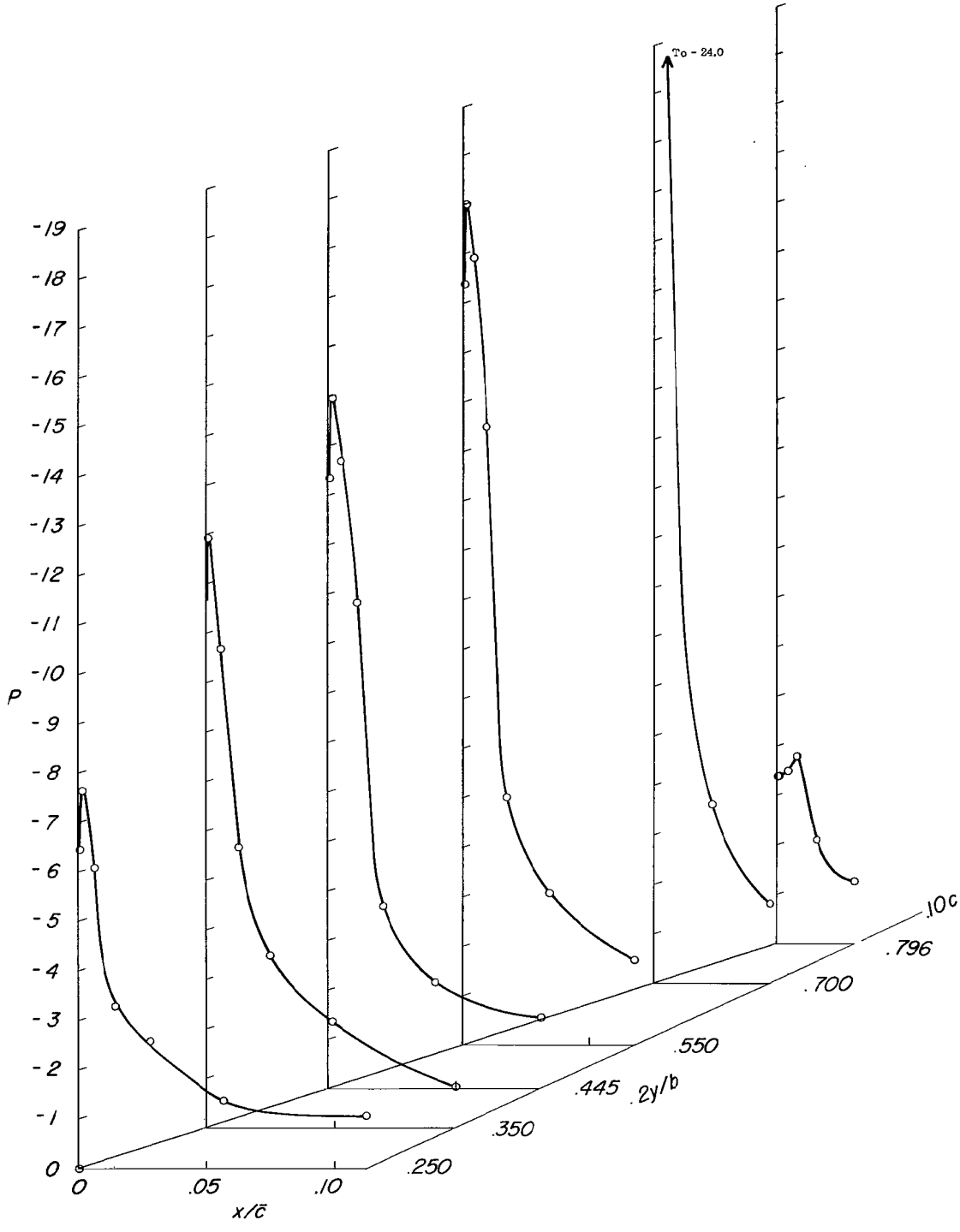

(c) $\alpha = 19.4^{\circ}$.

Figure 16.- Continued.

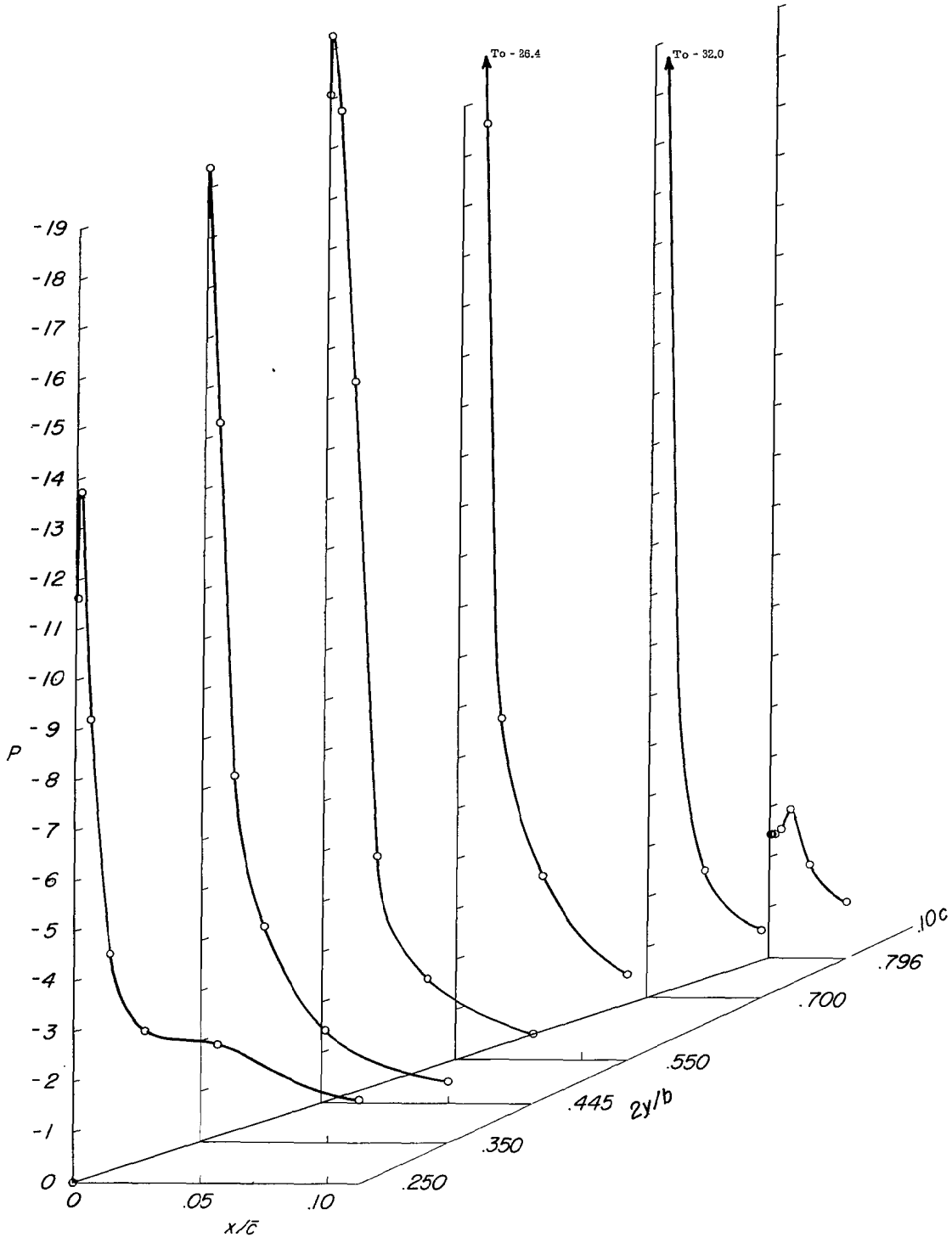

(d) $\alpha = 25.8^{\circ}$.

Figure 16.- Concluded.

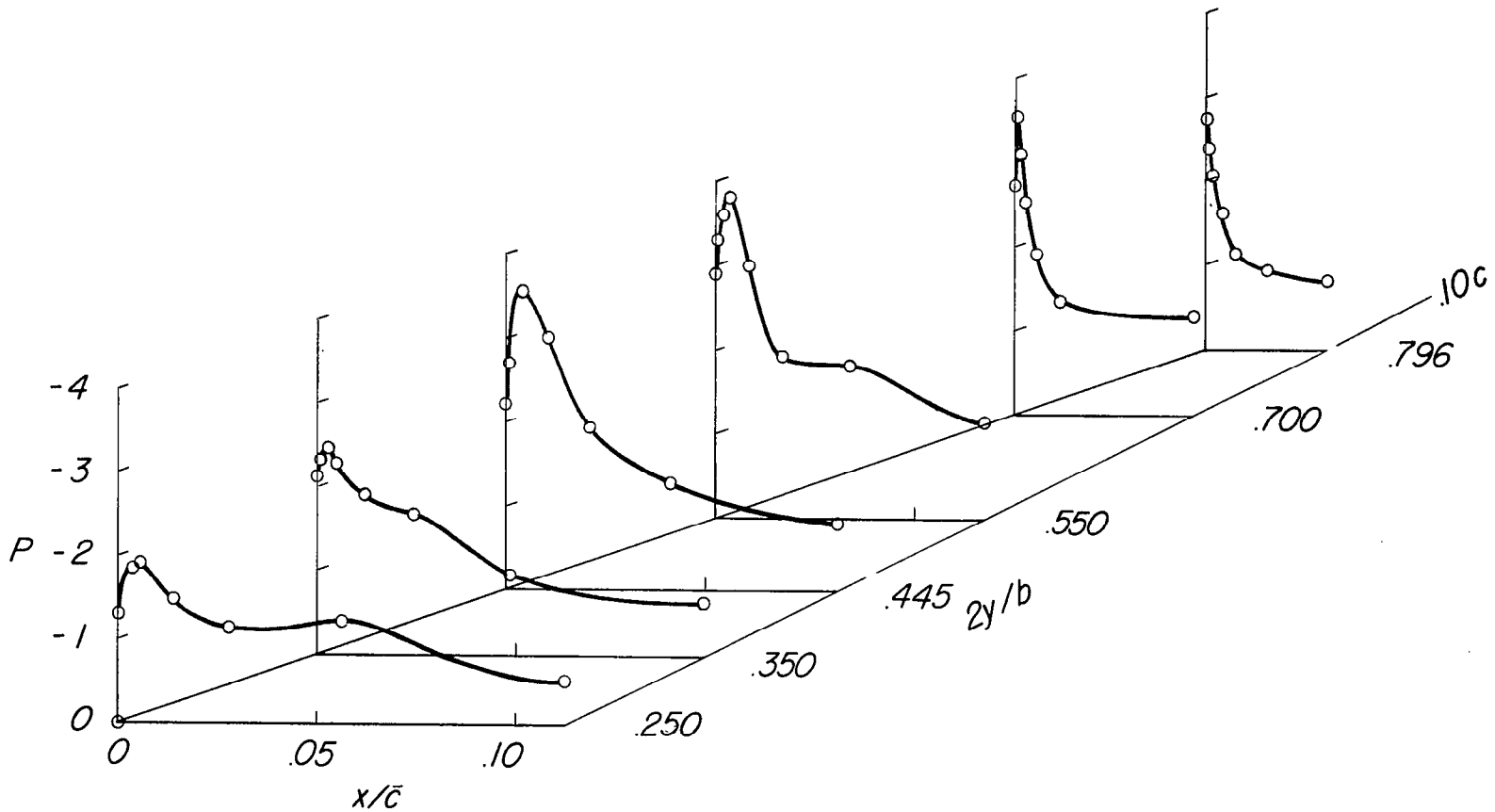

(a) $\alpha = 10.4^{\circ}$.

Figure 17.- Pressure distribution on the leading-edge upper surface of the delta wing. Leading edge sealed; M = 0.20; R = 17.4×10^{6}.

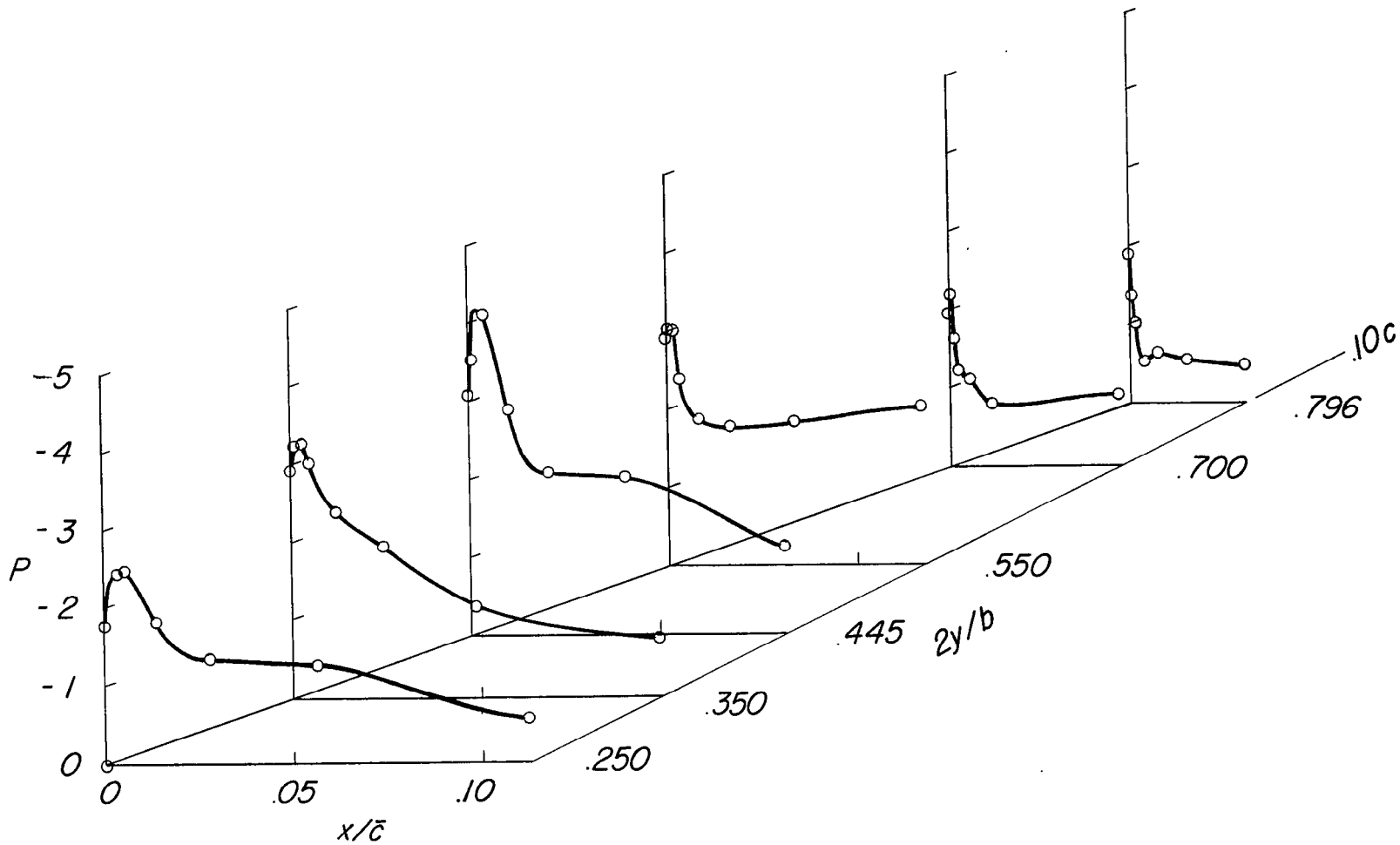

(b) $\alpha = 12.5^{\circ}$.

Figure 17.- Continued.

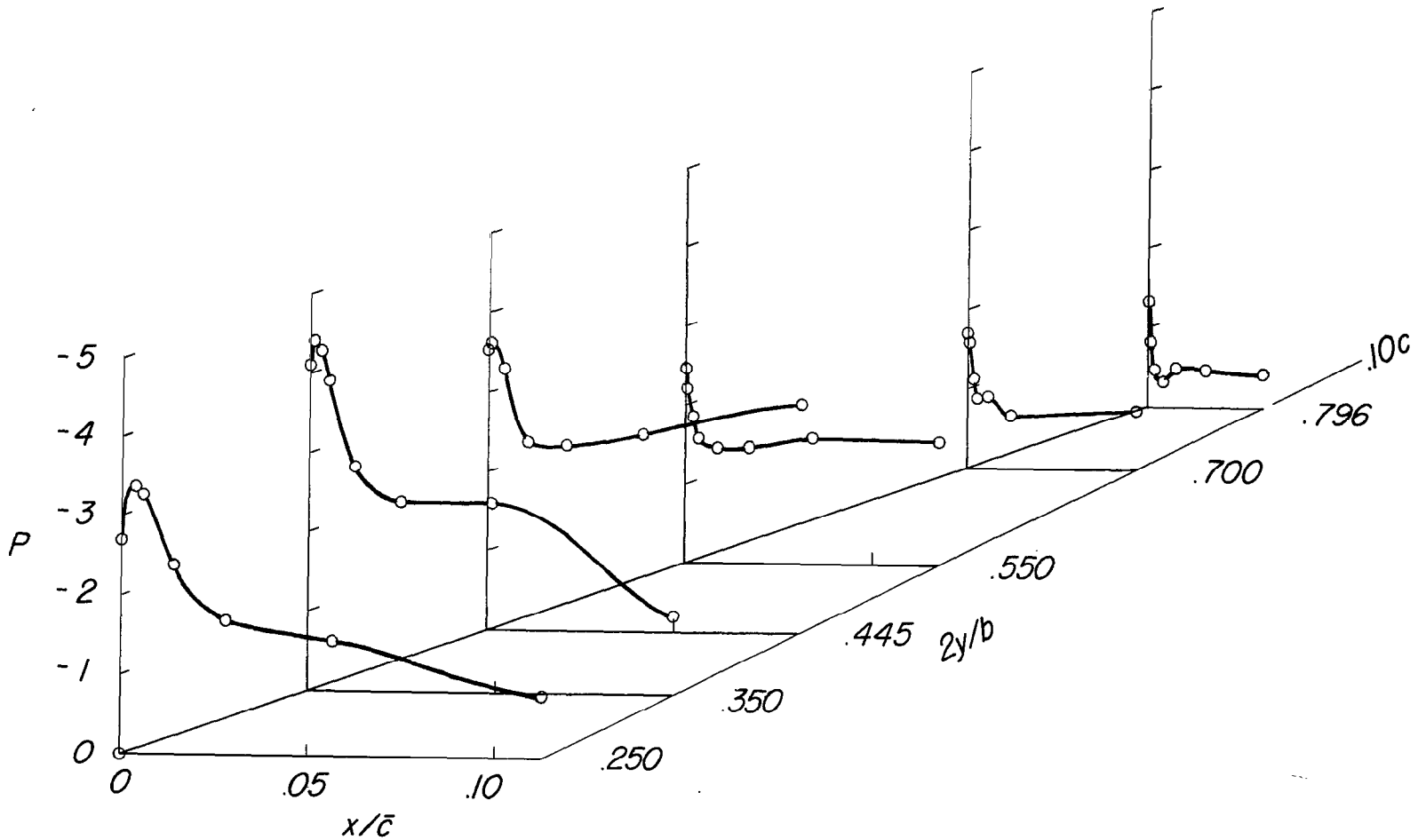

(c) $\alpha = 14.7^{\circ}$.

Figure 17.- Concluded.

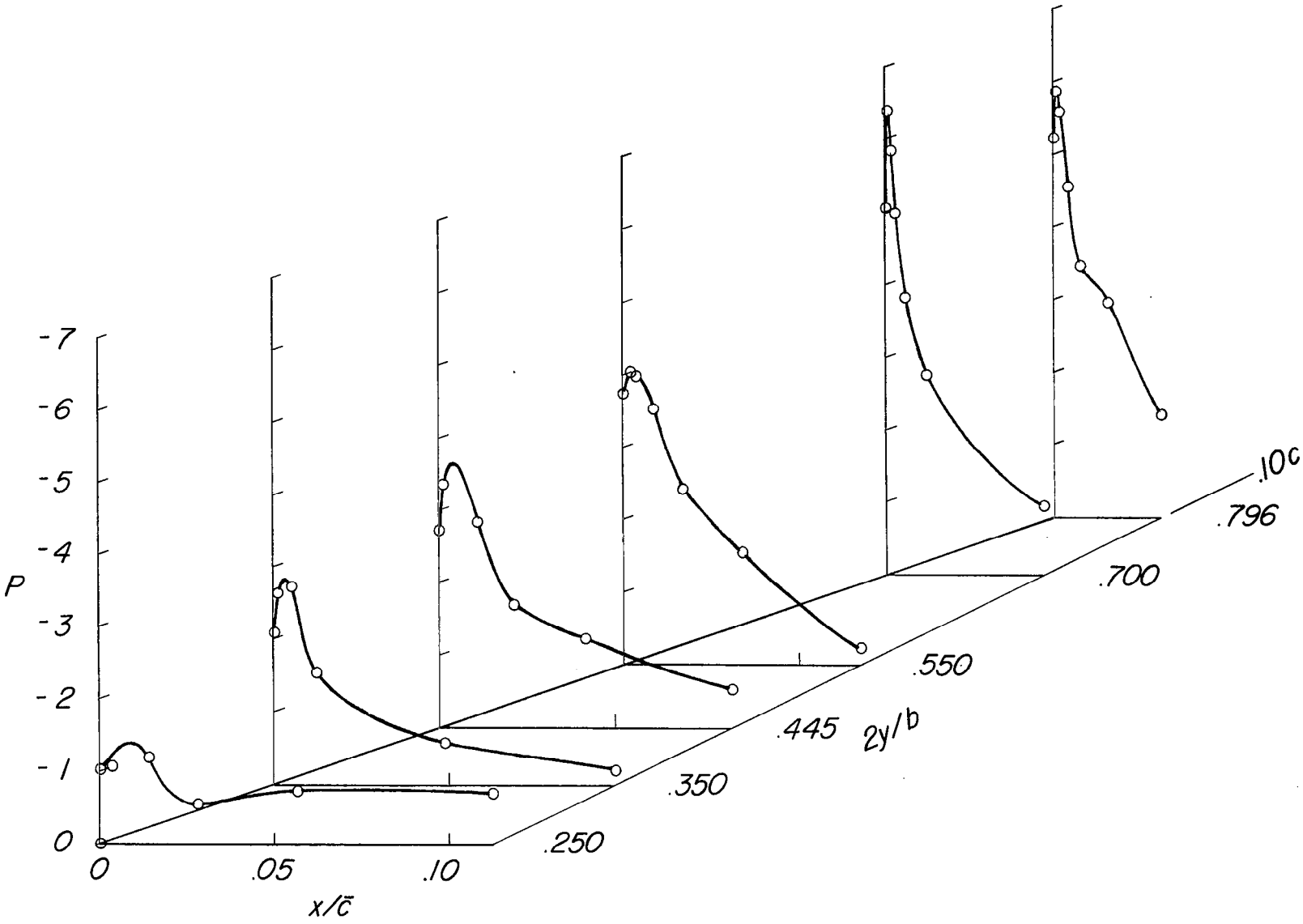

(a) $\alpha = 10.4^{\circ}$.

Figure 18.- Pressure distribution on the leading-edge upper surface of the delta wing. Configuration B; $C_Q = 0.0013$; $M = 0.20$; $R = 1.7 \times 10^6$

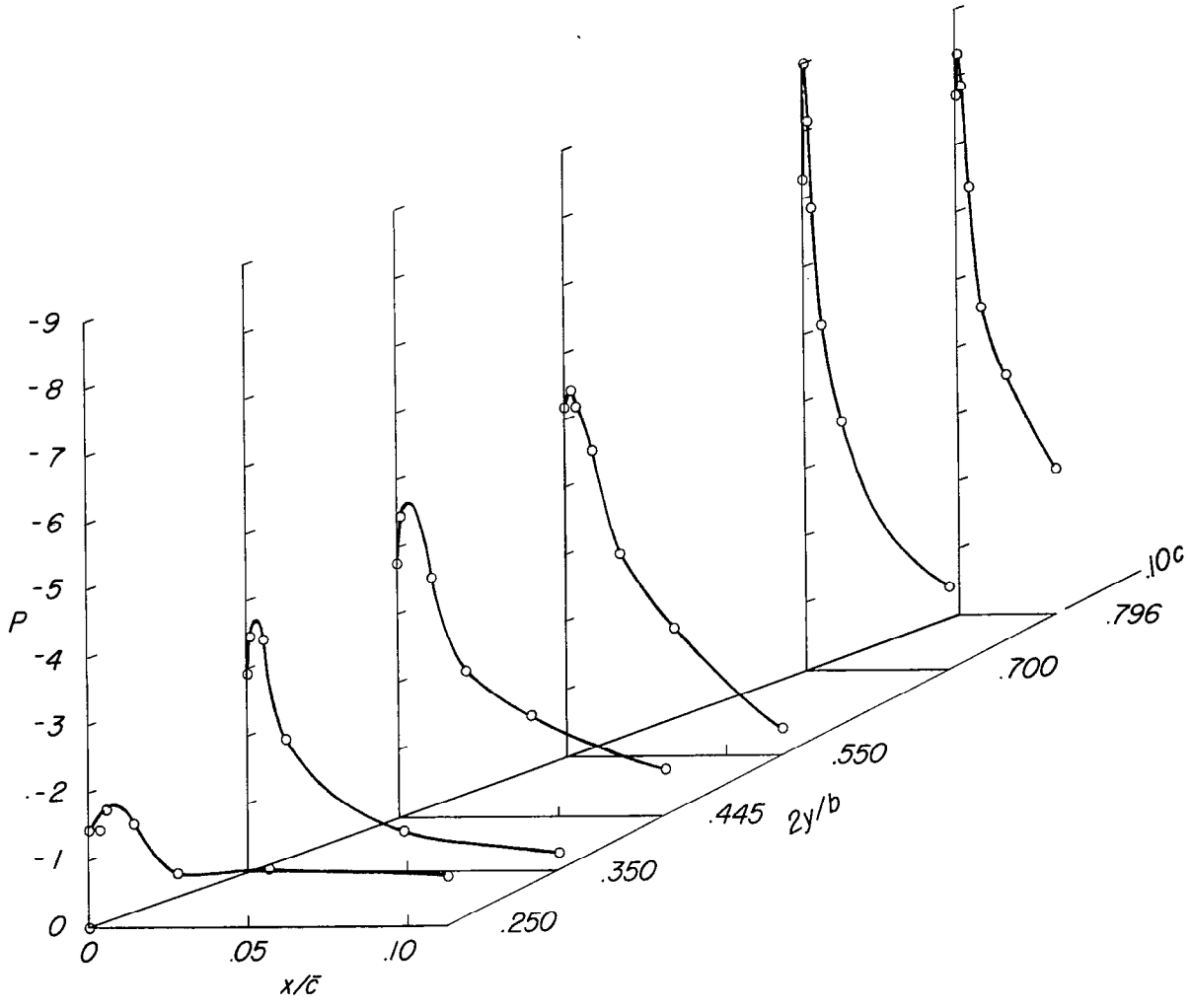

(b) $\alpha = 12.5^{\circ}$.

Figure 18.- Continued.

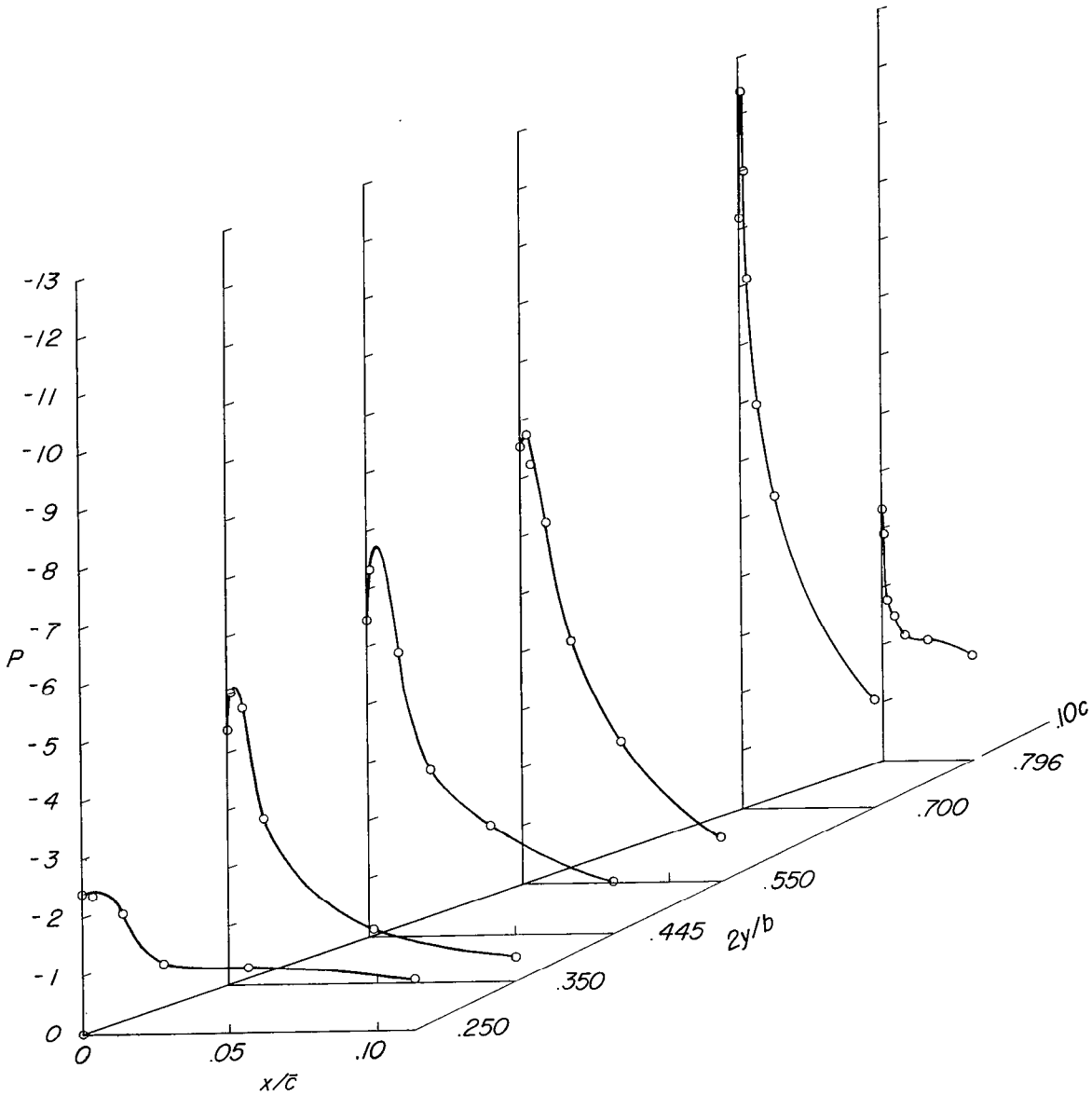

(c) $\alpha = 14.7^{\circ}$.

Figure 18.- Concluded.

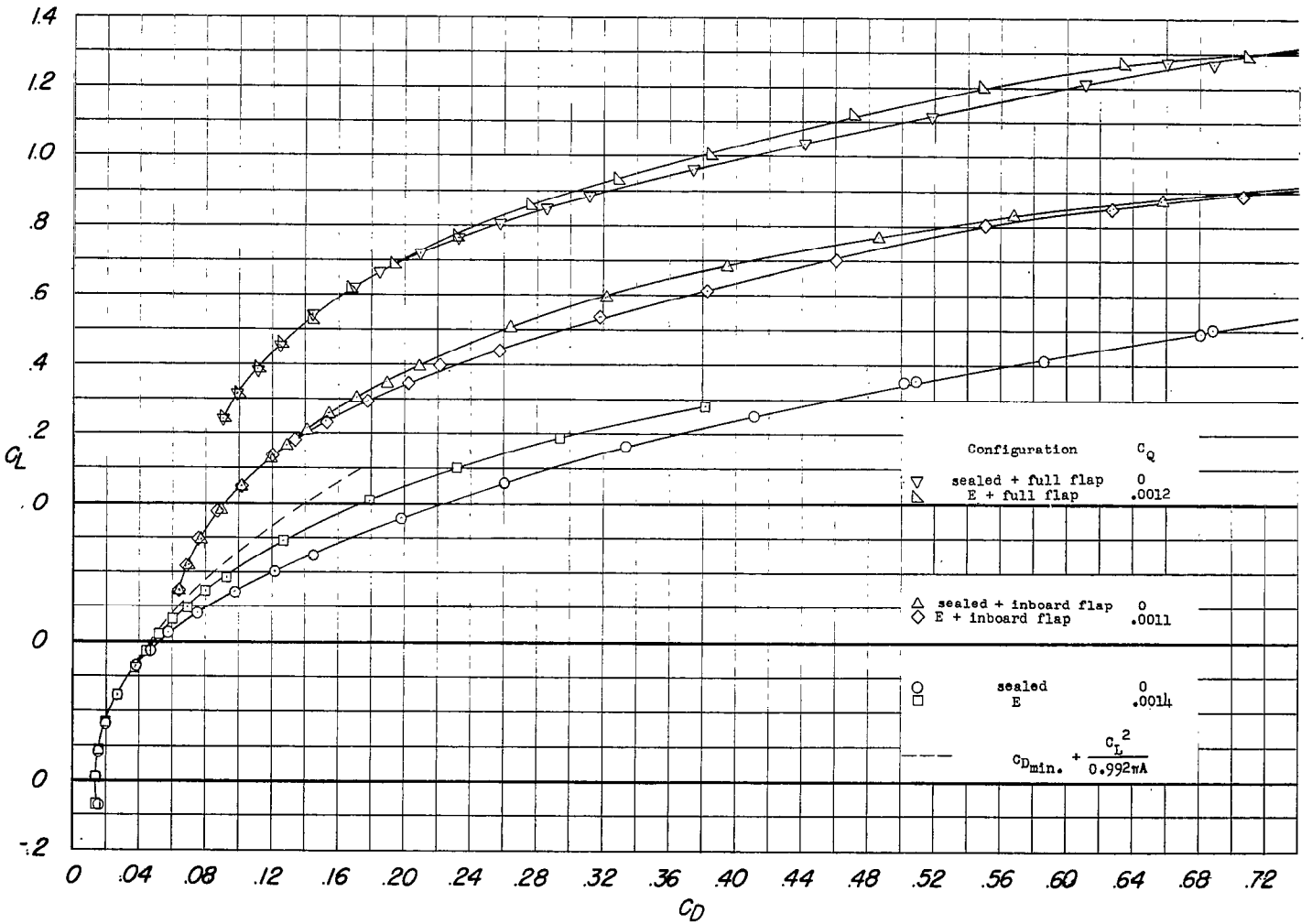

Figure 19.- Effect of suction on the drag of the clipped wing with and without 0.20c split flaps deflected 45° perpendicular to hinge line. M = 0.12; R = 10.7 × 10^6. Pump-power equivalent drag not included.

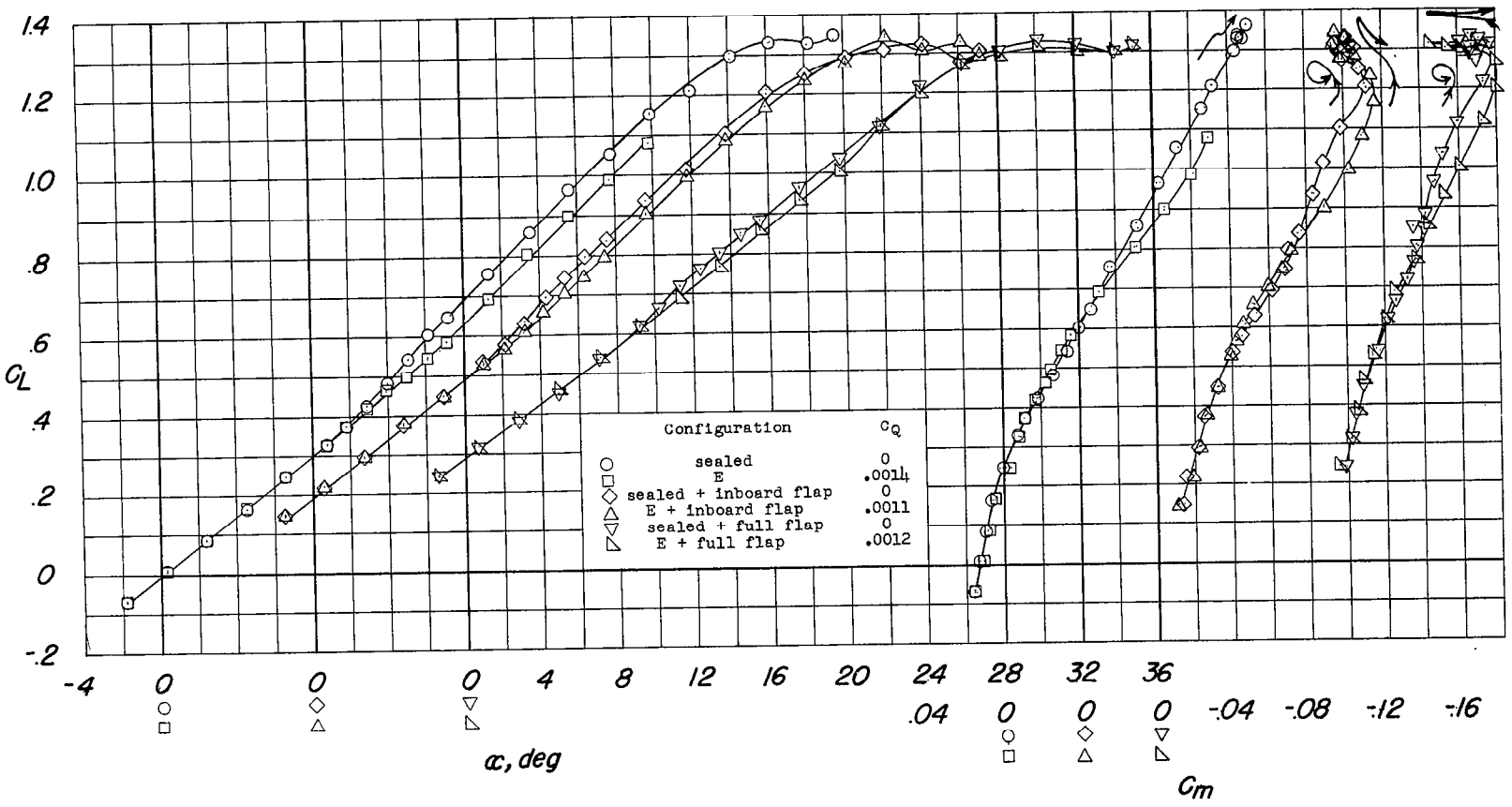

Figure 20.- Effect of suction on the lift and pitching-moment characteristics of the clipped wing with and without 0.20c split flaps deflected 45° perpendicular to hinge line. M = 0.12; R = 10.7×10^6.

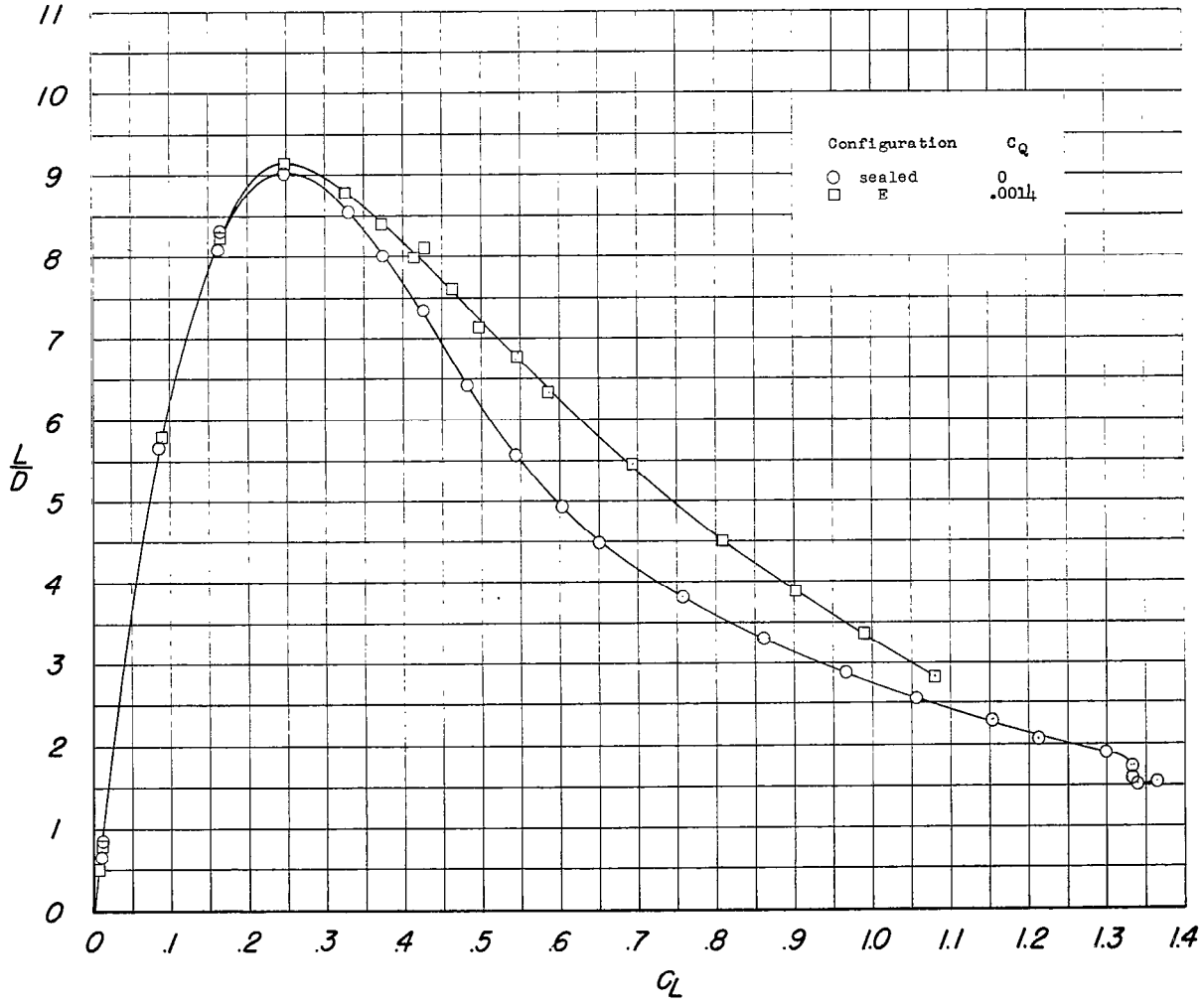

Figure 21.- Effect of suction on lift-drag ratio of clipped wing. $M = 0.12$; $R = 10.7 \times 10^6$. Pump-power equivalent drag not included.

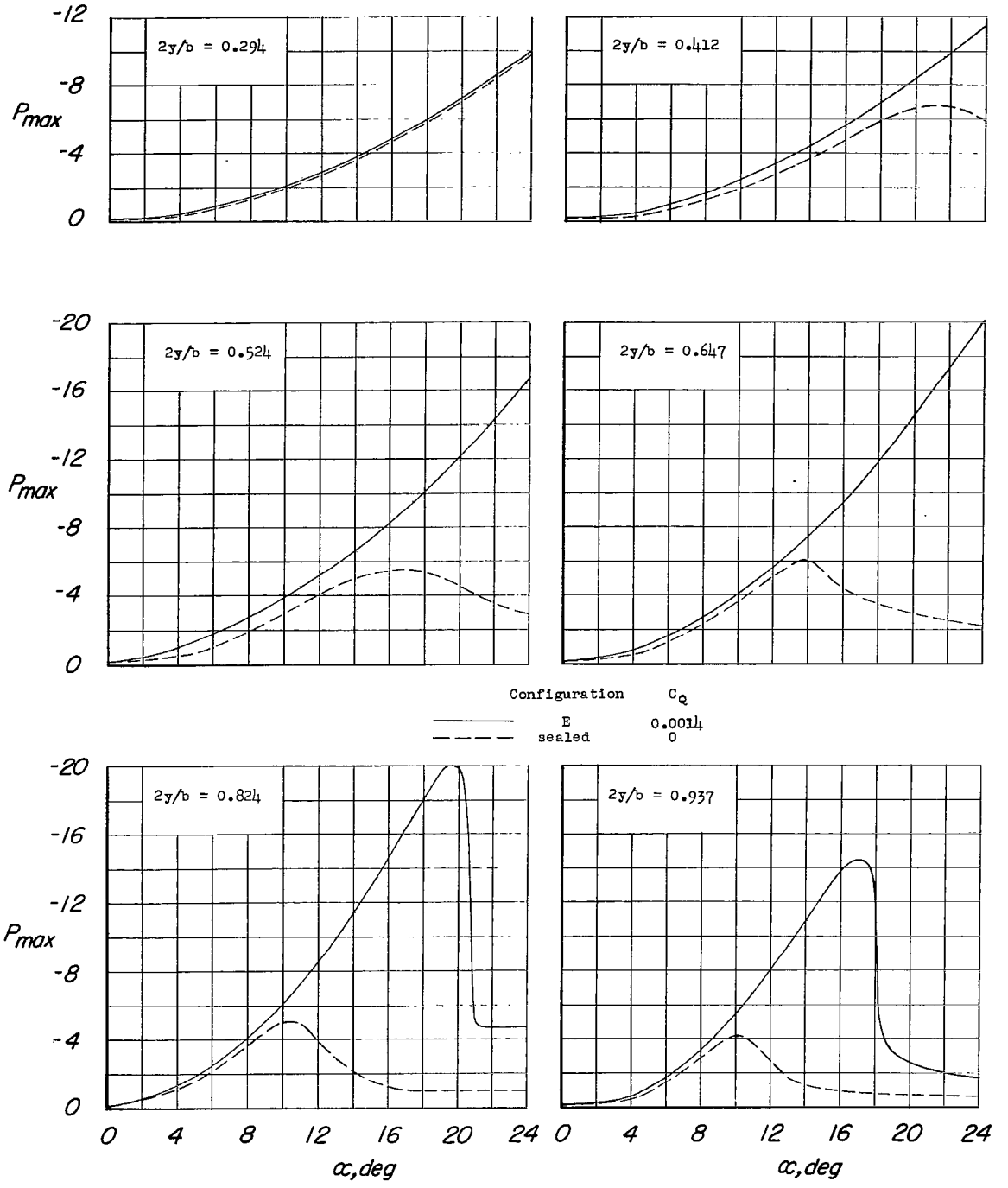

Figure 22.- Effect of suction on peak measured pressure at several spanwise stations on the clipped wing. $\frac{x}{c} = 0.001$; $M = 0.12$; $R = 10.7 \times 10^6$.

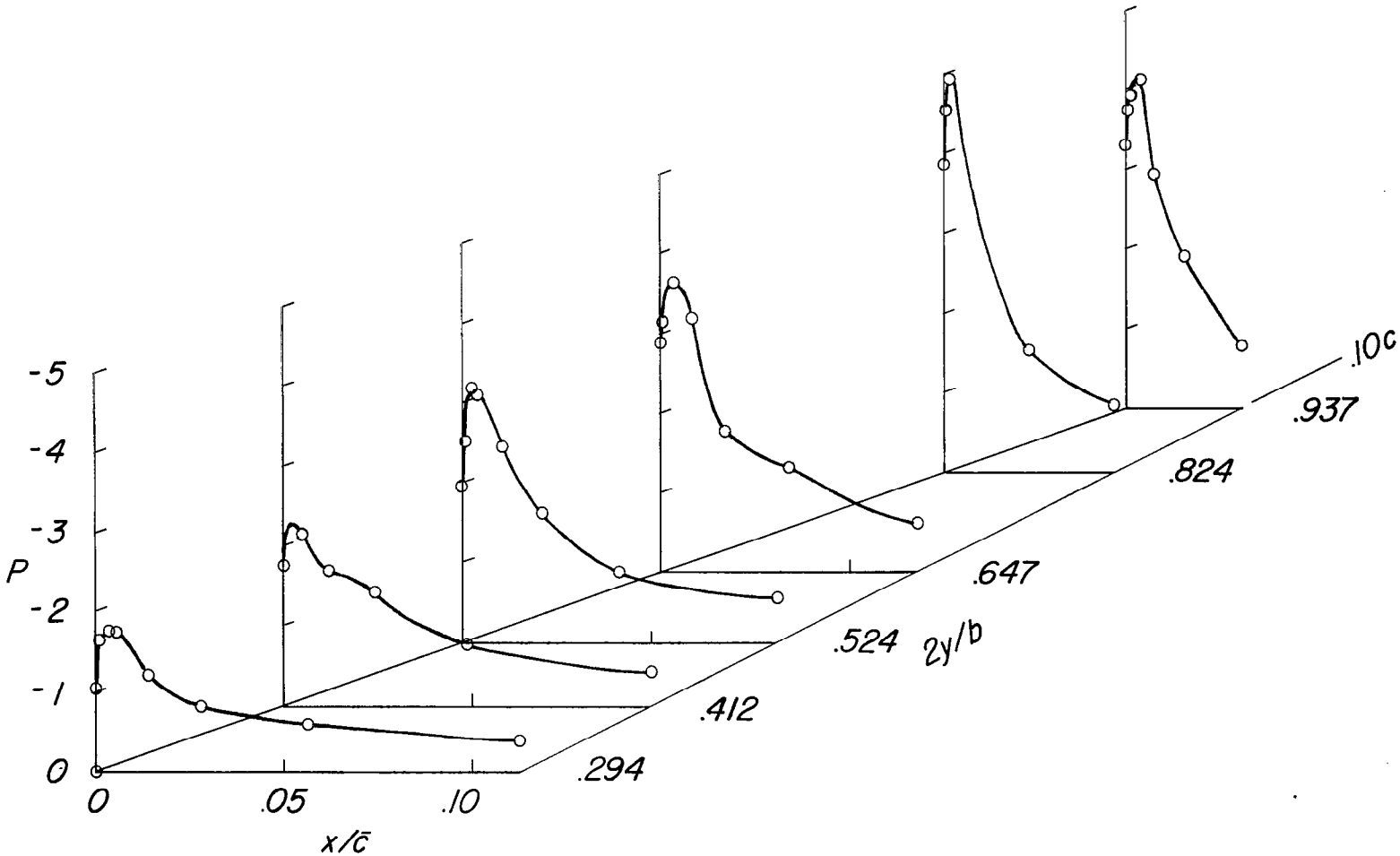

(a) $\alpha = 8.8^{\circ}$.

Figure 23.- Pressure distribution on the leading-edge upper surface of the clipped wing. Leading edge sealed; $M = 0.12$; $R = 10.7 \times 10^{6}$.

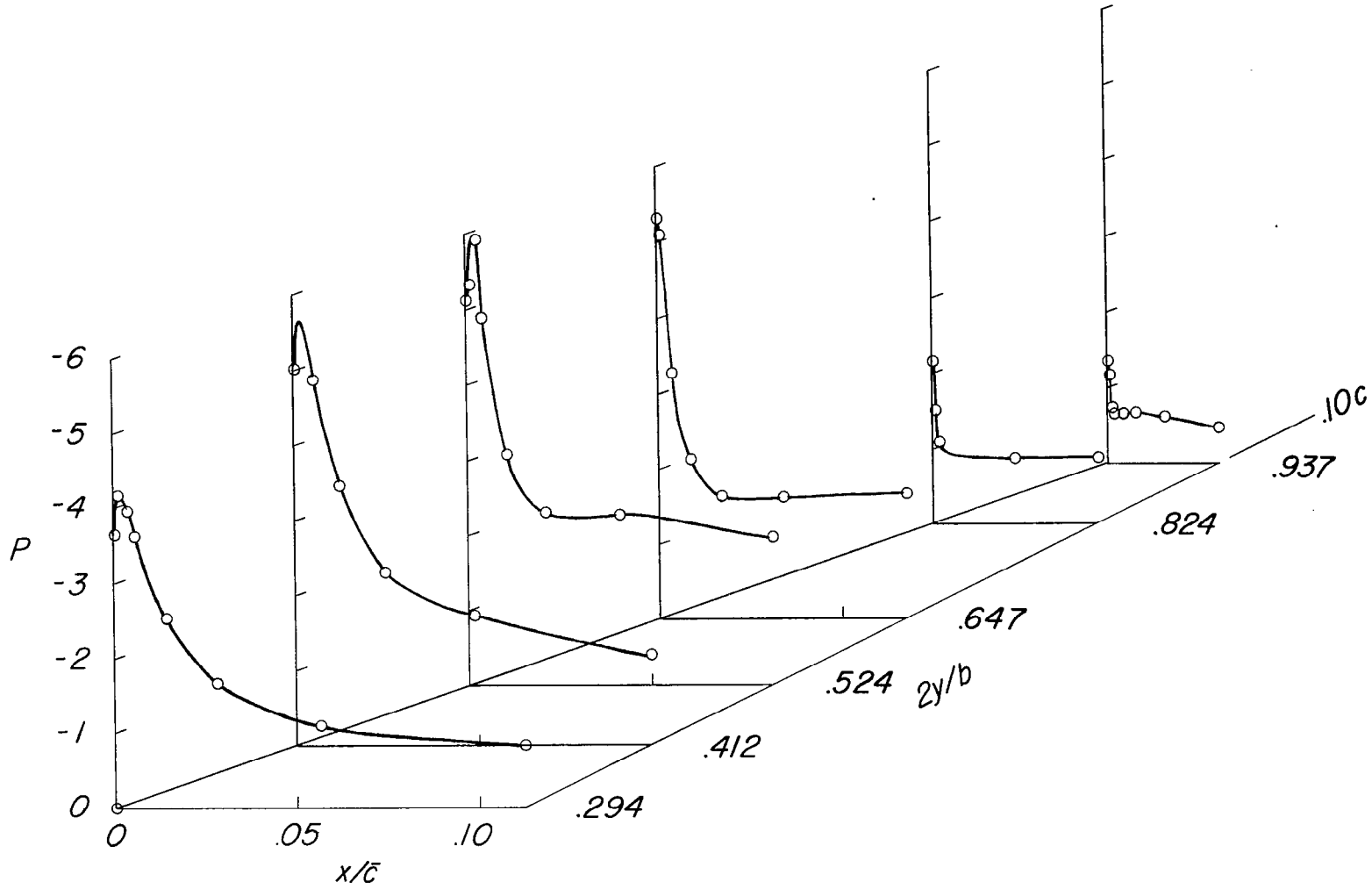

(b) $\alpha = 15.2^{\circ}$.

Figure 23.- Continued.

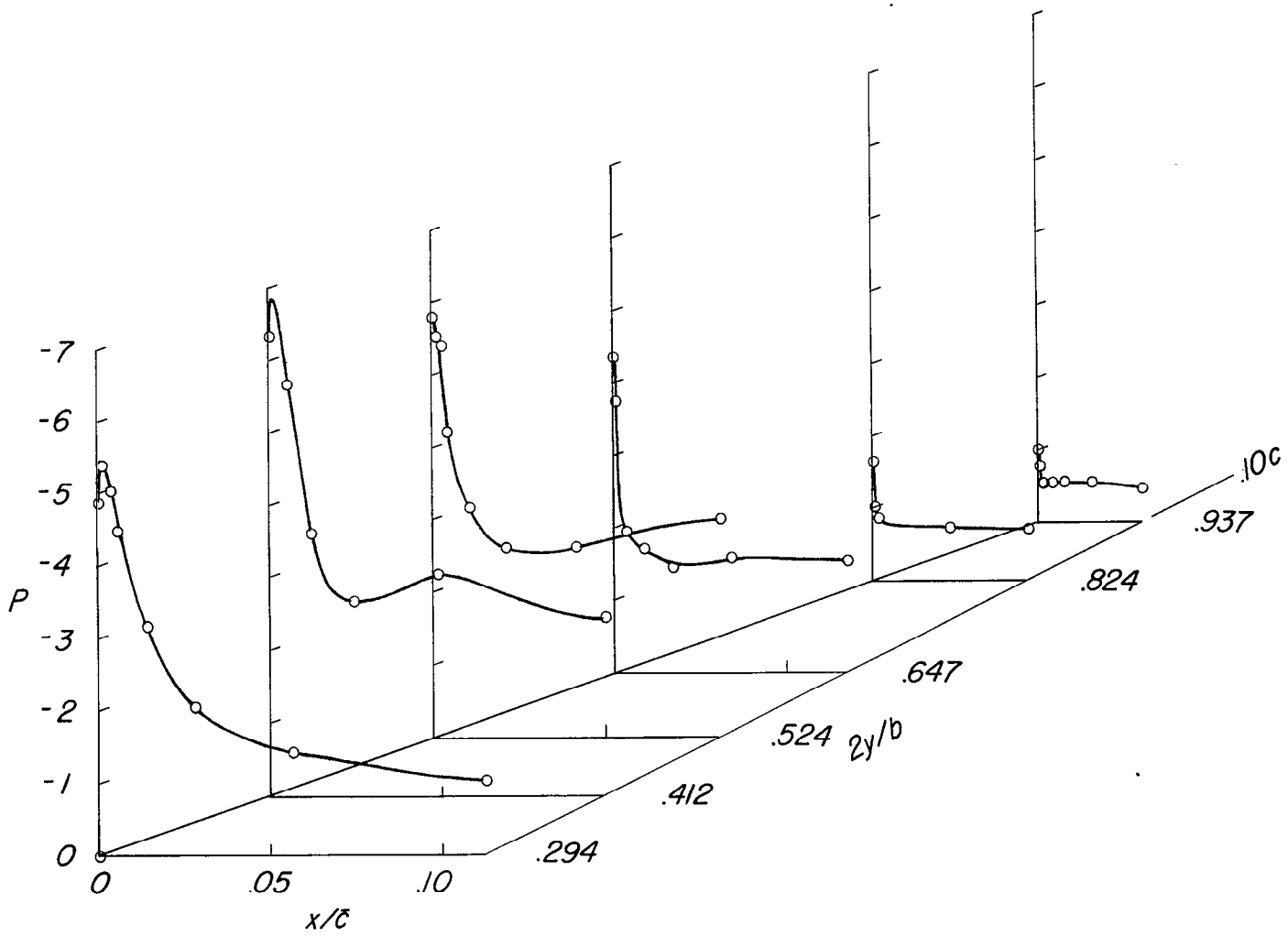

(c) $\alpha = 17.3^{\circ}$.

Figure 23.- Continued.

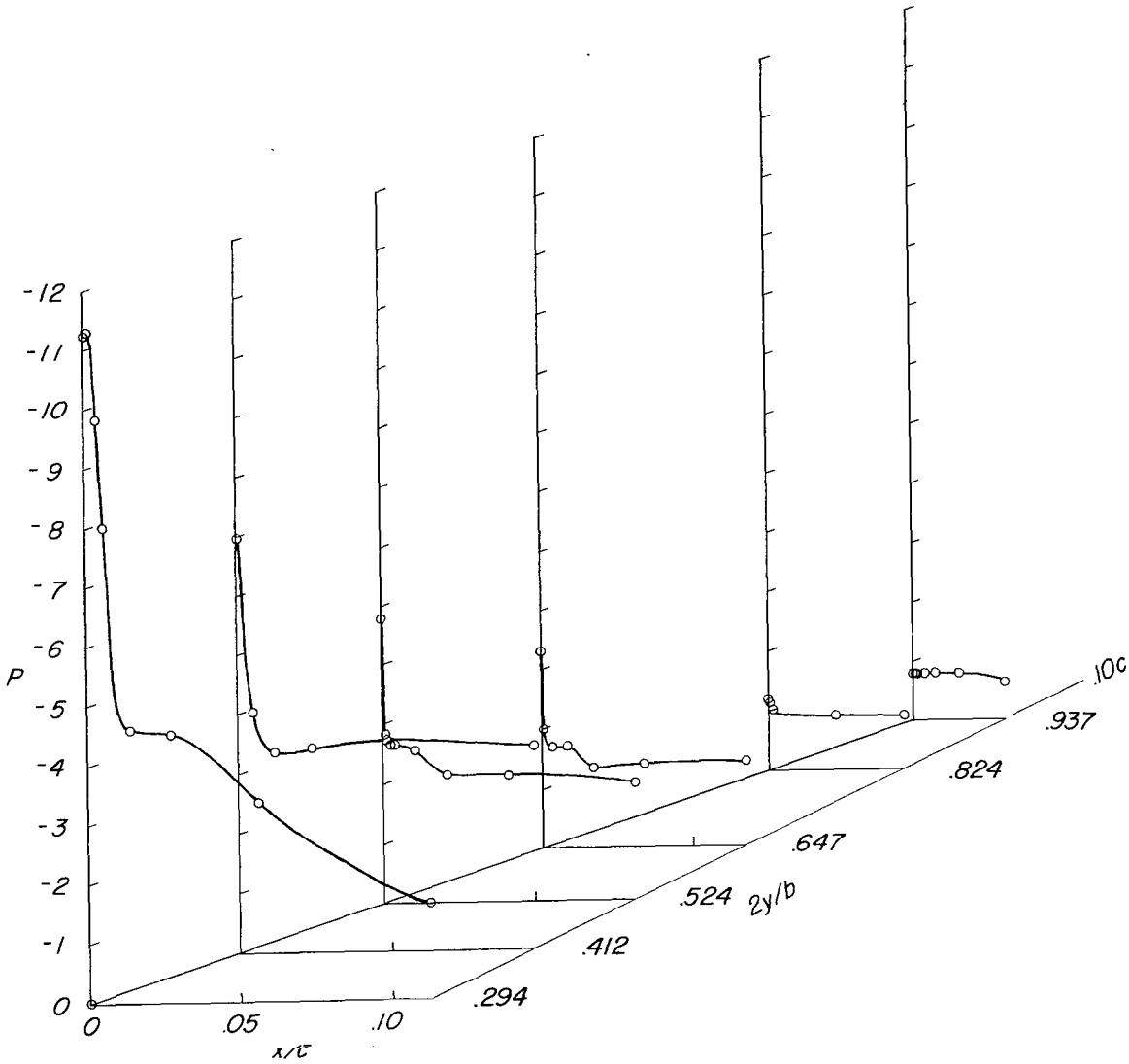

(a) $\alpha = 25.9^{\circ}$.

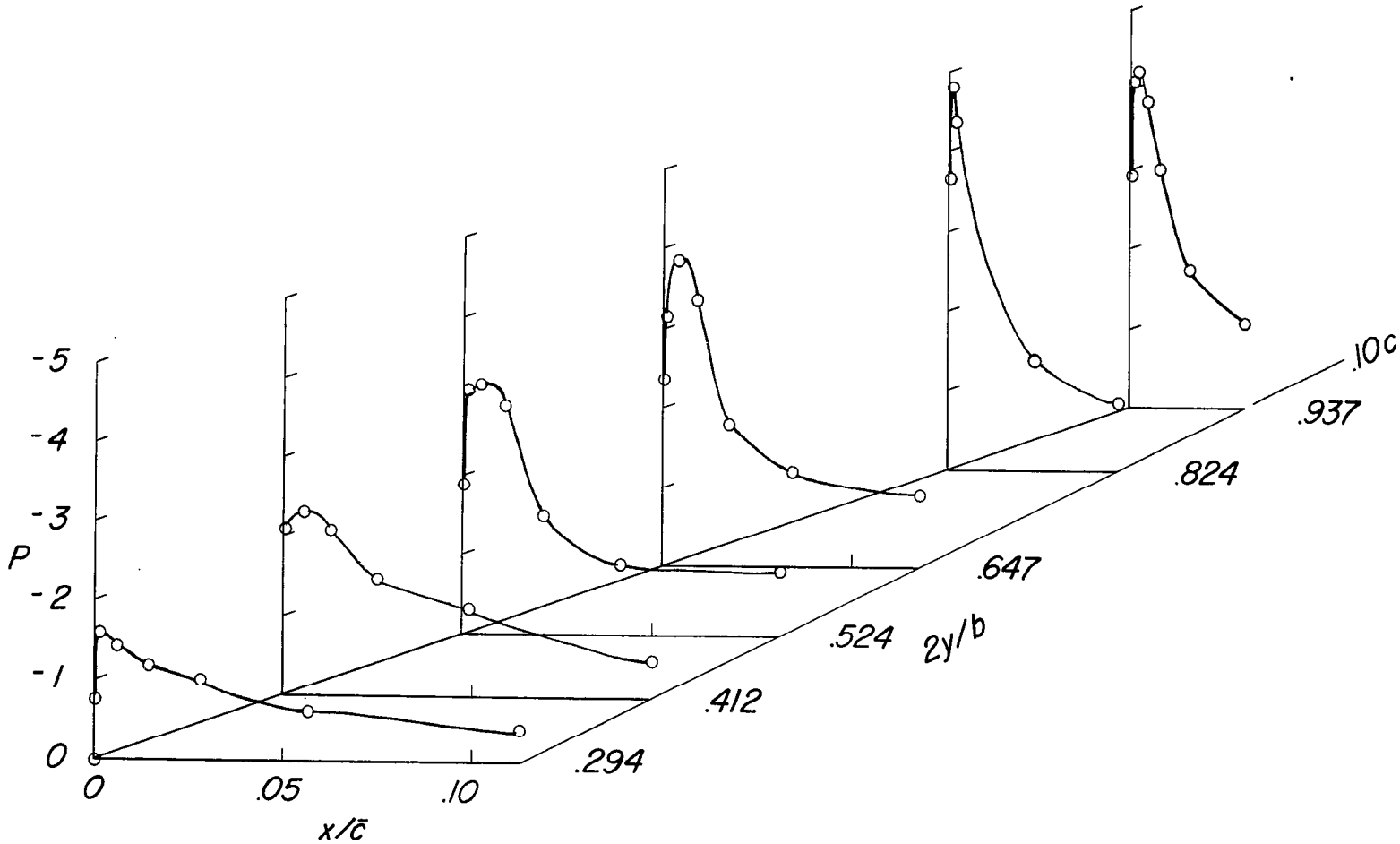

(a) $\alpha = 8.7^{\circ}$.

Figure 24.- Pressure distribution on the leading-edge upper surface of the clipped wing. Configuration E; $C_Q = 0.0014$; $M = 0.12$; $R = 10.7 \times 10^6$.

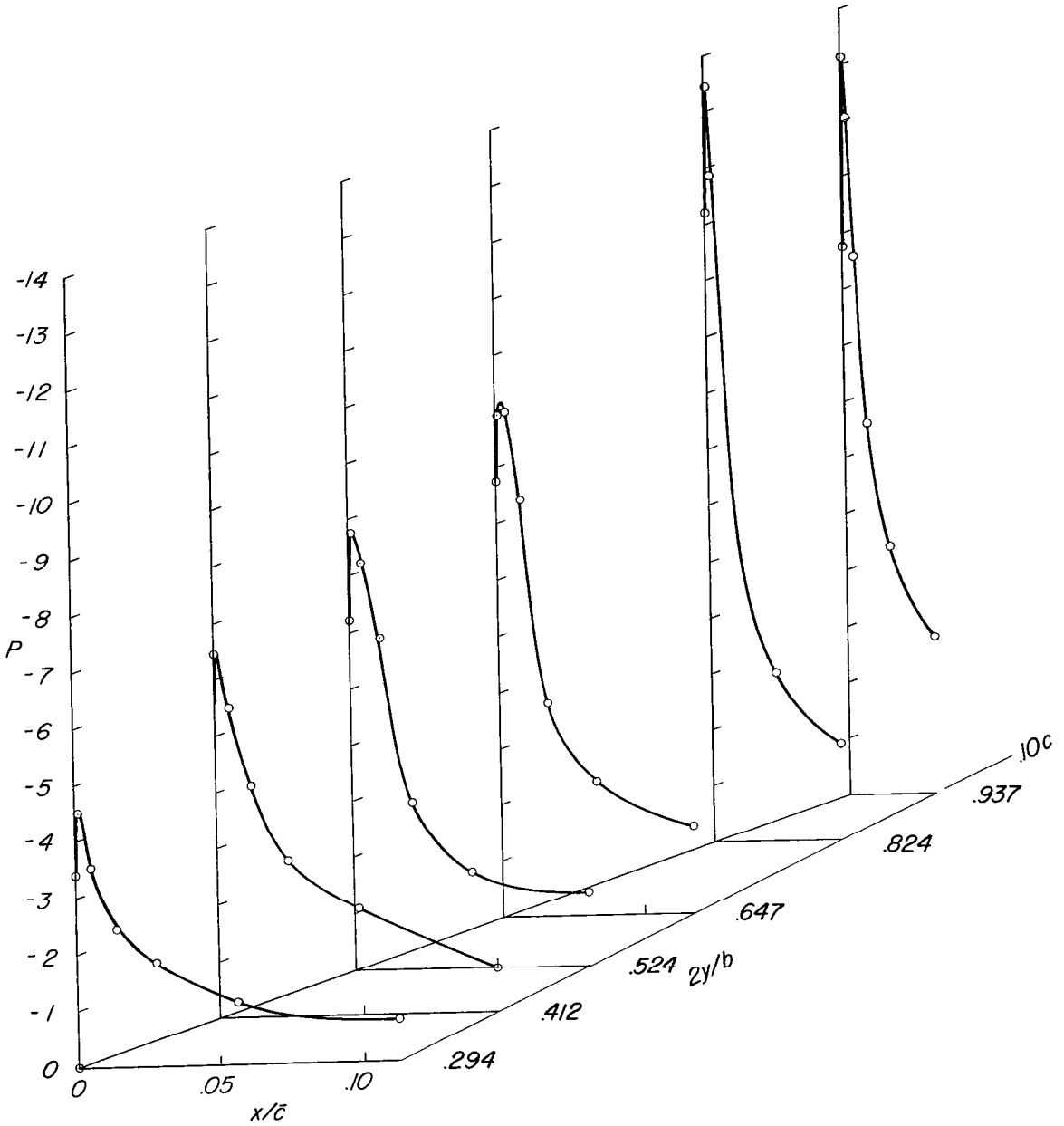

(b) $\alpha = 15.1^{\circ}$.

Figure 24.- Continued.

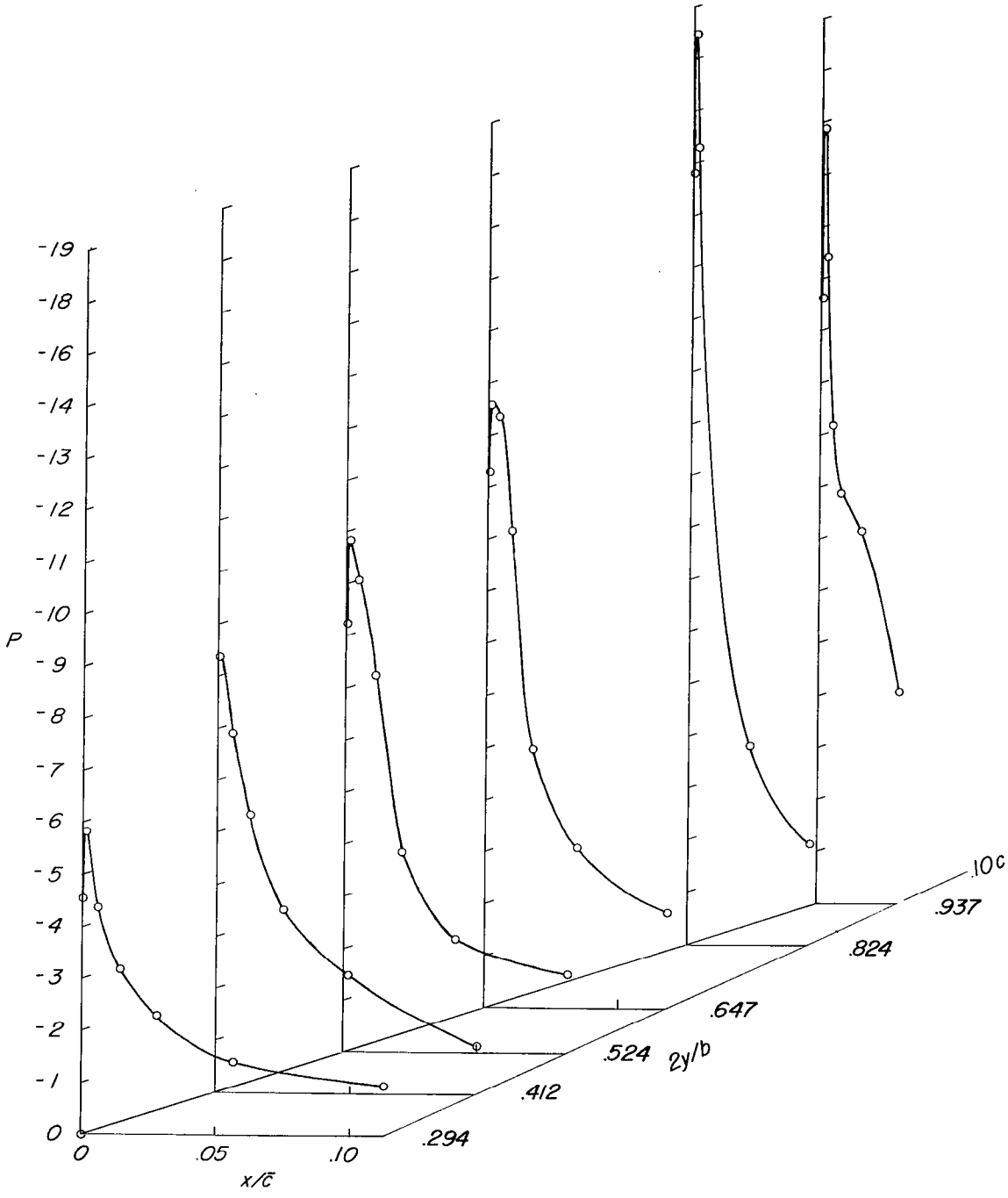

(c) $\alpha = 17.3^{\circ}$.

Figure 24.- Continued.

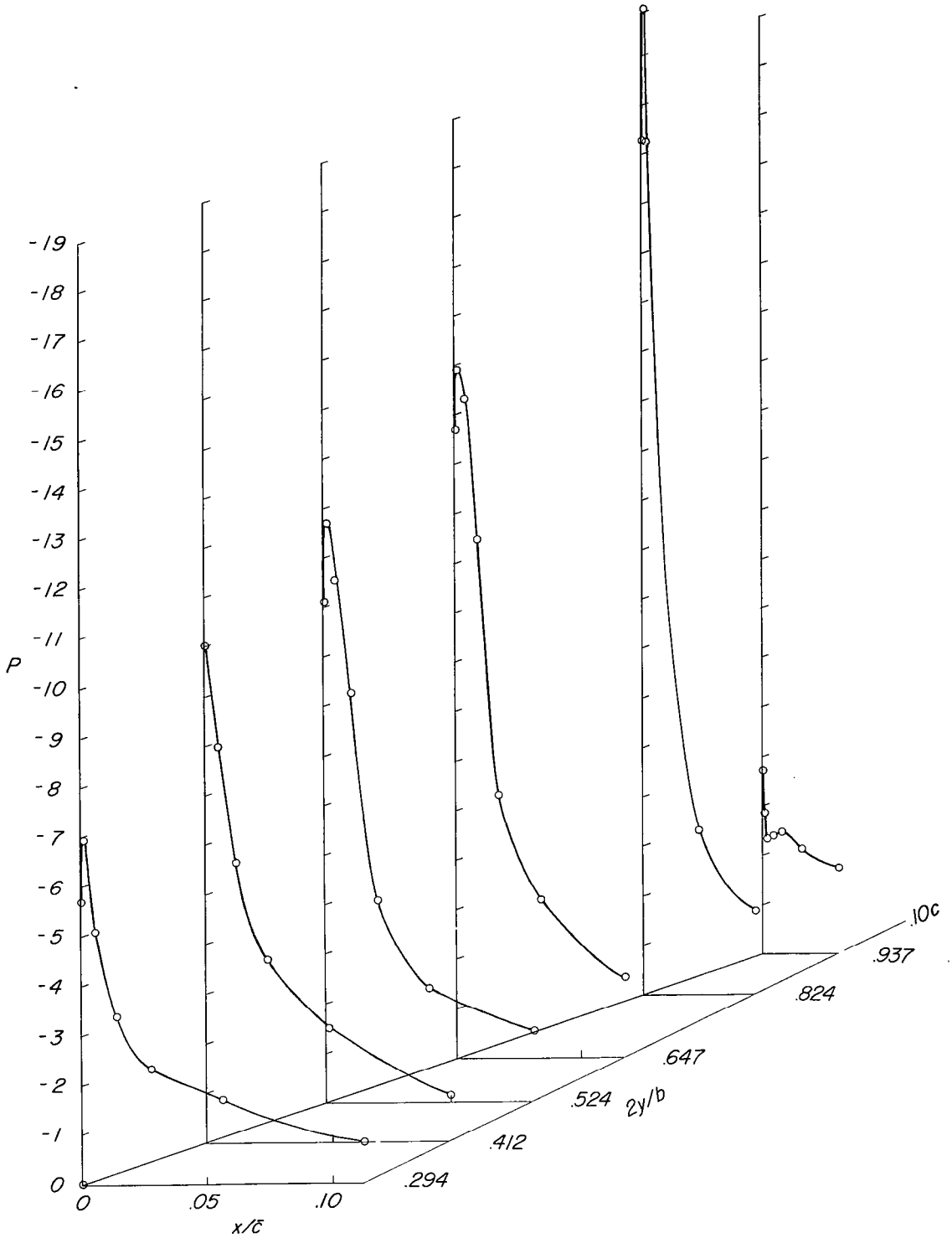

(d) $\alpha = 19.4^{\circ}$.

Figure 24.- Continued.

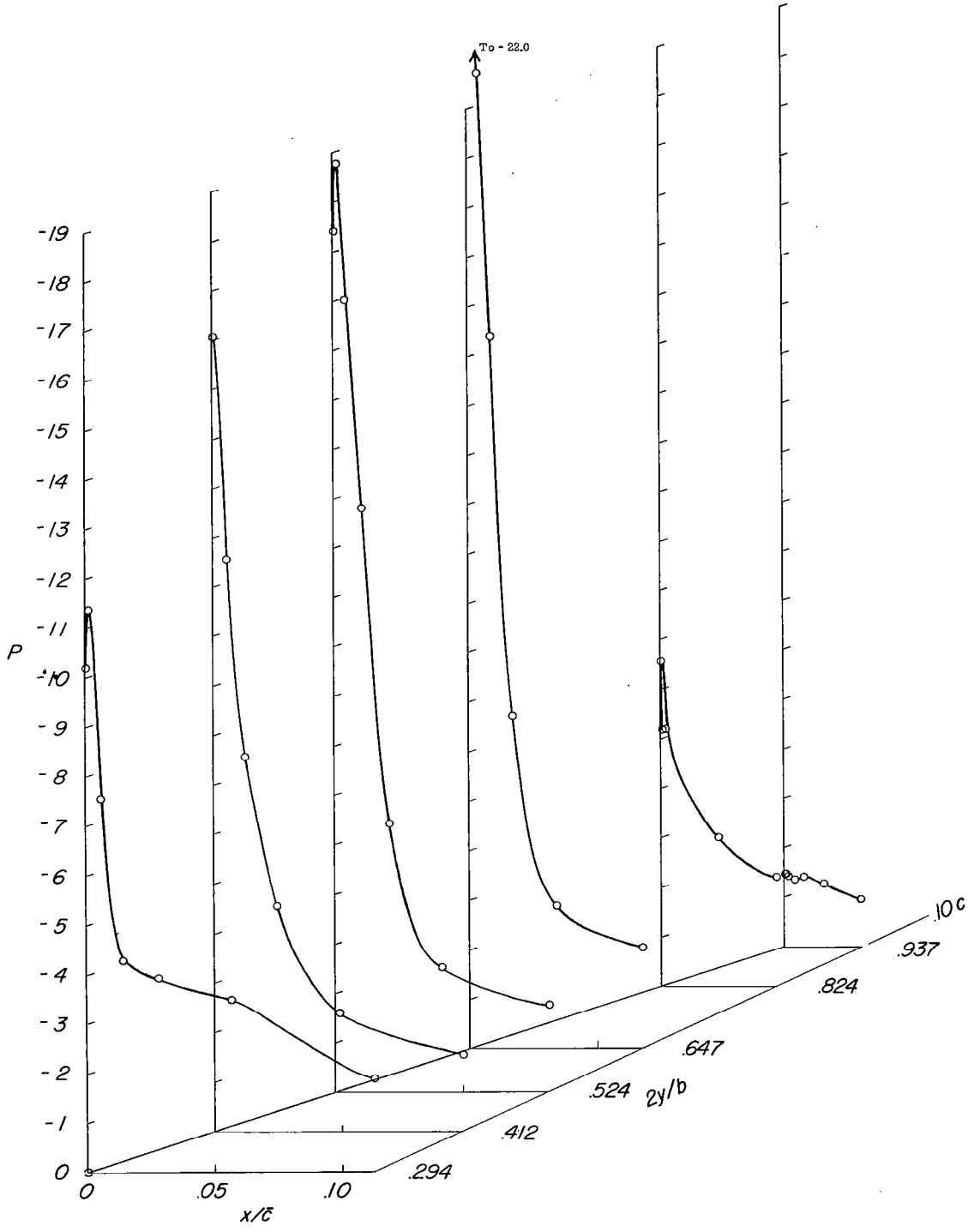

(e) $\alpha = 25.8^{\circ}$.

Figure 24.- Concluded.

[redacted]

NASA Technical Library
3 1176 01437 1950

[redacted]